The Thesis Committee for Gwen Catherine Carris
Certifies that this is the approved version of the following Thesis:

The Effect of Polycarboxylate Admixtures on Early-Age Autogenous Shrinkage

APPROVED BY
SUPERVISING COMMITTEE:

Raissa Ferron, Supervisor

Kevin Folliard

The Effect of Polycarboxylate Admixtures on Early-Age Autogenous Shrinkage

by

Gwen Catherine Carris

Thesis

Presented to the Faculty of the Graduate School of

The University of Texas at Austin

in Partial Fulfillment

of the Requirements

for the Degree of

Master of Science in Engineering

The University of Texas at Austin

December 2018

Dedication

I dedicate this thesis to my fiancé Phillip D'Amore and my loving parents.

Acknowledgements

First and foremost, I thank my advisor Dr. Raissa Ferron for her guidance, support, and enthusiasm for reviewing data. Secondly, I am thankful to Stephen Stacey, whose incredible volume of work, energy, and persistence laid the groundwork for this paper. I thank the Texas Department of Transportation for funding this project.

Mike, Jose, Nick, and Bruno: thank you for teaching me how to mix concrete, how to use a drill press, and all of the other ways of the concrete lab. Sanjida and Savitha, thank you for your help with cement chemistry and crack mapping, and your dedication to your work.

Lastly, I am grateful for the intelligence, time, curiosity, assiduousness, and labor of the undergraduate researchers: Esteban Gonzalez, Pamela Ruiz, Zige Zhang, and Jessica Milligan.

Abstract

The Effect of Polycarboxylate Admixtures on Early-Age Autogenous Shrinkage

Gwen Catherine Carris, M.S.E.

The University of Texas at Austin, 2018

Supervisor: Raissa Ferron

Autogenous shrinkage tests were performed on cement paste mixtures containing varying dosages of different types of polycarboxylate-based high range water-reducing admixtures (HRWRA). The autogenous shrinkage testing was performed using corrugated tubes according to ASTM C1698 on three specimens at once and with measurements taken multiple times a minute. The repeatability of the ASTM C1698 test results in comparison with the results of previous work in literature was presented. In general, a correlation between increased dosage of polycarboxylate admixture and decreased autogenous shrinkage was noted. It was determined that, for 75% of cases, the largest dosage of admixture, resulted in the lowest amount of shrinkage. Additionally, autogenous shrinkage results for typical mixtures used in precast concrete applications (i.e., mixtures incorporating viscosity modifiers and fly ash) are presented.

Table of Contents

List of Tables

List of Figures

I. INTRODUCTION

Background and Motivation

The motivation of studying these particular low water-to-cement ratio (w/c) mixtures was to understand the influence that autogenous shrinkage could have on microcracking in precast concrete beams. The appearance of the microcracking at precast plants in Texas [1,2,3] coincided with several of the plants shifting from using high range water reducing admixture (HRWRA) based on naphthalene-sulfonate chemistry to polycarboxylate ether chemistry. As a result, it was hypothesized that this transition resulted in increased autogenous shrinkage, which would explain the microcracking [1,2]. One aim of this study was to evaluate whether this hypothesis was true. A secondary aim of this study was to understand the effect of mixture parameters on autogenous shrinkage to mitigate shrinkage.

Organization of Document

Part II contains a literature review. The literature review consists of: (i.) background on autogenous shrinkage mechanisms, measurement, and the impact of autogenous shrinkage on microcracking; (ii.) an overview of polycarboxylate-ether (PCE) admixtures in concrete; and (iii.) a review of the effect of PCE's on autogenous shrinkage in literature. Part III details the materials and methods used and Part IV presents the results from these methods with an integrated discussion throughout. Part IV is organized into 4 parts discussing the observed effects of the following mixture parameters on autogenous shrinkage: 1.) Influence of HRWRA dosage, 2.) Influence of w/cm ratio, 3.) Influence of Admixture Type, and 4.) Influence of Fly Ash Replacement and VMA addition. Part V contains the conclusions from observations in the results and discussion section in the context of the Literature Review from Part II.

II. LITERATURE REVIEW

Autogenous Shrinkage

THE MECHANISM OF AUTOGENOUS SHRINKAGE

Autogenous shrinkage is the result of volumetric change due to the reaction of water and cementitious material without any interaction with the environment, specifically in terms of ambient temperature or evaporation. It is measured by placing cement paste within a sealed, isothermal vessel and driven by a combination of chemical shrinkage and self-desiccation. Chemical shrinkage occurs purely as a result of the reaction of cement and water. This reaction creates hydration products, primarily C-S-H gel, which does not take up as much room as the cement and water separately.

0.23 grams water are chemically bound per gram of cement reacted [4,5]. This water becomes part of the C-S-H gel solid and is nonevaporable. The volume reduction due to this reaction has been quantified as about 6.4 ml/100 g cement reacted [5]. Water takes two other forms in a cement paste: capillary water and physically bound water (referred to as gel water). Capillary water is unbound water that is free to be used in ongoing hydration. It is present in the coarse capillary pores. Physically bound water is adsorbed to the surface of the gel solid. 0.19 grams of water per gram of cement is physically bound during cement hydration [5]. When all capillary water has been converted into chemically bound water, hydration slows significantly. Complete hydration of cement paste only occurs at w/c ratios about 0.42 w/cm as this corresponds to the point that there is 0.23 g of water chemically bound and 0.19 g of water physically bound for every 1 g of cement (0.42=0.19+0.23) [4,5]. At w/cm ratios lower than 0.42 w/cm, the cement hydration reaction attempts to react with the physically bound water, creating a force via capillary pressure. The capillary pressure is directly proportional to the size of the pore within which the physically bound water is located. Capillary pressure causes compaction of the hydrating cement grains, a process which is referred to as self-desiccation. Autogenous shrinkage post-set is characterized by this self-desiccation. Figure 1 from the Portland Cement Association shows the relationship

between chemical shrinkage and autogenous shrinkage during the hydration process [6]. As the w/cm ratio lowers, the self-desiccation compaction force increases.

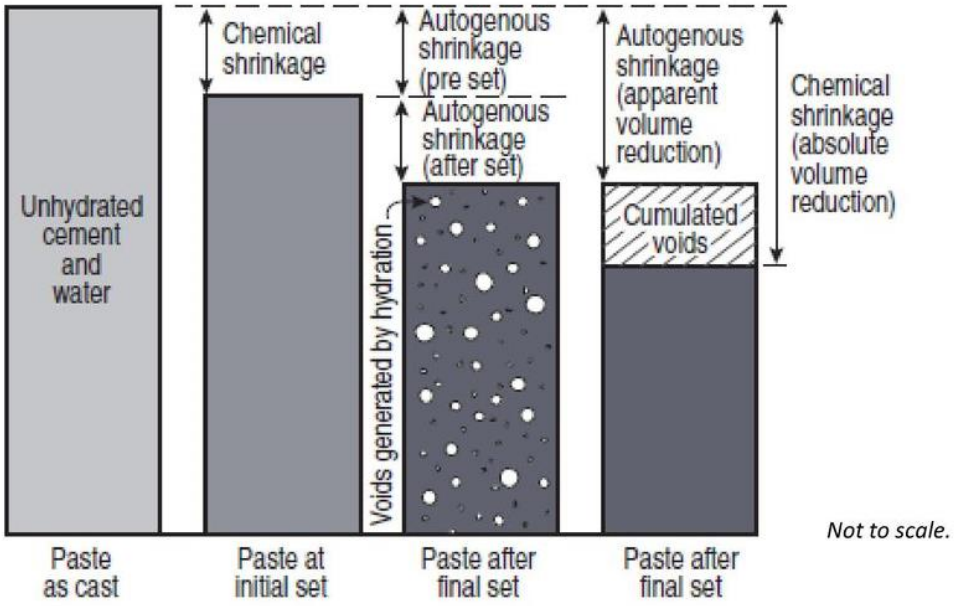

Figure 1: Chemical shrinkage and autogenous shrinkage volume change as illustrated by [6]

Bentz [7] explained that self-desiccation can be described by the Kelvin equation, which relates relative humidity or vapor pressure to the meniscus in a cylindrical pore of radius r:

$$\ln(RH) = \frac{-2\gamma V_m}{rRT}$$

$$RH = Relative\ Humidity$$

$$\gamma = surface\ tension\ \left(\frac{N}{m}\right)$$

$$V_m = Molar\ Volume\ \left(\frac{m^3}{mol}\right)$$

$$r = radius\ of\ the\ largest\ water - filled\ cylyndrical\ pore\ (m.)$$

$$R = universal\ gas\ constant\ \left(8.314\frac{J}{mol}K\right)$$

$$T = absolute\ temperature\ (K)$$

The capillary tension is therefore given by:

$$\sigma_{cap} = \frac{2\gamma}{r}$$

Based off of these classic equations, if w/cm ratio is held equal, the two critical parameters which affect autogenous shrinkage are:

1. the meniscus radius of the largest water-filled pore within the microstructure (or the pore size distribution within the cement paste over the time period measured as the radius of largest water-filled pore is constantly changing during the hydration process)
2. surface tension of pore solution

To address critical parameter 1, a coarser pore structure is desirable. In cement pastes there are 3 main classes of pores: air-voids, capillary pores, and gel pores [5,8]. Air voids occur during the mixing of concrete and range in size between 10 micrometers to 10 m, usually making up 1-2% of concrete mixtures. Capillary pores are created by the space in between cement grains and range from 10 nm and 10 micrometers. Initially they are filled with capillary water. Gel pores are voids in between gel particles and are a direct result of chemical shrinkage. Gel pores range between 0.5-10 nm. A coarser pore structure within a cement paste can be created by: using a coarser cement or incorporating fly ash (provided the fly ash is coarser or equal to that of the cement) [10, 13, 14]. Mixture parameters which contribute to a finer pore structure include: the inclusion of silica fume and HRWRA's [13, 14]. While many precast mixtures in the USA do incorporate fly ash, the necessity of high-early strength dictates the inclusion of HRWRA and very fine cement. A mitigation strategy for autogenous shrinkage addressing the second of the aforementioned critical parameters is to incorporate shrinkage-reducing-admixtures (SRAs) in to the mixture. SRAs function by reducing surface tension and potentially by changing the formation of portlandite [9]. However, SRAs create the following potential issues: they can potentially destabilize air void systems, retard hydration, and reduce strength [9]. These potential issues make it impractical to incorporate SRAs into precast mixtures.

MICROCRACKING AND AUTOGENOUS SHRINKAGE

Per RILEM TC-122-MLC, microcracks are defined as cracks with a crack width of less than 10 micrometer and refer to cracking induced by shrinkage, not external load [8]. However, a review of drying shrinkage microcracking observed that shrinkage cracking within a paste can lead to crack widths of up to 50 micrometers [8]. When these cracks occur at an early age, they can lead to weak points for durability issues to occur in future and be unsightly. The main sources of this form of cracking are known to be drying shrinkage (due to water evaporating to the environment) and autogenous shrinkage. The difference between the two mechanisms impact on cracking is that autogenous shrinkage is generally uniform throughout a cement paste, while drying shrinkage occurs nonuniformly due to a differential relative humidity gradient [8]. As concrete mixtures subject to significant autogenous shrinkage are used for high-strength structural applications, the issue of durability for these mixes is of great concern.

As previously discussed, up to the point of initial set, autogenous shrinkage is entirely the same as chemical shrinkage; a result of cement reacting with water, creating hydration products which do not take up as much room as the cement and water separately. As the system is purely fluid, this shrinkage purely causes strain, and not stress [11]. Beyond the point of setting, the pore structure formed within cement paste creates capillary stresses via Le Chatelier's principle, a process known as "self-desiccation" [11,12]. It has been established that paste mixtures with water-to-cementitious materials ratio (w/cm) lower than 0.42 reach a point during hydration at which there is not enough available water to react with the cement [4,5]. This causes capillary pressure to develop on the pore walls of the paste microstructure. As the microstructure develops, relative humidity within the paste lowers, creating rigidity within the paste. The increased rigidity of the paste creates restraint against these capillary forces. At the point of initial set, the strain *does* cause stress within the paste which can result in small cracks. Such small cracks could develop into larger cracks later on. Microcracks can be significant for high performance concrete mixtures, because at an early-age of hydration, the tensile strength of high performing concrete mixtures is at its lowest and most vulnerable to cracking.

MEASUREMENT OF AUTOGENOUS SHRINKAGE: THE "TIME-ZERO" PROBLEM

Autogenous shrinkage researchers refer to the time at which autogenous shrinkage transitions from pure chemical shrinkage to self-desiccation as 'time-zero.' How to identify the exact dividing point beyond which autogenous strains cause stress in the paste structure has been reviewed by Sant and a systematic study of time-zero by Huang et. al. [11,15]. Sant concluded that the "knee" in the autogenous shrinkage curve, or point at which the strain rate changes, correlates +/- 15 minutes to the Vicat final setting time and has been found to be a good indicator of the point at which stress commences from autogenous strains [11]. ASTM 1698, the ASTM standard for measuring autogenous shrinkage, also recommends final setting time determined by Vicat be used as time-zero and most researchers over the past decade have used Vicat testing to normalize their autogenous shrinkage data [18]. However, variation of +/-15 minutes of autogenous shrinkage data can have a profound impact upon the results and interpretation. In a 2017 study Huang et. al monitored RH in cement pastes and defined time-zero as the onset of internal RH drop, signifying stiffening occurring within the paste (a good metric based off of the previously discussed Kelvin equation) [11]. The study was conducted on Type I cement mixtures and PCE admixture. Huang concluded that Vicat final setting time occurs earlier than the stiffening point of the paste based off of RH data. Based off of RH data, time-zeros based off of the point of the 'knee' in the data were determined to be more accurate.

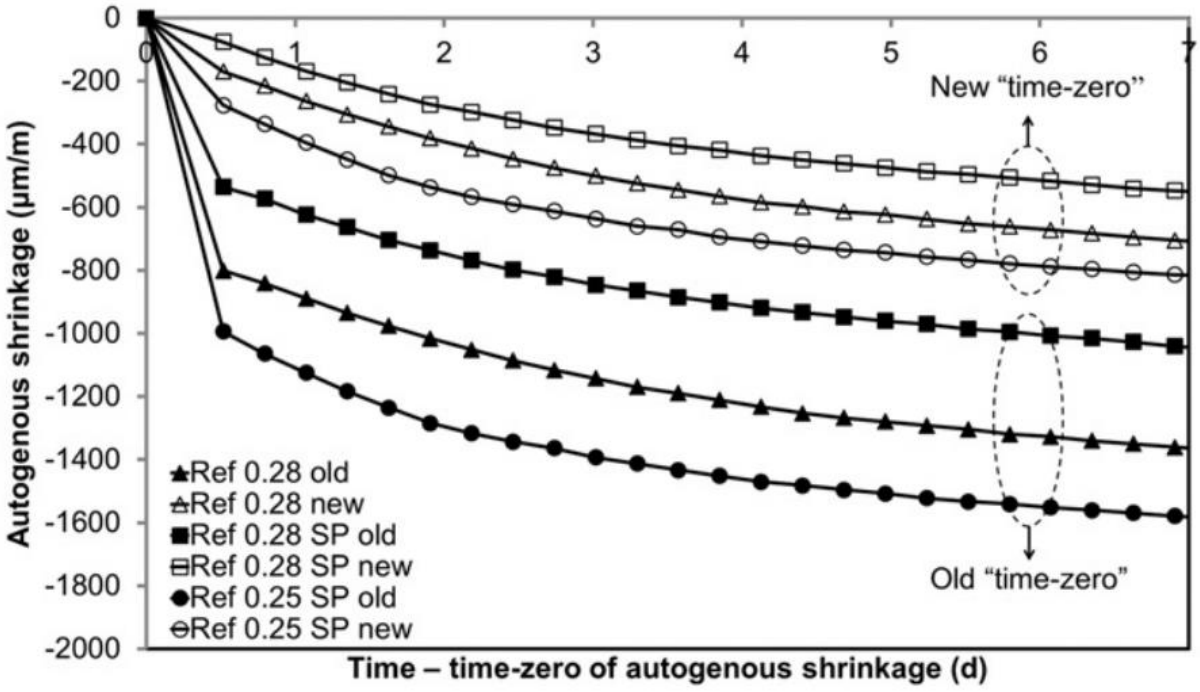

Figure 2: Time-zero shifts of autogenous shrinkage data by Huang et. al. [15]

There are two method types of measuring autogenous shrinkage: volumetric methods and longitudinal methods. The main volumetric method monitors the volume change of cement paste sealed within a condom via buoyancy over time [16]. The results presented here were conducted using the corrugated tube method according to the standardized method of measurement developed by Jensen and Hansen: ASTM C1698, Test Method for Autogenous Strain of Cement Paste and Mortar [17,18]. An additional adjustment to the procedure recommended by Gao et. al was also incorporated: the use of non-contact LDVT sensors to reduce frictional losses [19]. The corrugations of the tube provide rigidity in the radial direction and freedom to shrink in the linear direction so that displacement can be measured as accurately as possible [17]. Through previous labwork at the University of Texas and by Sant et. al, results from the linear corrugated tube test were determined to vary less than results from the buoyancy method [1,16]. Jensen and Hansen reported a typical standard deviation value of 200 μm/m before setting and 20 micrometers after

setting [17]. Gao et. al reported standard deviation values of 150 μm/m before set and 10 μm/m after set using a noncontact LDVT ASTM 1698 apparatus [19].

Besides the time-zero problem, an additional challenge presented to researchers of autogenous shrinkage are periods of expansion in the data (herein referred to as 'bleed bumps'). In measurement of autogenous shrinkage, after the initial period of linear increase of shrinkage over time due to chemical shrinkage, sometimes a period of expansion is observed. This autogenous expansion has been previously theorized to occur due to crystallization pressure (from growth of hydration products such as ettringite and portlandite), thermal dilation, and reabsorption of bleed water. Mohr and Hood demonstrated that by rotating the corrugated tubes during ASTM 1698 measurements, the expansion period becomes negligible [20]. Figure 3 demonstrates their findings which indicate that the expansion period is primarily due to reabsorption of bleed water, rather than thermal dilation or crystallization pressure. Mohr and Hood also observed that the period of expansion correlated with an increase in dosage of PCE admixture.

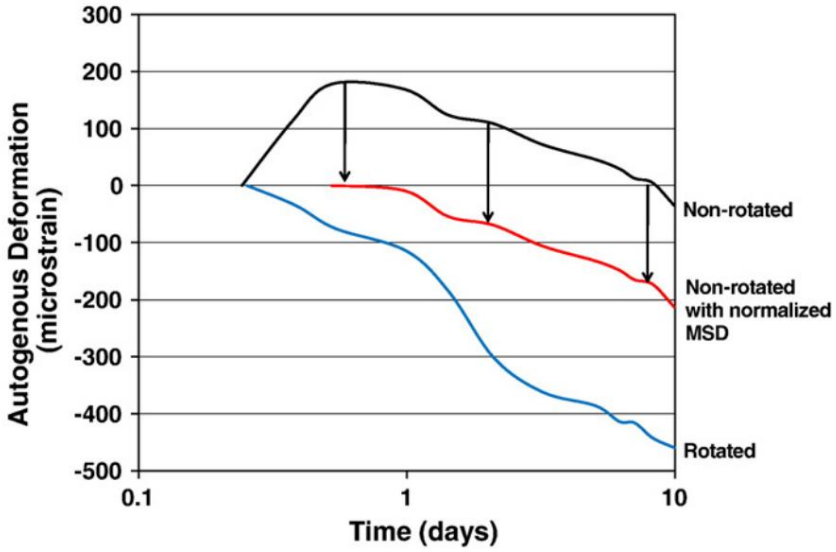

Figure 3: A comparison of the bleed bump or 'maximum strain differential' between non-rotated and rotated samples from [20]

This thesis focuses purely on autogenous strain created within low w/cm cementitious systems (0.28, 0.31, and 0.33). These mixtures are more susceptible to cracking caused by autogenous shrinkage stresses than high w/cm cementitious mixtures. To focus as much as possible on the relevant portion of autogenous shrinkage, all autogenous strain vs. time plots were normalized from the initiation of a clearly defined "bleed bump" in the shrinkage data at which point the autogenous strain rate changed. The Matlab code written to analyze the data is provided in Appendix A. The code accomplishes three primary tasks:

1. The data was converted from length change to strain via the equation:

$$\varepsilon = \frac{\Delta L}{L_0}$$

$$where\ \Delta L = length\ change\ and\ L_0 = initial\ length$$

2. The data was smoothed using the *rlowess* function (see Figure 4)

3. Then the peak in the strain data during the first stage of the deformation was established as time-zero and the strain data were shifted accordingly (identified in Figure 5).

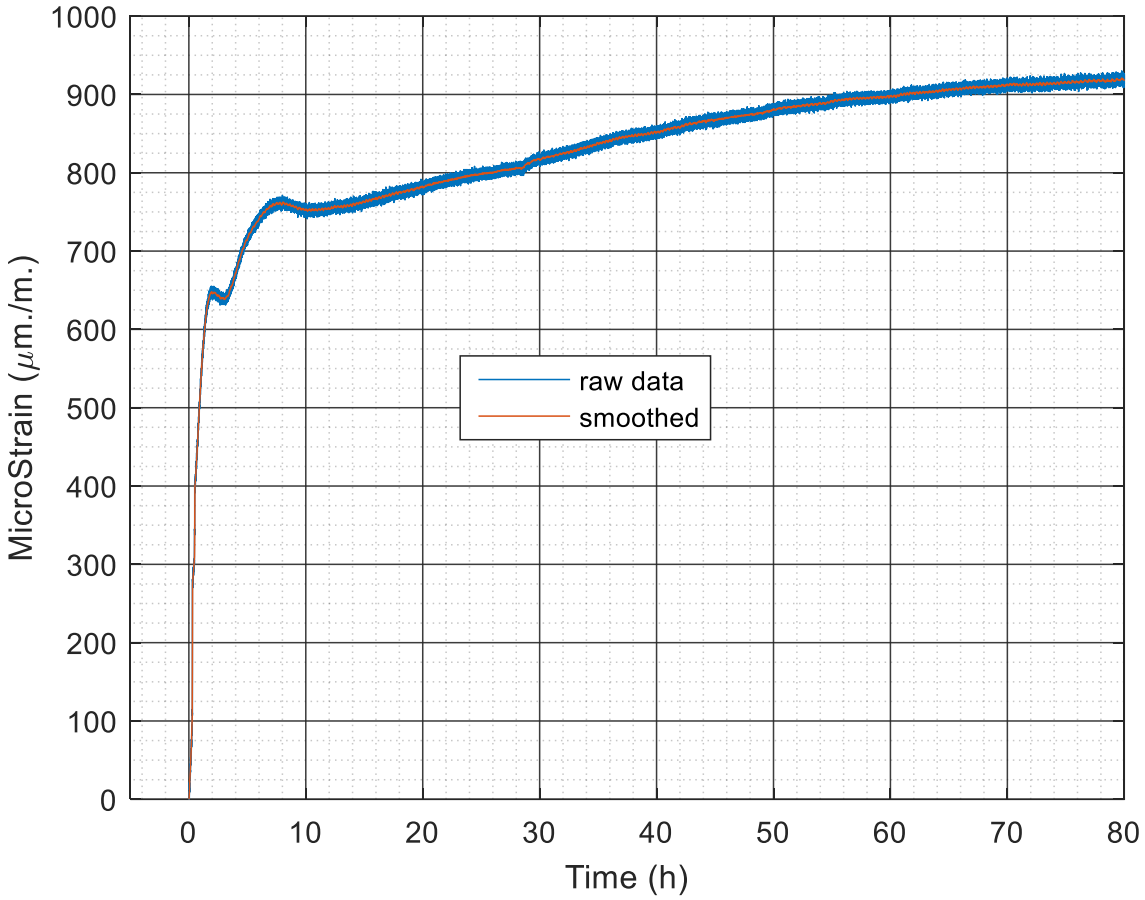

Figure 4: A sample of data is compared with the rlowess smoothed values. Amplitudes have already been converted into microstrain values, but the shift of the curve based on bleed bump values has not yet been applied. The rlowess smoothed strain values are used to determine the time-zero shift applied to the data.

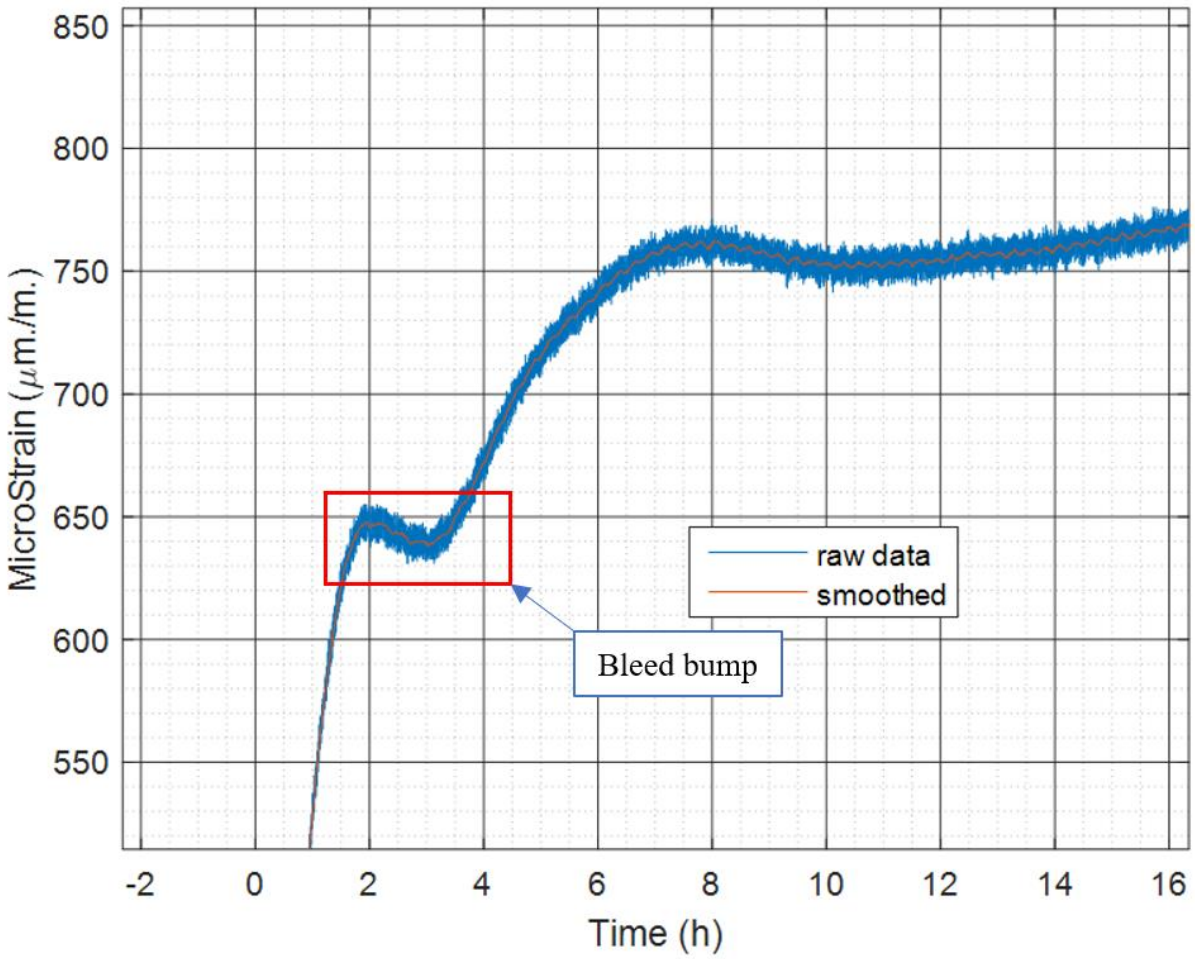

Figure 5: A zoomed in view of Figure 4, with bleed bump denoted. The strain data will be shifted 2 hours to the left based on the point at which expansion begins (provided it occurs within a reasonable range of Vicat setting times determined for mixtures in [1]).

An Overview of PCE Technology

Over the course of the 20th century, the concrete industry has advanced through three major generations of water-reducing admixtures: lignosulfates (discovered in the 1930's), sulfonated melamine and naphthalene condensates (1970's), and polycarboxylates (1990's) [21]. All water-reducing admixtures operate by preventing cement grains from grouping together in flocs during

cement hydration [21]. Cement grains are attracted to each other via Van Der Waals forces and repelled by electrostatic repulsive forces [22,23,23]. Both forces are dependent upon the distance between particles. Within about 1 nm, the magnitude of Van der Waals force overcomes electrostatic repulsive forces and cement grains stick to each other [23]. Figure 6 from [23] provides a conceptual illustration of the variation of attraction and repulsion energy with distance between cement particles.

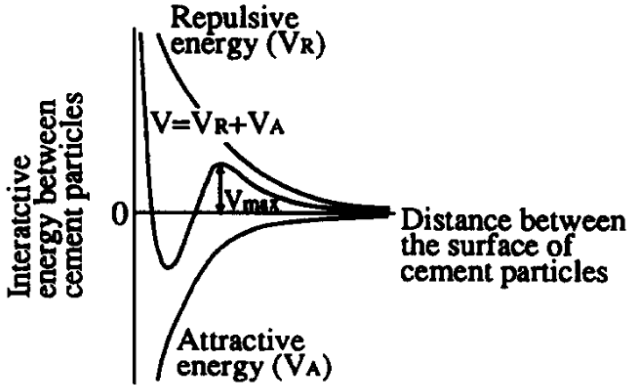

FIG. 1.
Relationship between distance and interactive energy of cement particles.

Figure 6: This figure from [23] illustrates the variation in attractive forces between cement grains (consisting of Van der Waals forces) and repulsive forces between cement grains (consisting of electrostatic repulsive forces). The figure shows that within a certain distance between cement grains, the attractive forces overcome the repulsive forces.

These groups of cement, called flocs, trap water. Trapped water within a floc is not available to lubricate paste. Additionally, flocs reduce the amount of exposed cement grain surface area, reducing the rate of hydrolysis. To prevent flocs, lignosulfates and melamine and naphthalene condensates primary mechanism of preventing flocs from forming is by dispersive action [22]. They adsorb onto the cement grain via a polar chain. Their anionic polar head makes the cement

hydrophilic and leads to repulsive forces between cement grains [22]. Additional dispersion is created by repelling negatively charged aggregate particles and air-entrained bubbles [22]. However, their water-reducing impact is limited to a short period of time [22,24]. Via this mechanism of dispersive action, melamine and naphthalene admixtures have a water reduction potential of up to 30%, but a high rate of slump loss [22,24]. Polycarboxylate-ether superplasticizers (PCE) consist of ether with a flexible polar chain carrying negative functional groups and long hydrophilic side chains [22]. Like lignosulfates and melamine/napthalene-based admixtures, the polar chain is adsorbed onto the cement grain. In addition to a negative charge from the polar chain, the long side chains physically help hold the cement grains apart, a mechanism referred to as steric hindrance [23,23]. Therefore, PCE s can achieve up to 40% water reduction [21]. Additionally, PCE's have a much lower rate of slump loss.

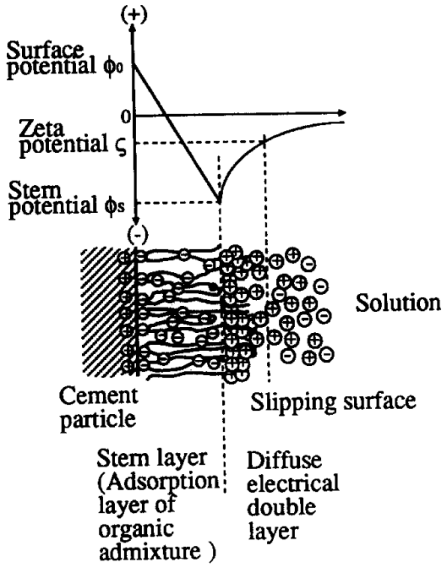

FIG. 2.
Schematic explanation of interfacial electric double layer formed on the cement particle absorbing organic admixture.

Figure 7: This figure from [23] illustrates the steric hindrance mechanism observed by Uchikawa et. al. The ether side chains of the admixture physically separate the particles. Steric hindrance increases the distance between particles and therefore reduces the effect of attractive Van Der Waals forces between cement particles.

There are currently a variety of types of PCE's. The 7 main chemical forms include: MPEG, APEG, VPEG, HPEG, IPEG, PAAM, and Organo-silane modified [25]. It has been shown that the variation between types of admixtures (characterized by side chain length and density) has an effect on fluid properties of the paste, including retardation of hydration [26]. Despite the variation in types of PCE's, many researchers do not present the molecular structure of the admixture used [26].

A great deal of research on PCE's is related to their appropriate dosage in a mixture. Any dispersant's effect on fluidity of a mixture increases linearly with its dosage up to the point of saturation. Critical dosage is defined as the point at which the dosage of admixture begins to increase the fluidity of the mixture. Saturation dosage is defined as the point at which increased dosage of admixture does not increase fluidity of the mixture. Figure 8 shows these dosage points.

Both dosage points relate to the rate of adsorption of polymers onto cement particles and (over time) the amount of polymer remaining in solution [27].

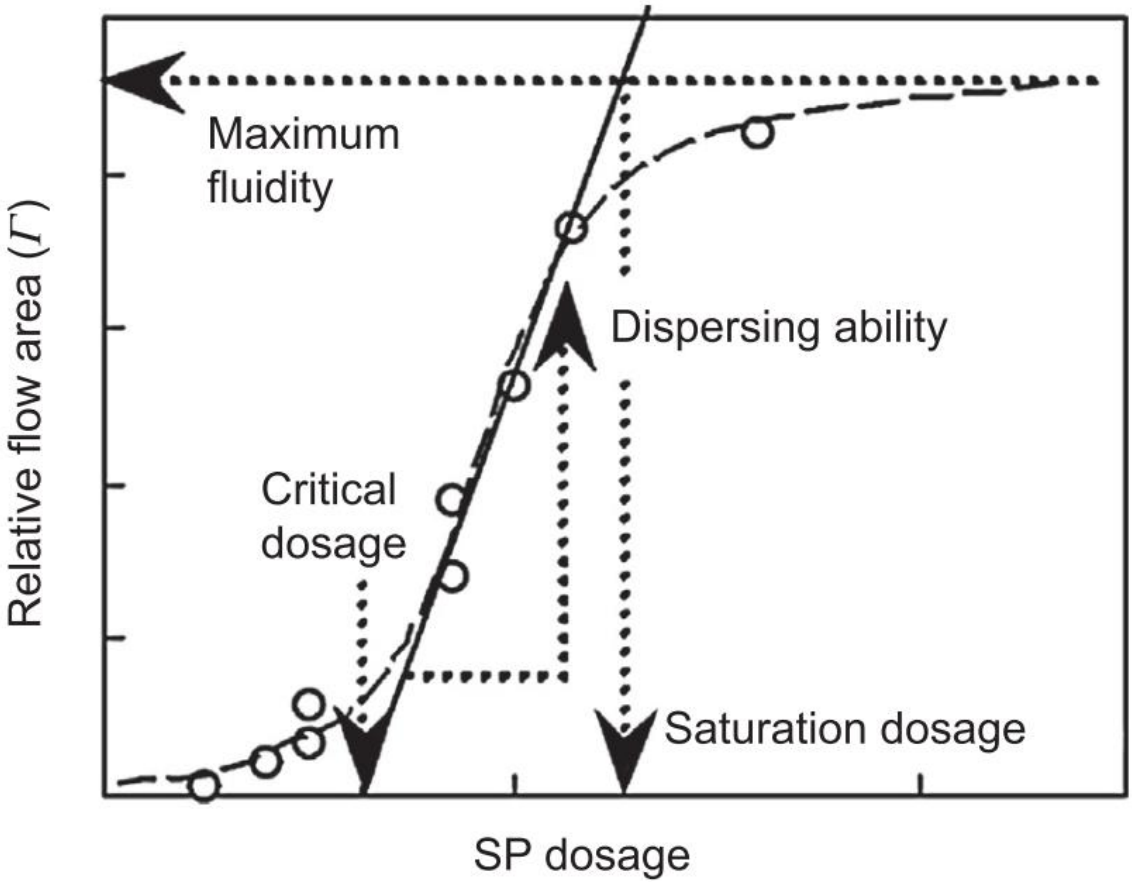

Figure 8: A conceptual plot of the relationship between flow area and admixture dosage showing the points of critical dosage and saturation dosage [27]

Polymers preferentially adsorb onto the aluminate phases of cement. Marchon et. al. theorize that during the hydrolysis and induction periods of hydration, polymers are preferentially adsorbing onto the aluminate phases to the point that aluminates are at full surface coverage, but silicates are not [27]. Polymers in solution could continue adsorbing onto partially covered silicate surfaces over time, contributing to a reduction in slump loss [27].

The Effect of PCE on Autogenous Shrinkage

A survey of literature review for studies on the effect of PCE of autogenous shrinkage focused on the studies presented and summarized in Table 1.

Work on naphthalene and melamine HRWRA's by Holt correlated increased dosages of admixture or any dosage of admixture whatsoever with an increase in autogenous shrinkage [11]. Based on those findings, Holt has recommended limiting admixture dosage to prevent autogenous shrinkage [28]. The theoretical background is intuitive: admixtures increase the degree of hydration of cement and result in the formation of a finer pore structure, as supported by MIP data [29]. The more refined the pore structure, the greater the capillary pressure created during self-desiccation of the paste. However, the results for PCE admixtures summarized in Table 1 find an inverse relationship between PCE HRWA and autogenous shrinkage, unlike the findings for naphthalene and melamine HRWA by Holt [11].

Table 1: A survey of papers evaluating the influence of PCE's on autogenous shrinkage.

Author	Cem Type	W/cm ratios	PCE Dosages	W or D?*	Time-Zero	Methodology	Std. Deviation Presented	FINDING***
Li et. al [30]	I	0.2-0.22	0.4, 0.8, 1.2 % cem wt	W	Final Vicat Set	ASTM 1698	No	A
Mohr and Hood [20]	I/II	0.30-0.45	0.62-4.32 microliters/ g cem	W	Final Vicat Set	ASTM 1698 + rotation of tubes	Yes**	A
Tiburzi [2]	III	0.28-033	5-29 oz/cwt****	D	Final Vicat Set	Buoyancy Test	No	A
Fontana et. al [31]	II	0.26-0.30	0.65-2.0 % cem wt	D	Knee Point	ASTM 1698 + LDVT Apparatus	No	A

**W=workability determined dosage of superplasticizer; D=Dosage specified by researcher arbitrarily for ease of comparison*

***8 tests were completed for every sample*

****Finding A=positive correlation between PCE dosage and autogenous shrinkage and B=an inverse correlation between PCE dosage and autogenous shrinkage*

*****Tiburzi also tested one melamine admixture and found higher autogenous shrinkage in mixtures with the melamine admixture compared with mixtures made with PCEs*

All studies listed in Table 1 on the effect of PCE on autogenous shrinkage found a correlation between increasing dosage of PCE admixture and decreasing autogenous shrinkage. One possible explanation for this is the impact of PCE on surface tension. As shown by, Mora-Ruacho et. al (see Figure 9), PCE admixture had a similar surface tension reducing effect to that of an SRA admixture [32].

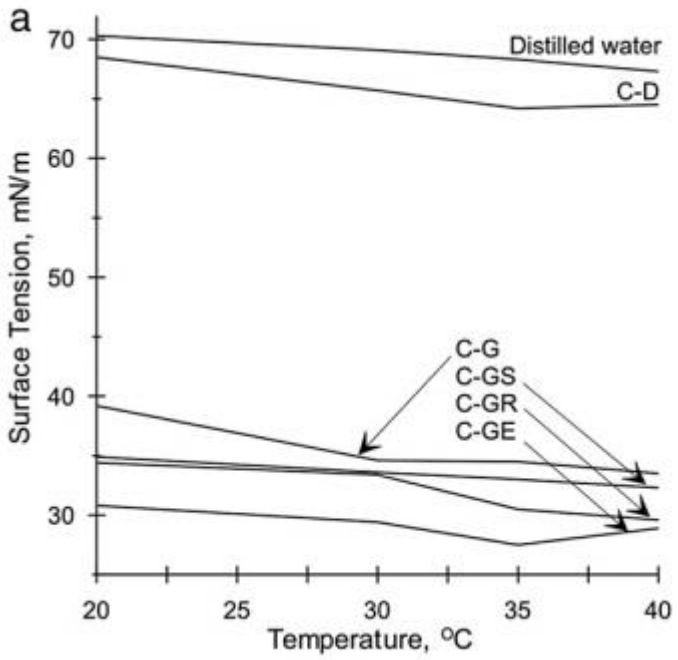

Figure 9: Comparison of the effect of water reducers and shrinkage reducing admixtures on surface tension of water from [32]. G indicates the polycarboxylate admixture tested, while D indicates the melamine admixture tested. S, R, and E are various types of SRA.

III. MATERIALS AND METHODS

MATERIALS

Autogenous deformation measurements and mini slump tests were conducted on the mixes displayed in Table 5. Three tubes were cast for each mix evaluated. All paste mixes were made with a Type III Portland cement (Alamo brand). The Blaine fineness of the cement was measured as 486.3 $m.^2/kg$ [1]. Three different types of polycarboxylate HRWRA were used: Sika 2100, Sika 4100, and BASF 7700. These are called HR-P1, HR-P2, and HR-P3, respectively. A VMA (Sika Stabilizer-4R) and Rockdale Type F fly ash were also incorporated in some mixtures to simulate compositions more similar to that of self-consolidating concrete (SCC) mixtures. The mixture proportions and materials were selected because of their widespread use in the Texas precast industry [1].

Table 2: Oxide Analysis of Alamo III Cement by mass % from [1]

SiO_2	$Al2O_3$	$Fe2O_3$	CaO	MgO	SO_3	Na_2O	K_2O
19.8	4.3	3.1	61.1	0.6	4.1	0.1	0.7

Bogue composition: 64.9% C3S, 7.9%C2S, 6.2% C3A, and 9.4% C4AF

Table 3: Oxide Analysis of Class F Fly Ash from [1]

SiO_2	$Al2O_3$	$Fe2O_3$	CaO	MgO	SO_3	Na_2O	K_2O
52.1	23.1	3.95	11.7	2.1	0.5	0.4	0.74

Table 4: Admixture Manufacturer Data

Manufacturer Name	Code Name	Admixture Type	Specific Gravity	% Solids	Recommended Dosage (fl.oz./cwt)
Sika Viscocrete 2100	HR-P1	HRWRA	1.08	40	1-12
Sika Viscocrete 4100	HR-P2	HRWRA	1.08	40	3-12
MasterGlenium 7700*	HR-P3	HRWRA	1.06	34	2-15

Sika Stabilizer-4R	VMA-1	VMA	1.01	40	0-7

Also referred to as BASF 7700

Table 5: Cement Paste Test Matrix

Series ID	Mix No.	HRWRA	HRWRA Dosage (oz/cwt)	VMA Dosage (oz/cwt)	Cement Content (g)	Fly Ash Content (g)	Water Content (g)
Series 1: Influence of Admixture Dosage- 0.28 w/cm	1	SIKA 2100	6.5	0.0	800	0	224
	2	SIKA 2100	8.25	0.0	800	0	224
	3	SIKA 2100	12	0.0	800	0	224
	4	SIKA 4100	6.5	0.0	800	0	224
	5	SIKA 4100	8.25	0.0	800	0	224
	6	SIKA 4100	12	0.0	800	0	224
	7	BASF 7700	6.5	0.0	800	0	224
	8	BASF 7700	8.25	0.0	800	0	224
	9	BASF 7700	12	0.0	800	0	224
Series 2: Influence of Admixture Dosage- 0.31 w/cm	10	SIKA 2100	6.5	0.0	761.87	0	236.2
	11	SIKA 2100	8.25	0.0	761.87	0	236.2
	12	SIKA 2100	12	0.0	761.87	0	236.2
	13	SIKA 4100	6.5	0.0	761.87	0	236.2
	14	SIKA 4100	8.25	0.0	761.87	0	236.2
	15	SIKA 4100	12	0.0	761.87	0	236.2
	16	BASF 7700	6.5	0.0	761.87	0	236.2
	17	BASF 7700	8.25	0.0	761.87	0	236.2
	18	BASF 7700	12	0.0	761.87	0	236.2
Series 3: Influence of Admixture Dosage- 0.33 w/cm	19	SIKA 2100	6.5	0.0	738.41	0	243.7
	20	SIKA 2100	8.25	0.0	738.41	0	243.7
	21	SIKA 2100	12	0.0	738.41	0	243.7
	22	SIKA 4100	6.5	0.0	738.41	0	243.7
	23	SIKA 4100	8.25	0.0	738.41	0	243.7
	24	SIKA 4100	12	0.0	738.41	0	243.7
	25	BASF 7700	6.5	0.0	738.41	0	243.7
	26	BASF 7700	8.25	0.0	738.41	0	243.7
	27	BASF 7700	12	0.0	738.41	0	243.7
Series 4: Influence of 28% Fly Ash Replacement by Mass @ 0.28 and 0.31 w/cm	28	SIKA 2100	8.25	0.0	800	200	280
	29	SIKA 2100	8.25	0.0	800	200	310
Series 5: Typical SCC mixtures (VMA & 28% Fly Ash Replacement by Mass)	31	SIKA 2100	6.5	2.75	800	326	315.3
	32	BASF 7700	8.25	2.75	800	326	315.3

PASTE MIXING PROCEDURE

The cement was sieved through a #20 sieve. De-aired water at room temperature was used. The ingredients were measured out and the admixture was shaken and then premixed into the water. The sequence of mixing consisted of:

1. Place water in Hobart mixer, then place cement in mixer. Record time of w/cm.
2. Mix on low for 30 seconds. Mix on high for 30 seconds. Let rest for 1 minute and 30 seconds. Use the spatula to scrape portions outside of the reach of the mixer during this period. Mix on high for 1 minute.

At that point, the autogenous shrinkage procedure was started.

There was one major difference in the mixing procedure for the 0.31 w/cm series mixes: these experiments were conducted earlier than the other mixes. The admixture bottle was not shaken before admixture was extracted from it. This potentially had a significant impact on the results as is discussed in Part IV.

AUTOGENOUS SHRINKAGE MEASUREMENTS

The procedure consisted of filling the tubes over a vibrating stand as shown in Figure 13 and placing the tubes in the apparatus. For a more detailed procedure, refer to Appendix C. Two modifications were made to the ASTM C1698 standard to reduce friction error and to reduce error due to temperature changes:

- the tubes were immersed in a mineral oil bath at 23°C until 72-hour measurement, and
- measurements of shrinkage were automated through the use of noncontact linear variable differential transformers (LVDT)

The apparatus used for this testing is shown in Figure 10. At one end of the corrugated tube a metal cap was attached with zip ties. This end of the tube was rigidly attached to an end of the steel

apparatus. The other end used the typical plastic caps sold by Germann Instruments. A ferromagnetic plate was epoxied to the plastic end. For more information on how the autogenous shrinkage apparatus was constructed, refer to [1].

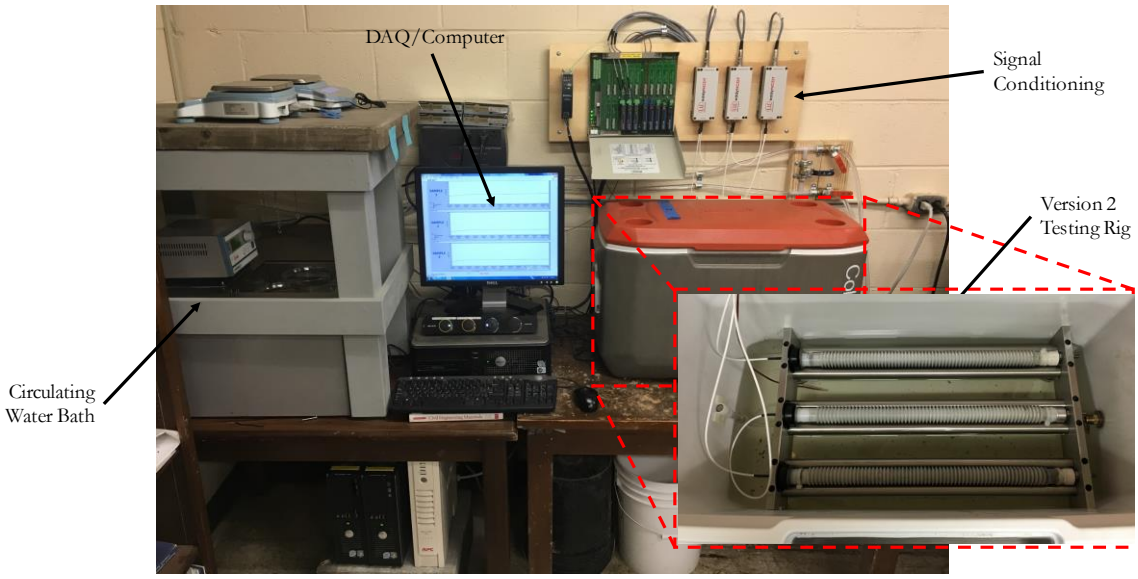

Figure 10: Autogenous shrinkage measurement apparatus [1]

Figure 11: Steel cap end which was tightened until the bolts were finger tight with a wrench, thus creating a fixed end of the tube [1]

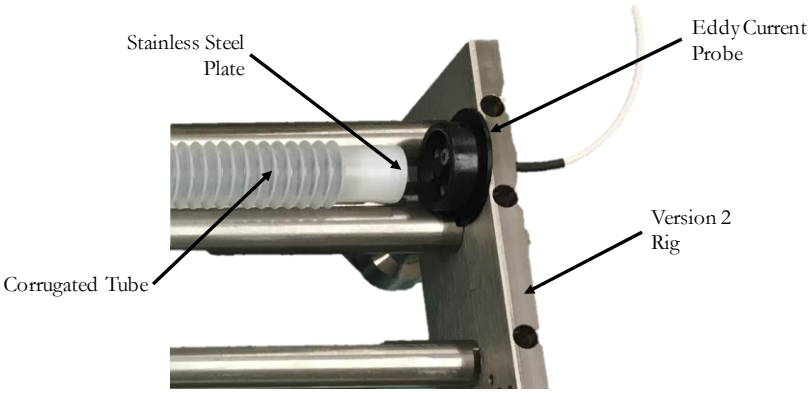

Figure 12: Plastic cap end of corrugated tube with steel plate that is free to shrink [1]

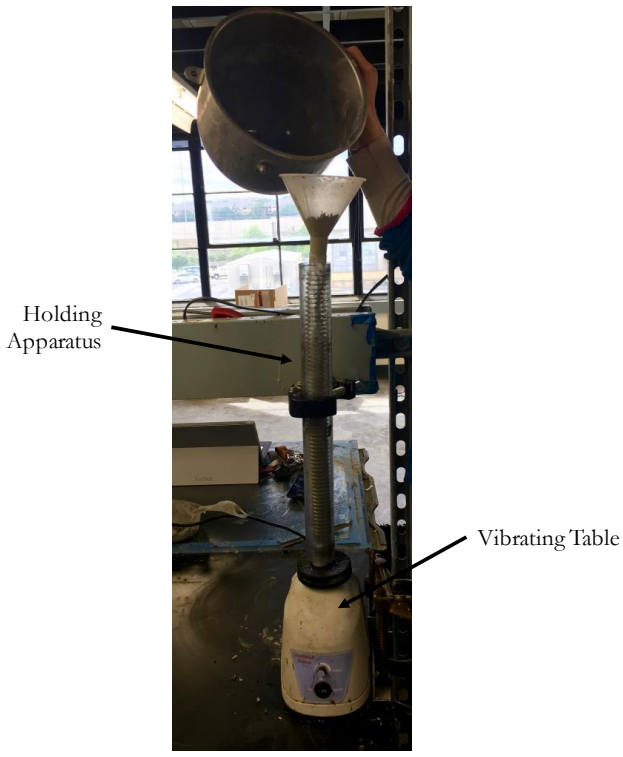

Figure 13: Photo of pouring the cement paste into corrugated tube as it is vibrated continuously from [1]

MINI SLUMP TEST

To evaluate cement paste workability a procedure based off of the ASTM working standard WK27311 was followed. A mini-slump apparatus (see schematic in Figure 14) was placed on a a plastic plate that was on top of a flat firm surface. Then a funnel or metal spoon was used to place the paste in to the mini slump apparatus, tamping and wiping the top of with a spatula to ensure the apparatus was entirely filled. Finally, the mini-slump apparatus was lifted up vertically. The paste was allowed to continue to spread as the corrugated tubes were filled for the autogenous shrinkage testing. As the mini slump test was conducted in tandem with the

corrugated tube test, the mini-slump was not consistently measured at a specific point, but rather at 10-20 after the water to cement contact time. At approximately 10 minutes, the slump flow area diameter was measured using a caliper. Appendix B contains a procedure sheet for more detailed information on the procedures of paste mixing, tube filling and placing, and slump flow testing.

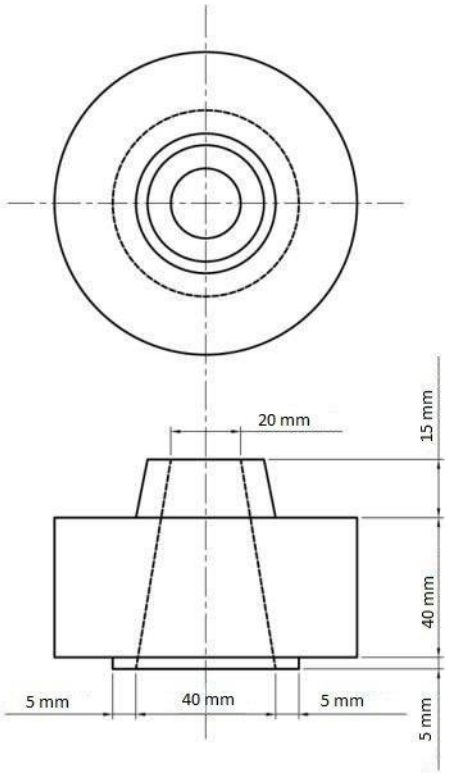

Figure 14: Schematic diagram of mini-slump apparatus used from [33]

IV. RESULTS AND DISCUSSION

The following sections present the results for autogenous shrinkage testing of the cement pastes samples. Part IV is organized into 4 parts discussing the observed effects of the following mixture parameters on autogenous shrinkage: 1.) Influence of HRWRA dosage, 2.) Influence of w/cm ratio, 3.) Influence of Admixture Type, and 4.) Influence of Fly Ash Replacement and VMA addition. The results are presented with shrinkage on the positive axis and expansion on the negative axis. Due to the high resolution of the testing (1 measurements taken per second), the time-zero was taken as the time at the peak of shrinkage prior to the period of expansion previously described as the bleed bump. The initiation of the bleed bump (where well-defined bleed bumps occurred) was chosen for ease of analysis and to reduce the effect to which bleeding could affect the results. The measurements shown here are the average of data from 3 different tube tests of the same mixture which was smoothed using *rlowess* in Matlab (code shown in Appendix A). Several tests had clearly flawed data which was removed from consideration. In these cases, a representative sample was selected. For example, Figure 15 shows the 3 data sets for Mix 8. Clearly, the ferromagnetic plate fell over or shifted in Samples A and C (this was not uncommon during testing). Therefore, only data from Sample B is presented.

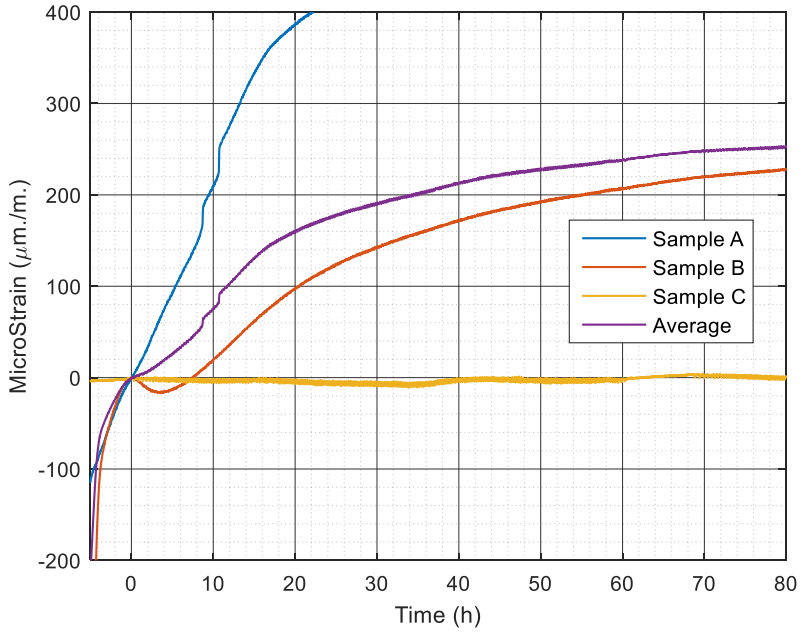

Figure 15: Paste Mix 8 corrugated tube measurements for each sample and the average results from the samples

Data resulting from solely one test is noted in Table 2 along with a 24-hour standard deviation and the maximum standard deviation over the period measured. Plots of the full standard deviations for each paste mixture are contained in Appendix C. Gao's record of an average standard deviation of 10 μm/m after set is a good benchmark to interpret the reliability of the data shown in Table 6 and Appendix C [19]. However, Gao only monitored the paste for 24 hours total, not 24 hours beyond final set. Additionally, Gao worked with a much coarser cement than the cement used in this research. (Note, the Blaine fineness of the cement used in Gao's work was 367 m^2/kg versus 486.3 $m.^2$/kg for the cement used in this work). Perhaps the fineness of the Type III cement and the duration of the measurements account for the larger standard deviations observed in the autogenous shrinkage testing of these pastes. Entrapped air was often

observed during the mixing procedure despite consistent vibration and could also account for the above expected standard deviations observed.

Table 6: Standard Deviation of Autogenous Shrinkage Data

Series ID	Mix No.	HRWRA	HRWRA Dosage (oz/cwt)	24 Hr Std Deviation (μm/m.)	Max Std Deviation over Period Measured (μm/m.)	Duration of Measurement beyond Time-Zero (h)
Series 1: Influence of Admixture Dosage- 0.28 w/cm	1	HR-P1	6.5	64	172	92
	2	HR-P1	8.25	24	82	68
	3	HR-P1	12	10	23	80
	4	HR-P2	6.5	2	64	80
	5	HR-P2	8.25	13	78	80
	6	HR-P2	12	32	72	77
	7	HR-P3	6.5	18	22	65
	8*	HR-P3	8.25	N/A	N/A	80
	9*	HR-P3	12	N/A	N/A	80
Series 2: Influence of Admixture Dosage- 0.31 w/cm	10*	HR-P1	6.5	N/A	N/A	60
	11	HR-P1	8.25	60	70	80
	12	HR-P1	12	38	50	50
	13	HR-P2	6.5	65	80	55
	14*	HR-P2	8.25	N/A	N/A	82
	15	HR-P2	12	20	20	68
	16	HR-P3	6.5	25	60	45
	17	HR-P3	8.25	25	78	62
	18	HR-P3	12	25	50	38
Series 3: Influence of Admixture Dosage- 0.33 w/cm	19	HR-P1	6.5	58	80	68
	20	HR-P1	8.25	19	58	65
	21*	HR-P1	12	75	88	62
	22	HR-P2	6.5	25	39	77
	23	HR-P2	8.25	53	73	76
	24	HR-P2	12	28	70	64
	25*	HR-P3	6.5	30	70	57
	26	HR-P3	8.25	50	97	80
	27	HR-P3	12	5	10	62
Series 4: Influence of 28% Fly Ash Replacement @ 0.28, 0.31, and 0.33 w/cm	28	HR-P1	8.25	20	75	80
	29*	HR-P1	8.25	N/A	N/A	100
	32	HR-P3	8.25	35	58	80

**single representative sample is shown on result plots presented for comparison*

1. Influence of HRWRA dosage on Autogenous Shrinkage Results

Series 1: 0.28 w/cm pastes

Figures 16-18 show the effect of HRWRA dosage and type on autogenous shrinkage for pastes made with the lowest w/cm ratio explored in this research (w/cm=0.28). In Figure 16, the addition of admixture beyond the dosage of 8.25 oz/cwt correlates with a reduction in autogenous shrinkage. The difference in autogenous shrinkage between pastes made with a PCE dosage of 6.5 oz/cwt vs. 8.25 oz/cwt appears to be minimal. Another interesting trend in the data is the change in the shape of the curve at time-zero with addition of admixture. A period of expansion only occurs in the 8.25 oz/cwt and 12 oz/cwt dosage pastes. The pronunciation of the curvature of the bleed bump appears to increase with addition of Sika 2100, matching similar observations by Mohr and Hood that increase in dosage of HRWRA correlates with an increase in expansion due to bleed water reabsorption [20]. In Figure 17, the addition of the admixture for all dosages correlates with a reduction in autogenous shrinkage. The difference between the results for the 6.5 and 8.25 oz/cwt dosage pastes are very small, on the order of approximately 10 μm/m at 70 and 80 hours after time-zero, whereas the 12 oz/cwt dosage mixture shrinkage was about 40 μm/m lower at 70 and 80 hours after time-zero. A bleed bump is only visible for the 12 oz/cwt dosage mixture. In Figure 18, the addition of the BASF HRWRA correlates with a reduction in autogenous shrinkage at all dosages, to a larger degree than for the Sika 2100 or Sika 4100 admixtures pastes. All mixtures in Figure 19 have a pronounced bleed bump, and the expansion of the bleed bump correlates with the dosage of admixture. An increase in the bleed bump expansion with increased dosage was observed for the BASF 7700 type series and the Sika 2100 series at 0.28 w/cm. However, the Sika 4100 series does not show a significant bleed bump,

except at the largest dosage of HRWRA. Figures 16-18 all show that at the highest dosage of HRWRA, the lowest autogenous shrinkage occurs.

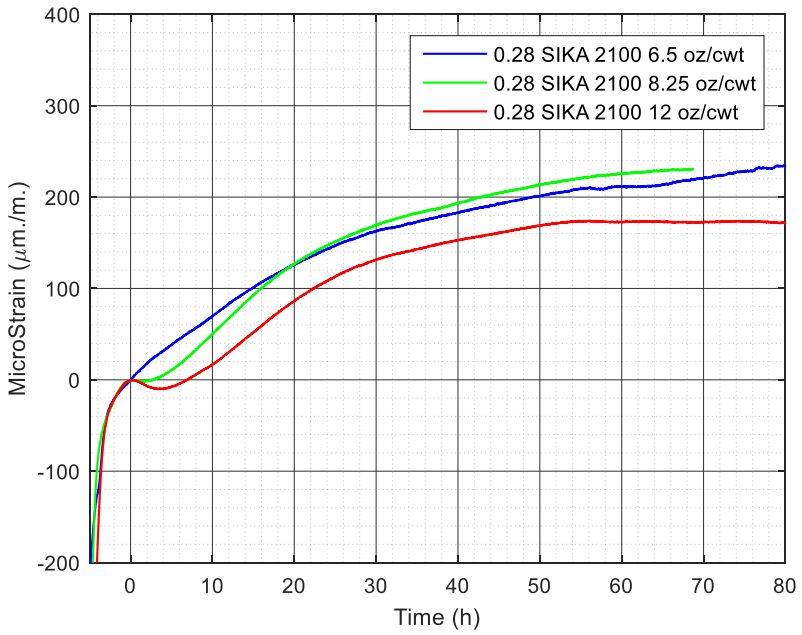

Figure 16: The effect of SIKA 2100 admixture dosage on the autogenous shrinkage of a 0.28 w/cm paste

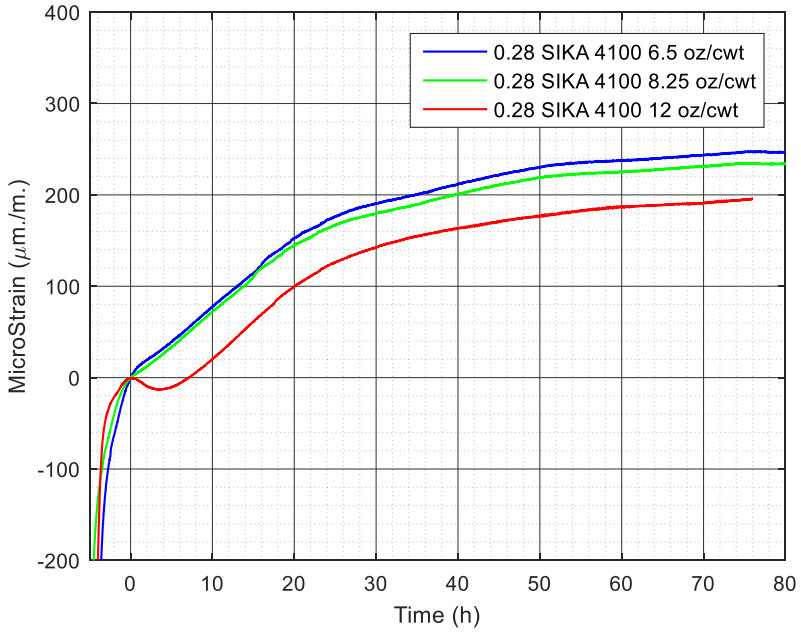

Figure 17: The effect of SIKA 4100 admixture dosage on the autogenous shrinkage of a 0.28 w/cm paste

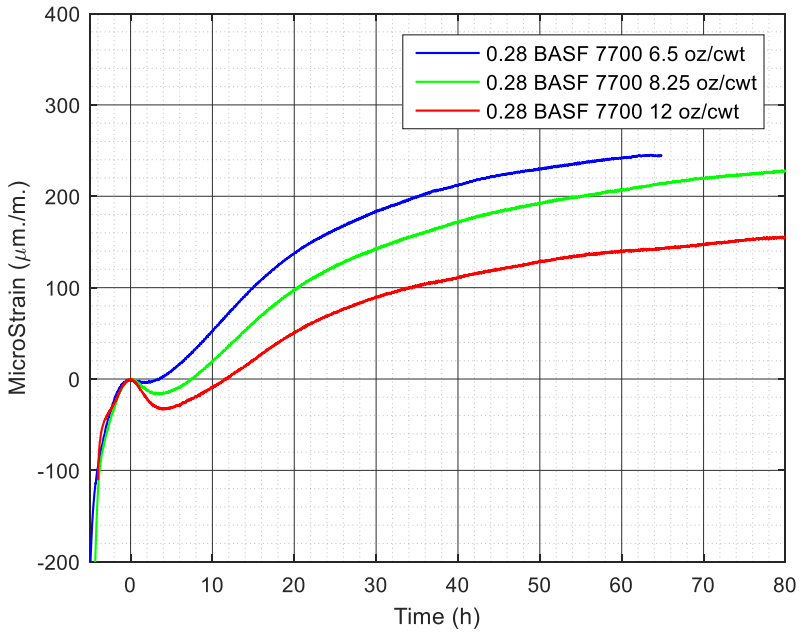

Figure 18: The effect of BASF 7700 admixture dosage on the autogenous shrinkage of a 0.28 w/cm paste

Figure 19 shows the mini-slump data for the same paste mixtures tested in Figures 16-18. This data provides insight to the fluidity of the mixture as well as to the degree of dosage for the mixture. The results in Figure 19 suggest that Sika 2100 transitioned through a critical dosage point at a dosage between 8.25 oz/cwt and 12 oz/cwt due to the significant increase in slump diameter at 12 oz/cwt. At 12 oz/cwt, beyond the critical dosage point, the autogenous shrinkage of the Sika 2100 mixture does reduce. However, the same result is observed for the Sika 4100 pastes which show fairly linear fluidity trends during the dosage range explored in this work so no correlation between the mini slump data and the autogenous shrinkage data is observed.

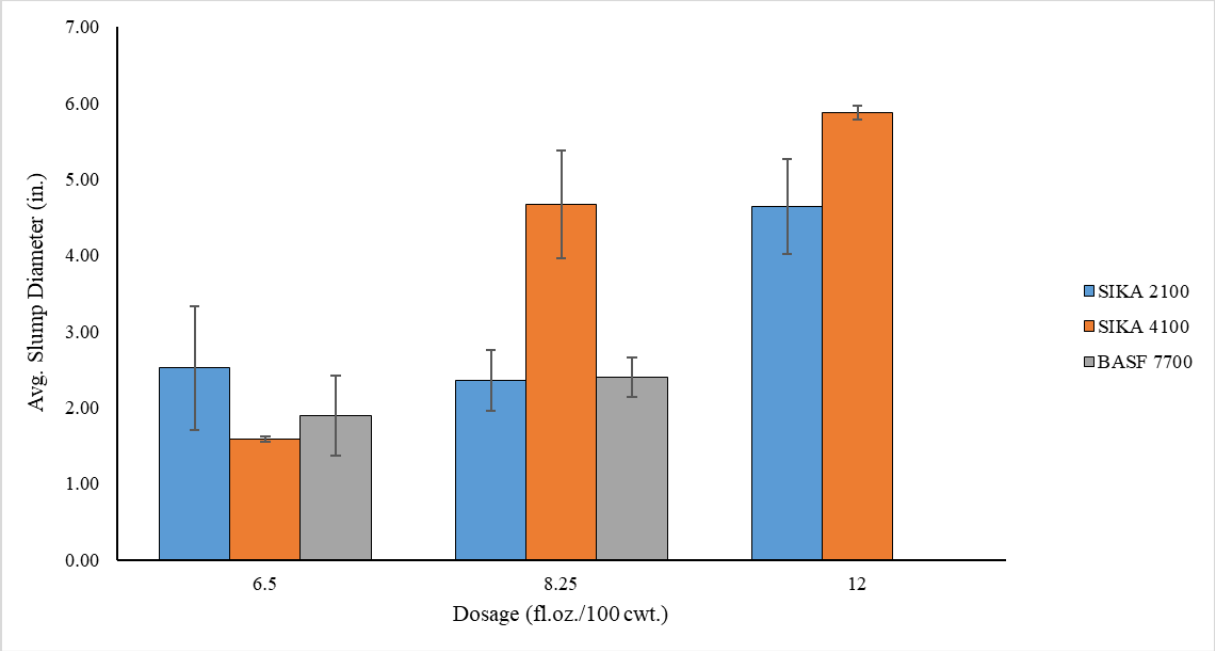

Figure 19: Comparison of fluidity of mixture with dosage of admixture

Series 2: 0.31 w/cm ratio pastes

Figures 20-22 show the effect of HRWRA dosage and type on autogenous shrinkage for pastes made at w/cm = 0.31. As noted in the materials and methods section, these pastes were made with HRWRA that was not agitated before the mixing procedure, unlike the 0.28 w/cm and 0.33 w/cm series pastes. Figure 20 shows an inverse relationship between autogenous shrinkage and

admixture dosage at every dosage when SIKA 2100 is used. Whereas, when SIKA 4100 is used (see Figure 21), similar shrinkage results for 6.5 oz/cwt and 12 oz/cwt occurred. There appears to be two unique periods of expansion in the 12 oz/cwt mixture in Figure 21, which is unique among the 0.28 w/cm and 0.31 w/cm and unusual in literature. This is interesting because double bleed bumps or multiple periods of bleed water absorption are not usually observed in autogenous shrinkage data in the literature; the observance of the double bleed bumps in this work may be due to the high resolution of the data or the fineness of the cement. The 6.5 oz/cwt mix shows a distinct bleed bump that is mirrored in the 8.25 oz/cwt dosage paste results. While there is only very early-age data provided for the BASF HRWRA, Figure 22 shows that as the dosage of HRWRA increased, autogenous shrinkage decreased. Figures 20-22 do not show any clear trend between admixture dosage and autogenous shrinkage.

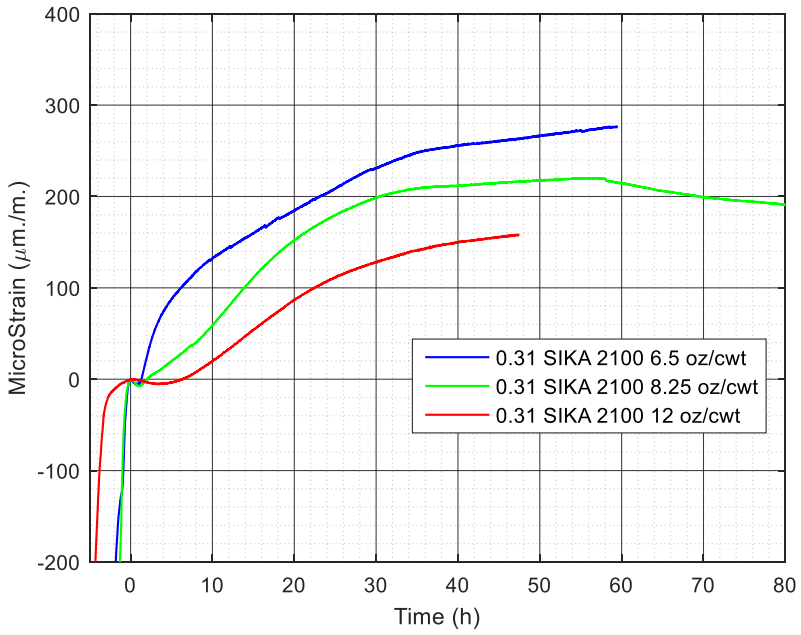

Figure 20: The effect of SIKA 2100 admixture dosage on the autogenous shrinkage of a 0.31 w/cm paste

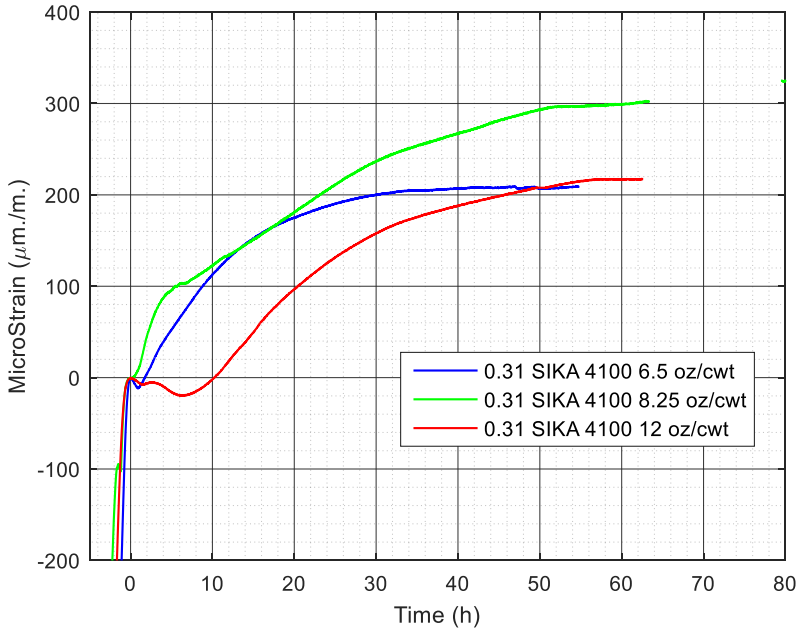

Figure 21: The effect of SIKA 4100 admixture dosage on the autogenous shrinkage of a 0.31 w/cm paste

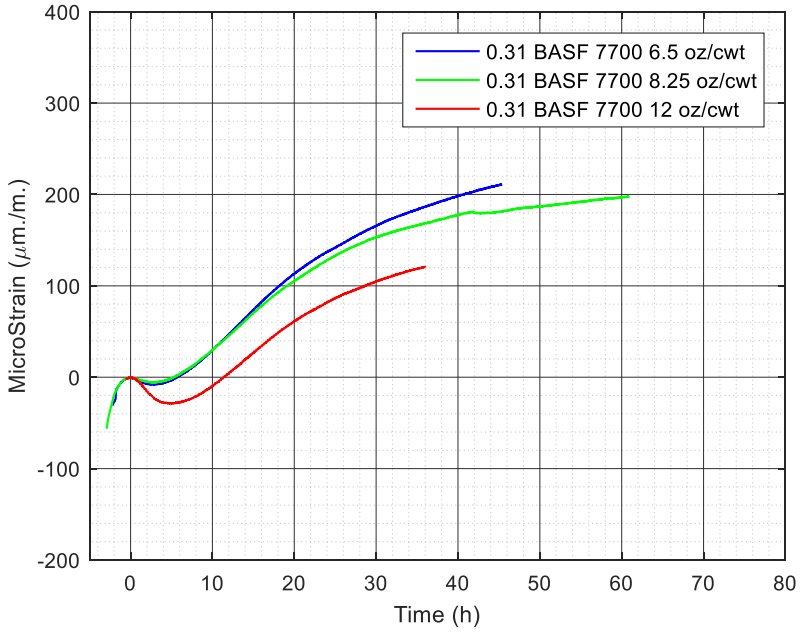

Figure 22: The effect of BASF 7700 admixture dosage on the autogenous shrinkage of a 0.31 w/cm paste

Figure 23 shows the mini-slump data for the mixtures discussed in Figures 20-22. Figure 23 suggests that BASF 7700 transitioned through a critical dosage point at a dosage between 8.25 oz/cwt and 12 oz/cwt due to the significant increase in slump diameter at 12 oz/cwt. Sika 2100 and Sika 4100 both show a linear increase in slump diameter with increase in PCE dosage, and thus it is not clear if the critical dosage point was achieved yet for those mixtures. This can be due to the differences in HRWRA chemistry and structure since the BASF 7700 HRWRA was made by a different manufacturer than the other two admixtures. Interestingly, the BASF 7700 admixture paste is the only paste in this series that does show a clear decrease in autogenous shrinkage at the dosage rate of 12 oz/cwt, which suggests that beyond the critical dosage point increases HRWRA reduces autogenous shrinkage. Further research should be conducted with a wider series of admixtures to validate this hypothesis.

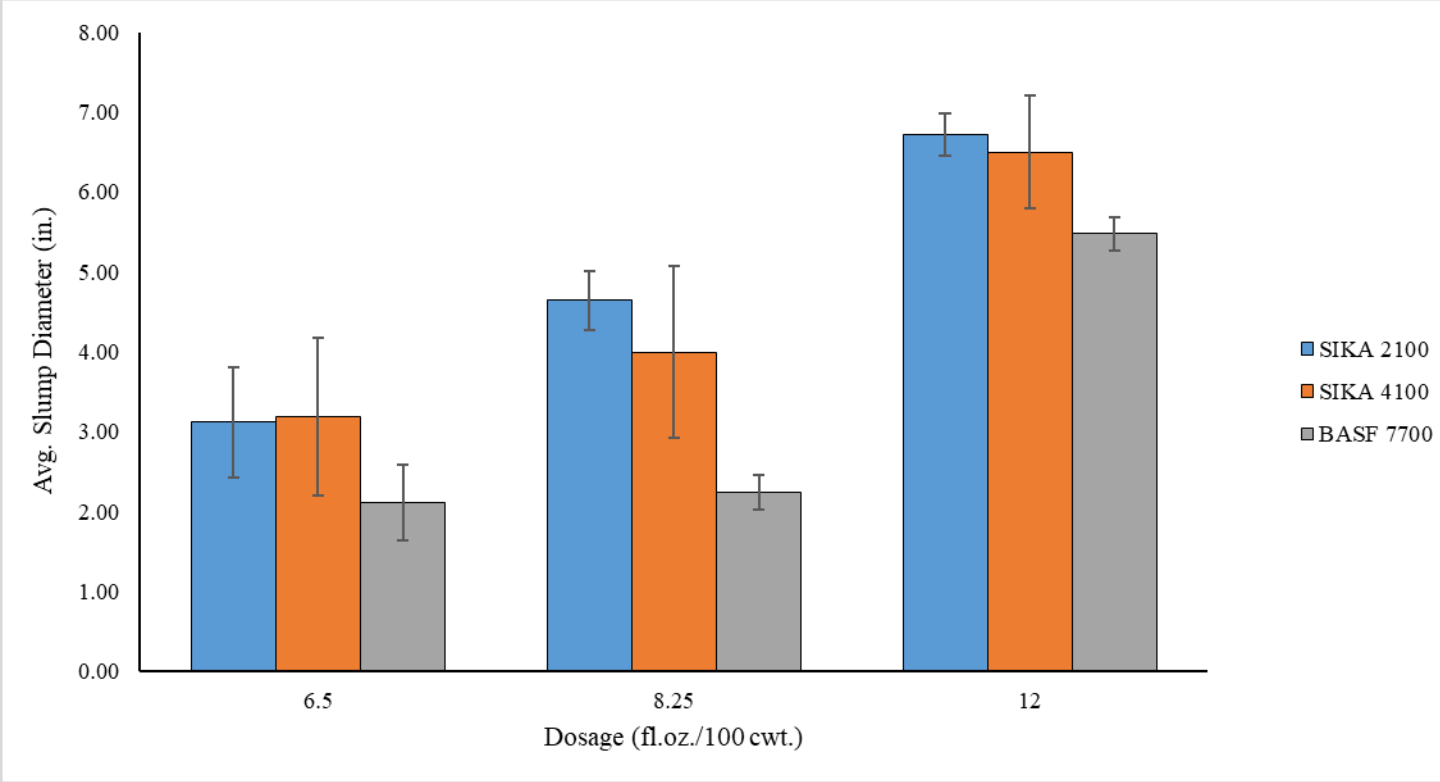

Figure 23: Comparison of fluidity of mixture with dosage of admixture

Series 3: 0.33 w/cm ratio pastes

Figures 24-26 show the effect of HRWRA dosage and type on autogenous shrinkage for pastes made using the highest w/cm ratio explored in this work (w/cm=0.33). Figure 24 shows overlapping shrinkage values at all dosages for pastes prepared using SIKA 2100. The bleed bump behavior is unusual as 2 periods of expansion are observed as in Figure 18. As was discussed in Series 2, multiple bleed bumps are not usually present in other researcher's autogenous shrinkage data. It is possible that the resolution of the data (one measurement was recorded for each second in this study) enabled this observation. It may also be unique to the materials used in this study. Figure 25 shows that when SIKA 4100 is used, an inverse correlation between increasing dosage and decreasing shrinkage occurs. However, it also highlights the importance of when time-zero is selected. If the second bleed bump of the 12 oz/cwt dosage mix in Figure 25 was selected as its time-zero, conclusions would be changed. Two periods of expansion or a double bleed bump are shown in the 8.25 and 12 oz/cwt mixtures, but not in the 6.5 oz/cwt mixture. Figure 26 shows a correlation between increasing dosage of PCE and reduction of autogenous shrinkage at all dosages. As was observed for the 0.28 w/cm data series, this reduction becomes more significant beyond the 8.25 oz/cwt dosage.

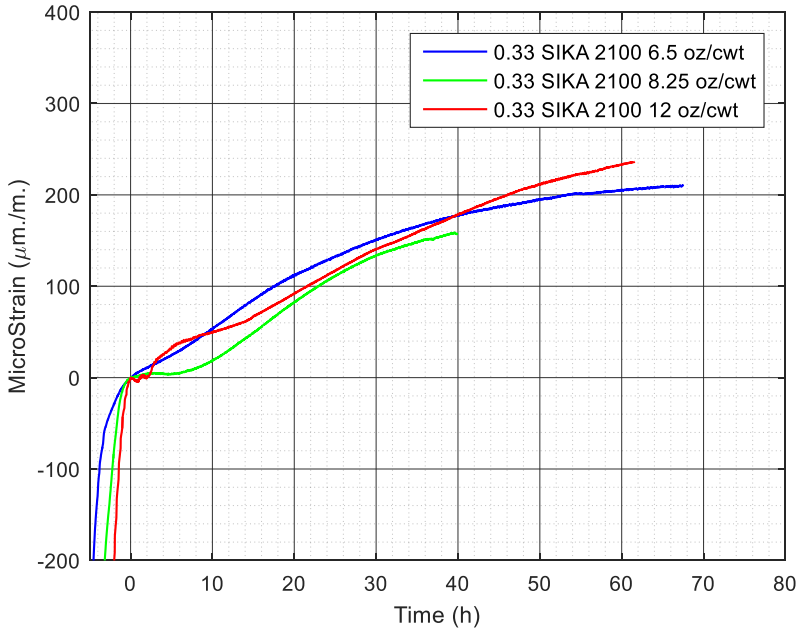

Figure 24: The effect of Sika 2100 admixture dosage on the autogenous shrinkage of a 0.33 w/cm paste

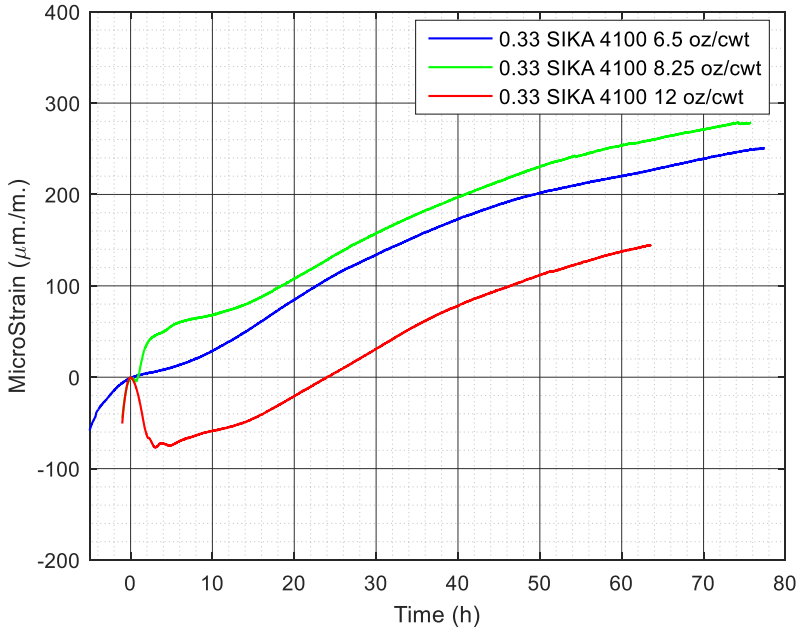

Figure 25: The effect of Sika 4100 admixture dosage on the autogenous shrinkage of a 0.33 w/cm paste

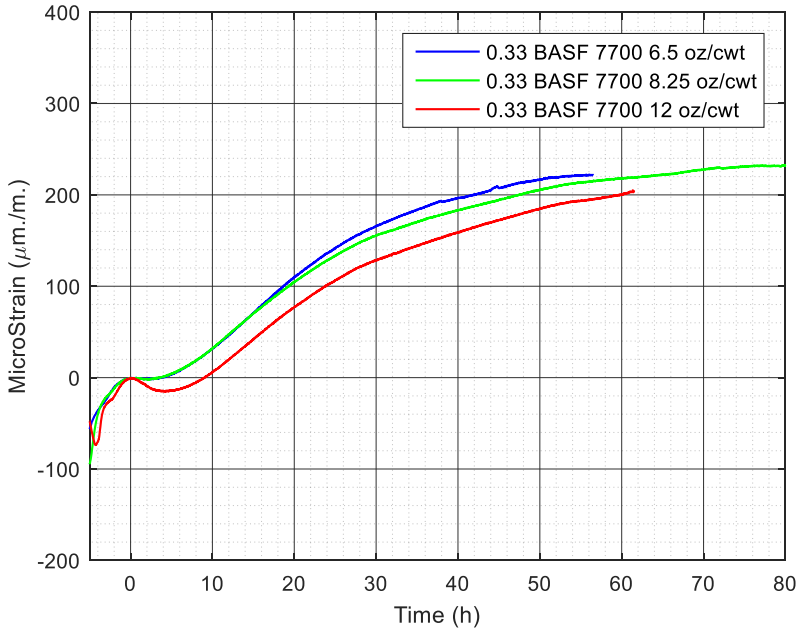

Figure 26: The effect of BASF 7700 admixture dosage on the autogenous shrinkage of a 0.33 w/cm paste

Summary of Influence of HRWRA Dosage on Autogenous Shrinkage

Results show that for 75% of cases presented in Figures 16-18, 20-22, and 24-26, the addition of admixture beyond 8.25 oz./cwt resulted in a decrease in autogenous shrinkage. The majority of the mixtures for which the trend did not hold were at a w/cm ratio of 0.31. These mixtures were made at the beginning of the project, before agitating of the PCE was included in the mixing procedures as was discussed in Part III. It is possible that the observed trend of decreasing autogenous shrinkage with increasing dosage of PCE is merely an artifact of making time-zero at the initiation of expansion in the mixture. However, the results correspond with four other studies discussed in Part II [2, 30, 31, 20]. All four studies documented a decrease in autogenous shrinkage with increasing dosage of polycarboxylate admixture. The repeatability of this finding is significant, as it has been recommended to limit the addition of superplasticizer because of concerns that superplasticizer causes an increase in autogenous shrinkage [28]. Previous findings

based on shrinkage and naphthalene and melamine superplasticizers should be re-examined for PCE's. None of the other studies found a threshold dosage for this reduction, which was observed in this study. Slump flow data included in this section offered little insight or correlation with the threshold dosage in terms of a critical dosage or saturation dosage indicating the threshold dosage being overcome.

2. Influence of W:CM on Autogenous Shrinkage Results

Admixture 1: Sika 2100 Series Results

Figures 27-29 show the effect of w/cm on autogenous shrinkage for pastes made using Sika 2100 admixture. Figure 27 shows that when the lowest admixture dosage was used for SIKA 2100, the 0.28 w/cm paste and 0.33 w/cm ratio paste have similar autogenous deformation, whereas the 0.31 w/cm ratio displays the largest amount of autogenous shrinkage by a significant margin. This can be explained by the unique mixing procedure for the 0.31 w/cm ratio series. Figure 28 shows that at the moderate admixture dosage level, 8.25 oz/cwt, the 0.33 w/cm ratio paste did have the lowest autogenous deformation by a large margin beyond the 0.28 and 0.31 w/cm ratio pastes. The autogenous deformation results for 0.28 and 0.31 w/cm mixtures overlapped at approximately 50 hours after time zero, beyond which the 0.28 w/cm ratio mix experienced a marginally greater amount of autogenous deformation. Figure 29 shows that at the highest admixture dosage for SIKA 2100, 12 oz/cwt, the 0.33 w/cm ratio paste experienced the largest amount of autogenous deformation by a large margin beyond the 0.28 and 0.31 w/cm ratio paste. The 0.28 and 0.31 w/cm ratio pastes overlapped very closely. Figures 27-29 do not show a consistent relationship between w/cm and autogenous shrinkage, even when disregarding the 0.31 w/cm series.

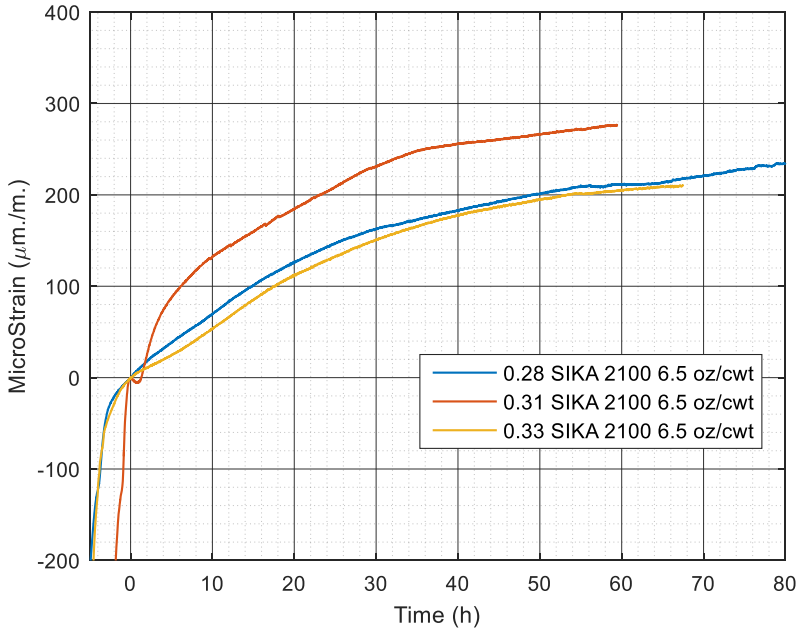

Figure 27: Effect of w/cm on Mixture with Sika 2100 admixture at 6.5 oz/cwt

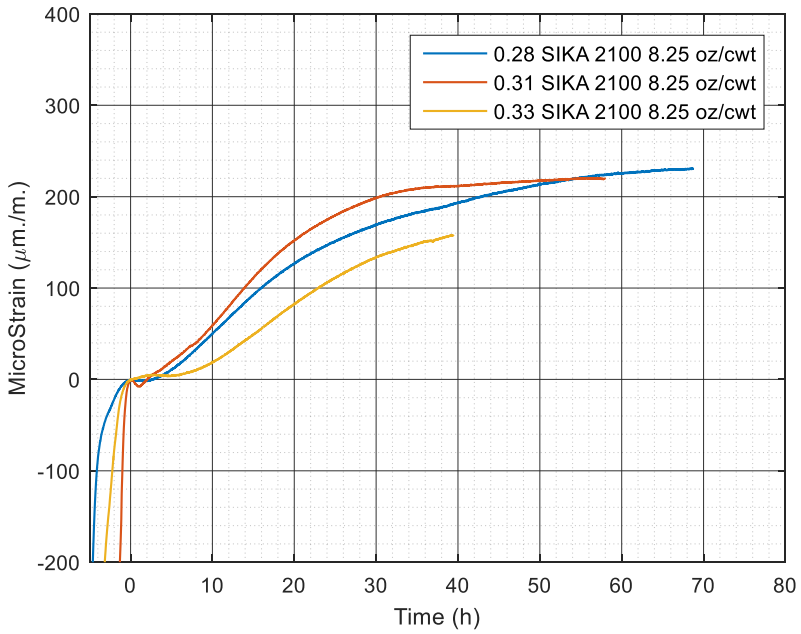

Figure 28: Effect of w/cm on mixture with Sika 2100 admixture at 8.25 oz/cwt

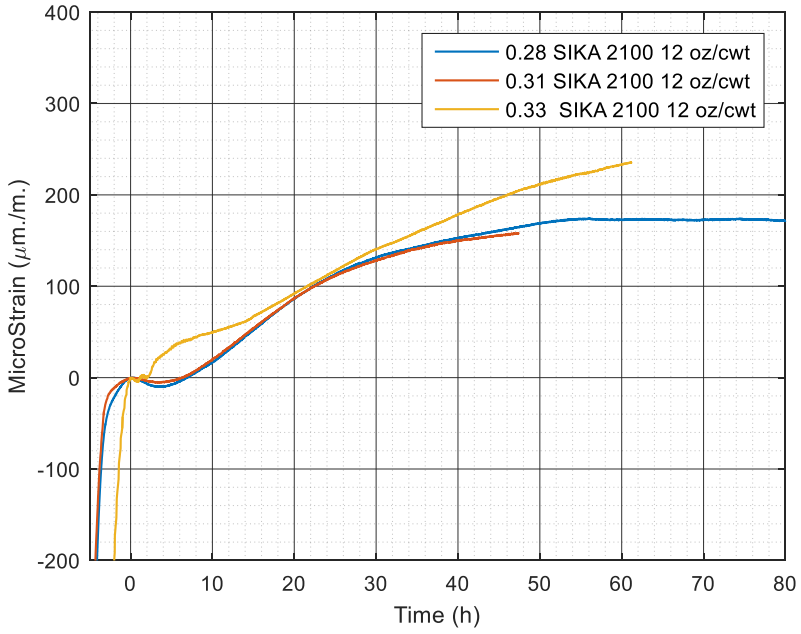

Figure 29: Effect of w/cm on Mixture with Sika 2100 admixture at 12 oz/cwt

Admixture 2: Sika 4100 Results

Figures 30-32 show the effect of w/cm on autogenous shrinkage for pastes made using Sika 4100 admixture. Figure 30 shows that when the lowest dosage was used, the 0.31 w/cm ratio paste experienced the largest rate of autogenous deformation change initially. At approximately 35 hours after time-zero, however, both the 0.28 and 0.31 w/cm ratio pastes show similar amounts of autogenous shrinakge. However the 0.31 w/cm ratio paste's autogenou shrinkage does not significantly change after the 35 hour time point, whereas the 0.28 w/cm ratio mix's autogenous shrinkage continues to increase. The 0.33 w/cm ratio paste shows a lower rate of initial autogenous shrinkage during the first 35 hours, but maintains its shrinkage rate beyond the 70 hour point. At the 70 hours point, the 0.33 w/cm ratio paste shrinks the most, which is the opposite of what is expected. Figure 31 shows that at the moderate admixture dosage range, the 0.33 w/cm ratio paste experienced the lowest amount of autogenous deformation overall by a significant margin while the 0.28 w/cm and 0.31 w/cm ratio mixes' autogenous shrinkage values overlapped at approximately 50 hours beyond time-zero. Beyond the 50 hour point, the 0.28 w/cm ratio

shrinkage continued increasing, while the 0.31 w/cm ratio mix's shrinkage rate of increase is almost zero. Figure 32 shows that at the highest admixture dosage level, the 0.31 and 0.33 w/cm ratio mixes' autogenous shrinkage overlapped over the course of the measurement period. At 50 hours beyond time-zero, both mixtures autogenous shrinkage rate slows significantly. The 0.33 w/cm ratio mix exhibits very different behavior, shrinking at an almost linear rate from the 15 hour point to the end of the recorded data.

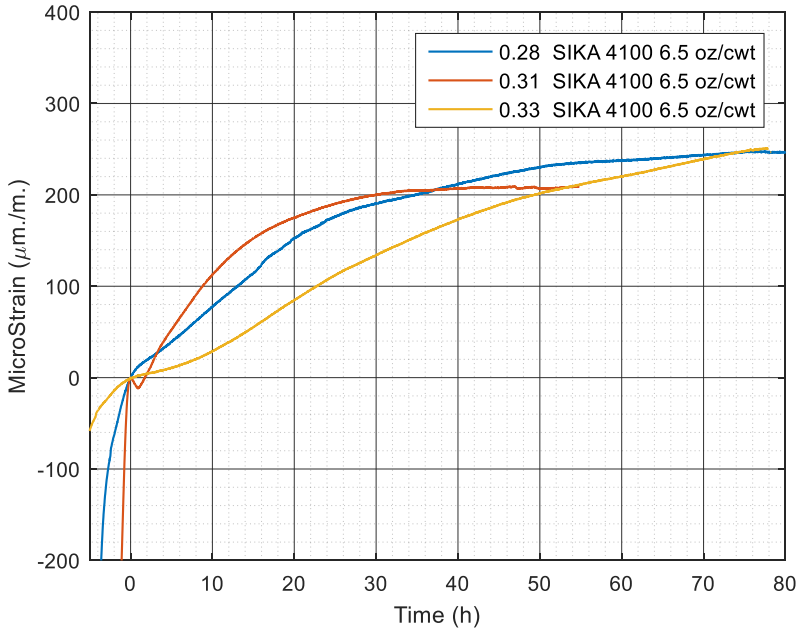

Figure 30: Effect of w/cm on mixture with Sika 4100 admixture at 6.5 oz/cwt

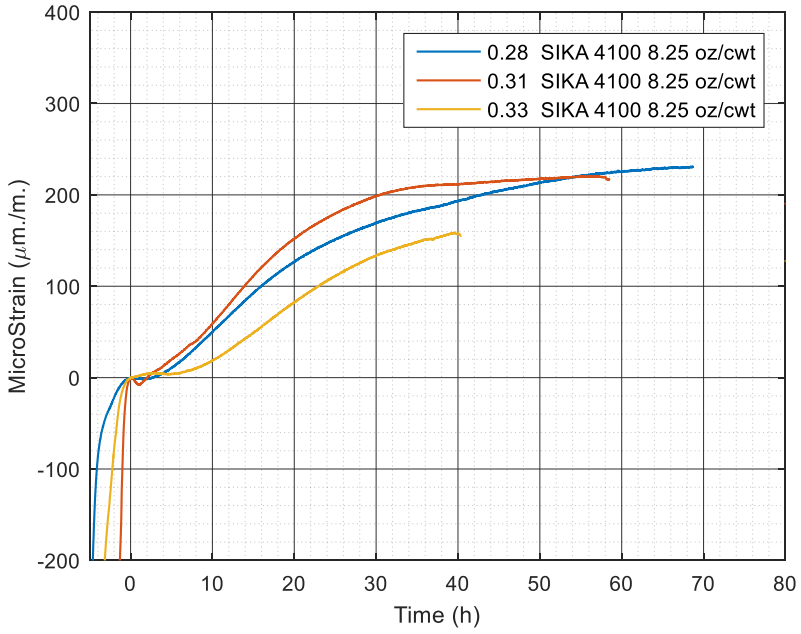

Figure 31: Effect of w/cm on mixture with Sika 4100 admixture at 8.25 oz/cwt

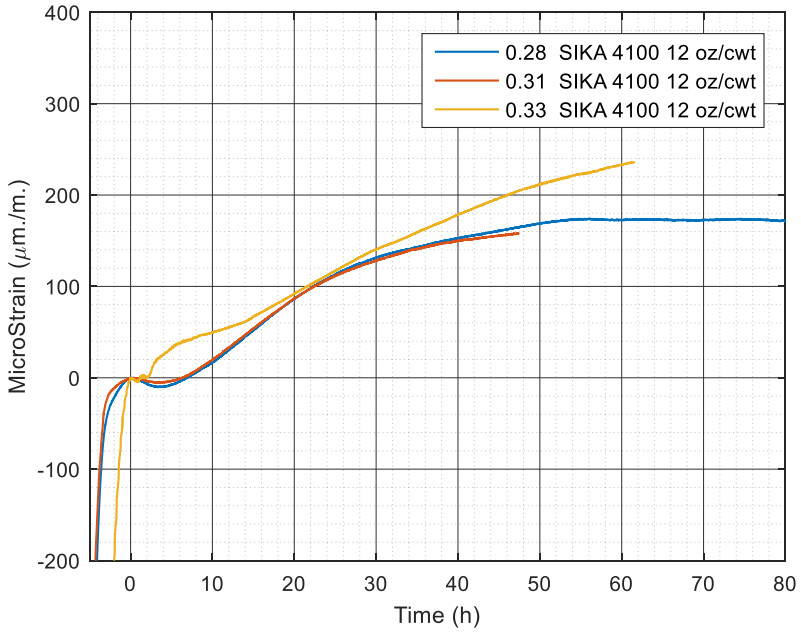

Figure 32: Effect of w/cm on mixture with Sika 4100 admixture at 12 oz/cwt

Admixture 3: BASF 7700

Figures 33-35 show the effect of w/cm ratio on paste mixtures prepared with the admixture BASF 7700. Figure 33 shows that when the lowest dosage was used, the 0.31 and 0.33 w/cm ratio pastes' autogenous deformation curve was very similar. The autogenous shrinkage of the 0.28 w/cm paste was slightly higher (by about 10 µm/m) than the 0.31 and 0.33 w/cm ratio paste's autogenous shrinkage. Whereas, at the moderate dosage of 8.25 oz/cwt (see Figure 34), the autogenous shrinkage of the 0.33 w/cm ratio paste was slightly higher than the autogenous shrinkage of the 0.31 and 0.28 w/cm ratio pastes. Autogenous shrinkage data for the 0.28 w/cm and 0.33 w/cm ratio pastes increased throughout the 80 hours of data shown, whereas the 0.31 w/cm ratio shrinkage rapidly levelled off at the 40 hour point. Figure 35 shows that the dosage of 12 oz/cwt an increase in w/cm ratio correlated with an increase in autogenous shrinkage, the opposite relationship of what was expected. Figures 33-35 do not show a consistent trend between w/cm ratio and autogenous shrinkage. In fact, no difference greater between the mixtures greater than 10 µm/m is observed, except at the greatest HRWRA dosage of 12 oz/cwt.

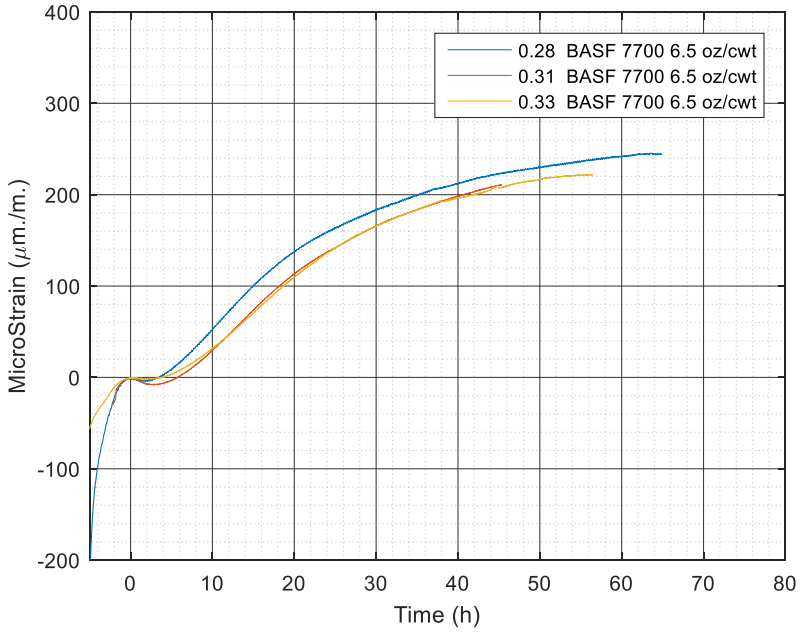

Figure 33: Effect of w/cm on mixture with BASF 7700 admixture at 6.5 oz/cwt

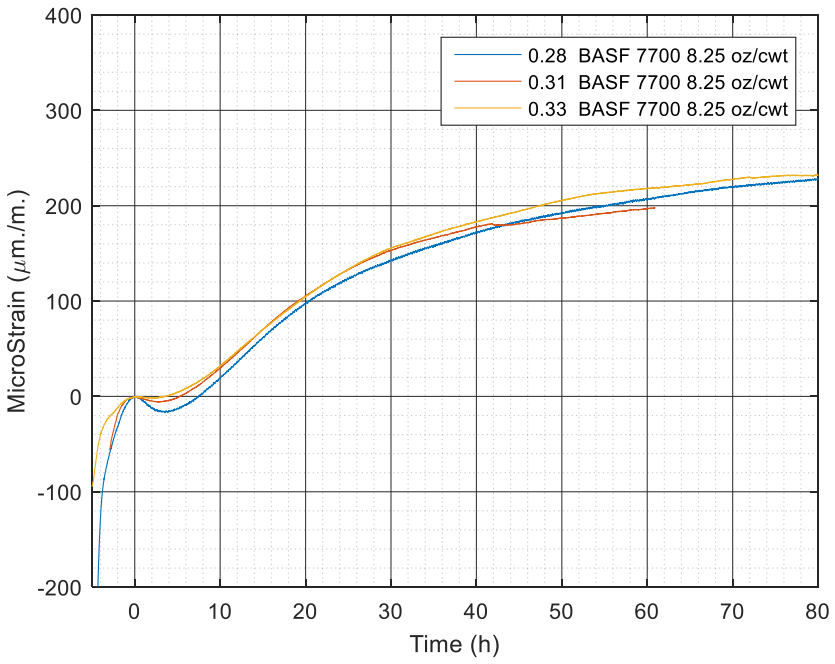

Figure 34: Effect of w/cm on mixture with BASF 7700 admixture at 8.25 oz/cwt

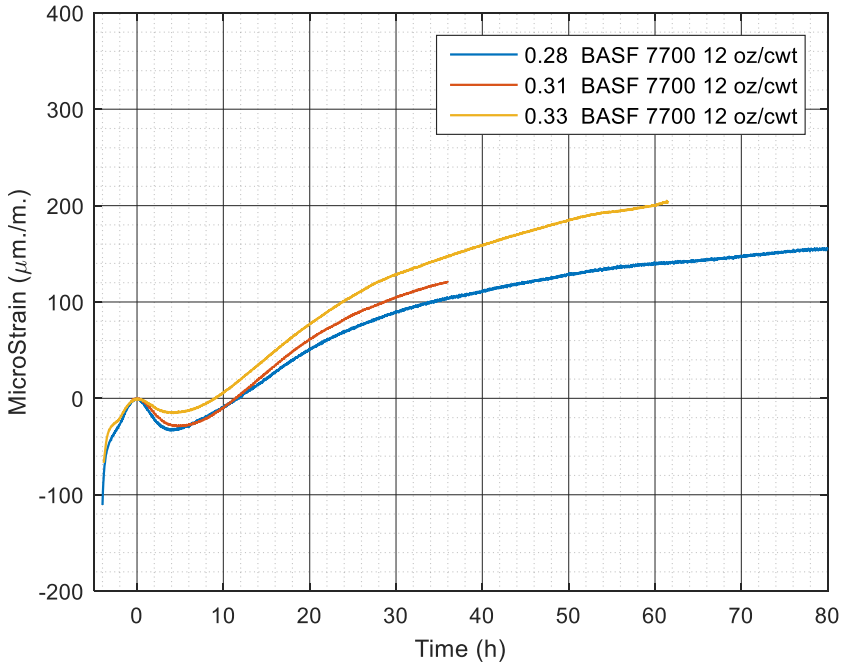

Figure 35: Effect of w/cm on mixture with BASF 7700 admixture at 12 oz/cwt

Summary of Influence of W/CM on Autogenous Shrinkage

As the mechanism of autogenous shrinkage, self-desiccation, is exacerbated by the reduction of the w/cm ratio, it was expected that the autogenous deformation of the pastes would increase as the w/cm decreased. However, no such clear trend was seen.

3. Influence of Admixture Type

Series 1: 0.28 w/cm ratio series

Figures 36-38 show the effect of w/cm ratio on autogenous shrinkage of admixture type on pastes made with the lowest w/cm ratio explored in this research (w/cm=0.28). Figure 36 shows that BASF 7700 and Sika 4100 pastes reached similar levels of autogenous shrinkage at 60 hours post time-zero. However, there are major differences in the BASF and Sika 4100 strain change rate over time, especially during the two hours after time-zero. Pastes incorporating Sika 2100 and Sika 4100 did not have a significant bleed water expansion period (defined as the difference in strain during the expansive period after time-zero), and simply exhibit a 'knee' in the curve where the shrinkage rate changes. However, pastes incorporating BASF 7700 exhibit a distinct bleed bump or period of expansion; after time-zero, the paste stops shrinking and expands (shown by the curve dipping below the x-axis approximately 4 μm/m). Figure 37 shows that at 8.25 oz/cwt pastes of each admixture reached a very similar level of autogenous shrinkage (within 10 μm/m) by 80 hours after time-zero. The Sika 4100 and BASF 7700 pastes both show a period of expansion, whereas the Sika 2100 paste still does not show a period of expansion. Figure 38 shows that at 12 oz/cwt, the Sika 2100 and Sika 4100 pastes' period of expansion overlaps. The BASF 7700 paste's period of expansion is larger in magnitude than the other pastes. At the largest dosage (12 oz/cwt), there is some significant difference in autogenous shrinkage among the mixes: at 70 hours past time-zero, the Sika 4100 mixture has shrunk about 10 μm/m more than the Sika 2100 mixture which shrinks 20 μm/m more than the BASF 7700 mixture.

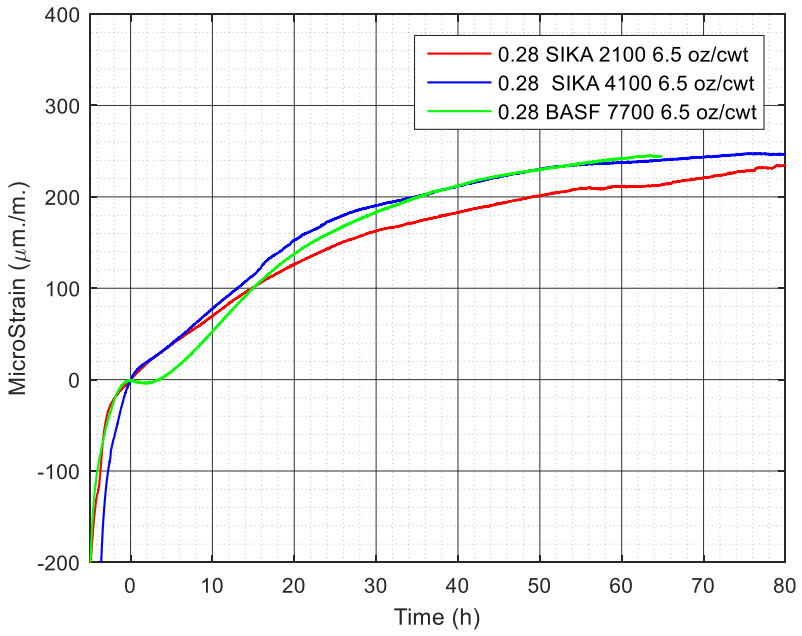

Figure 36: Effect of HRWRA type on autogenous shrinkage on 0.28 w/cm ratio pastes at dosage 6.5 oz/cwt

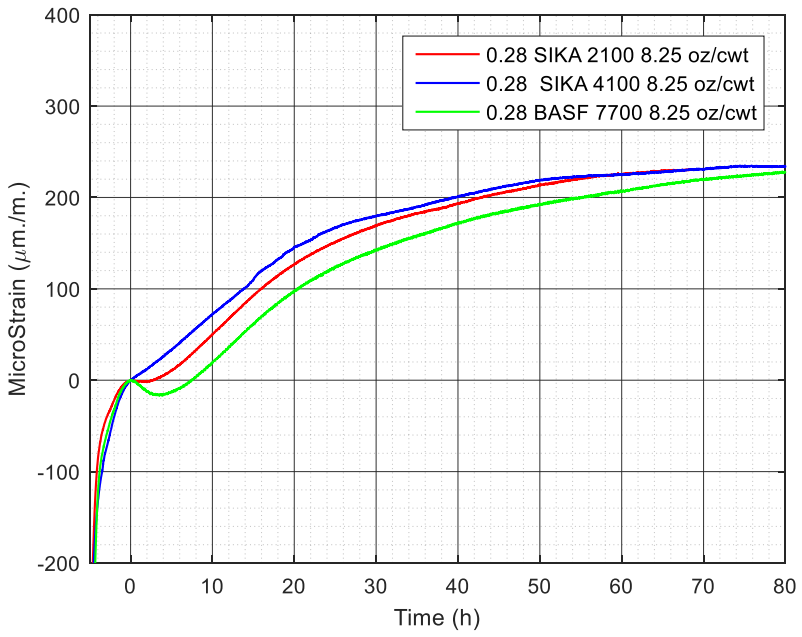

Figure 37: Effect of HRWRA type on autogenous shrinkage on 0.28 w/cm ratio pastes at dosage 8.25 oz/cwt

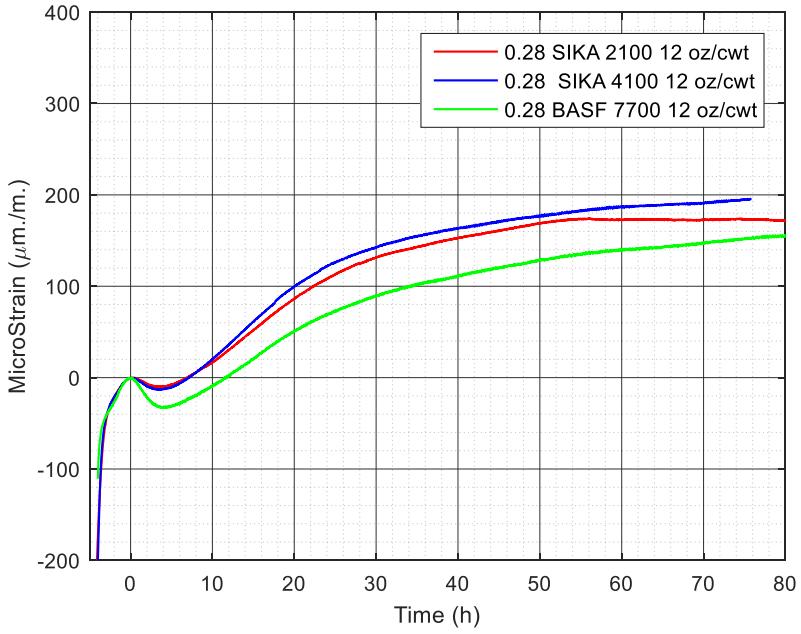

Figure 38: Effect of HRWRA type on autogenous shrinkage on 0.28 w/cm ratio pastes at dosage 12 oz/cwt

Series 2: 0.31 w/cm ratio series

Figures 39-41 show the effect of w/cm ratio on autogenous shrinkage of admixture type on pastes made with the 0.31 w/cm. Figure 39 shows that at the lowest dosage evaluated in this study, at 40 hours after time zero the shrinkage of the Sika 2100 paste is greater than the Sika 4100 and BASF 7700 paste, which overlap. At time-zero, the Sika 2100 and Sika 4100 both have a rapid period of expansion. The strain differential is similar to the BASF 7700 paste, but the period of time over which it occurs is much smaller. Figure 40 shows a significant difference in autogenous shrinkage based off of HRWRA type at 8.25 oz/cwt: the shrinkage of the Sika 4100 paste is greater than that of the Sika 2100 paste which is greater than the BASF 7700 paste. The same difference in bleed bump shape occurs as was observed in Figure 39 occurs: the Sika 2100 and Sika 4100 pastes have a shorter period of bleed water expansion. Figure 41 shows the same impact of HRWRA type on autogenous shrinkage at 12 oz/cwt dosage of PCE: the shrinkage of the Sika 4100 paste is greater than that of the Sika 2100 paste which is greater than the BASF 7700 paste. At time-zero, all pastes have similar time period lengths of bleed water absorption and expansion.

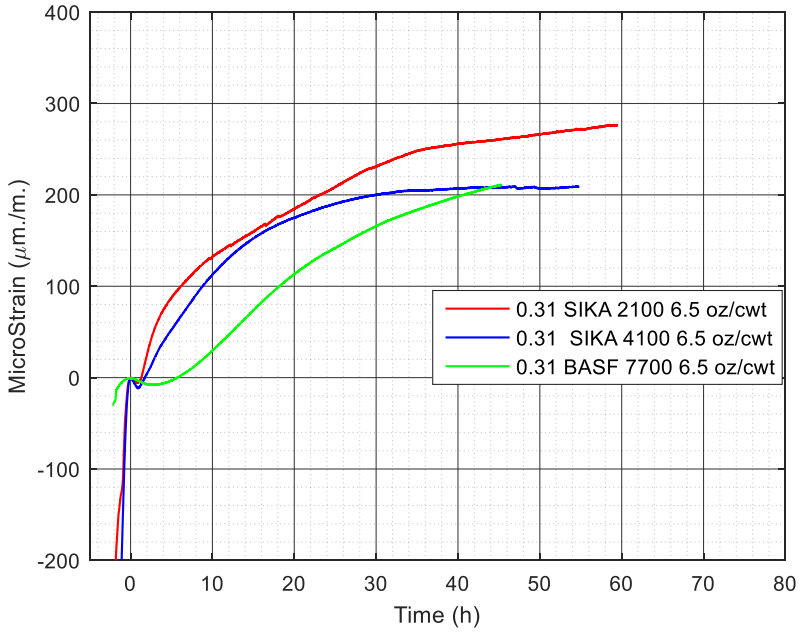

Figure 39: Effect of HRWRA type on autogenous shrinkage on 0.31 w/cm ratio pastes at dosage 6.5 oz/cwt

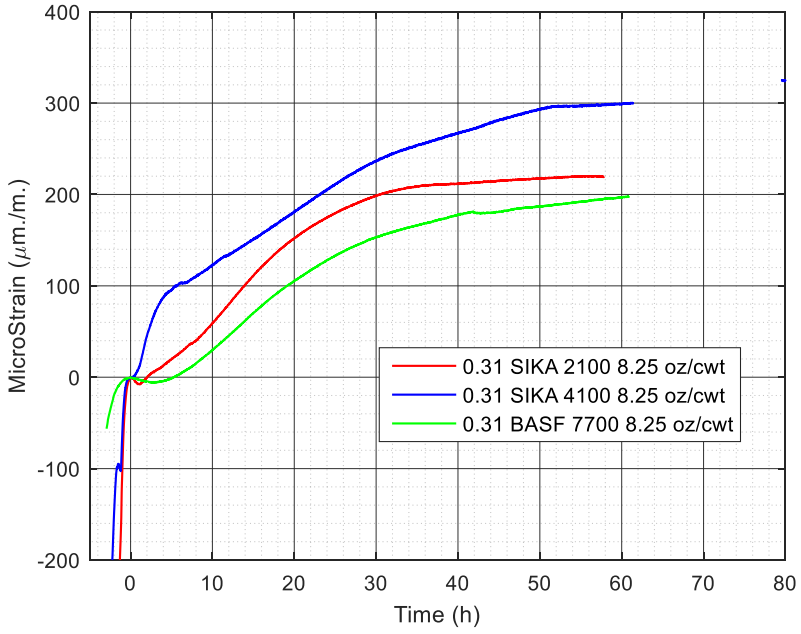

Figure 40: Effect of HRWRA type on autogenous shrinkage on 0.31 w/cm ratio pastes at dosage 8.25 oz/cwt

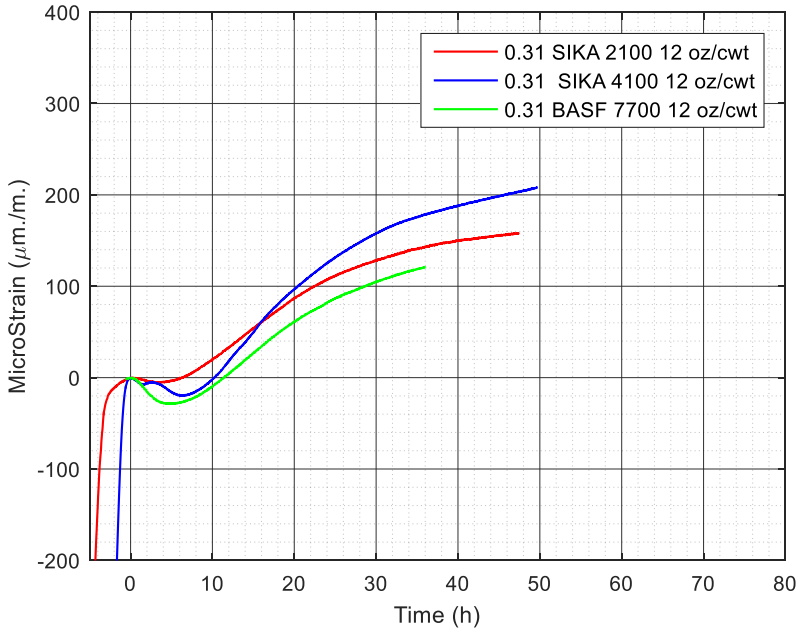

Figure 41: Effect of HRWRA type on autogenous shrinkage on 0.31 w/cm ratio pastes at dosage 12 oz/cwt

Series 3: 0.33 w/cm ratio series

Figures 42-44 show the effect of HRWRA type on autogenous shrinkage for pastes made using the highest w/cm ratio explored in this work (w/cm=0.33). Figure 42 and Figure 43 show similar magnitudes of autogenous shrinkage for all HRWRA types at the dosages of 6.5 oz/cwt and 8.25 oz/cwt, respectively. Figure 44 shows significantly different magnitudes for each HRWRA type: Sika 4100 shrinks more than BASF 7700 which shrinks more than Sika 2100.

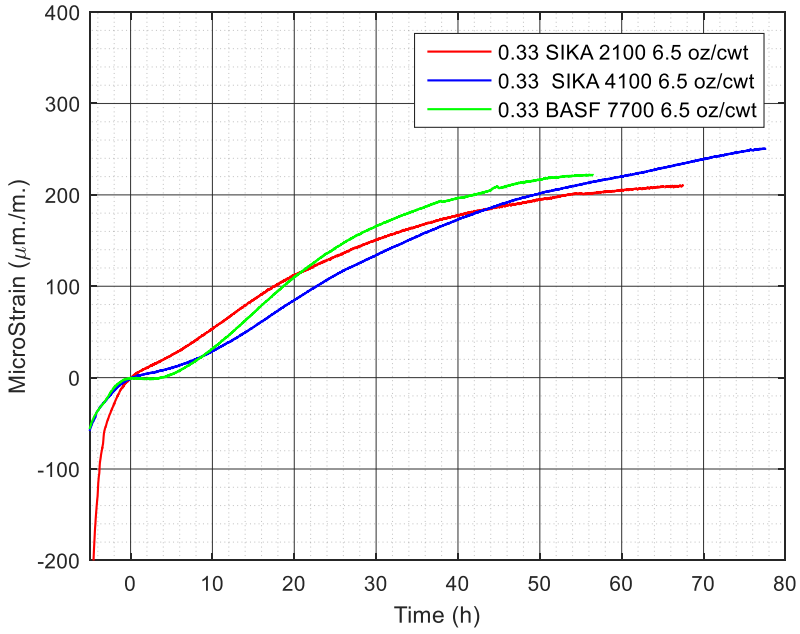

Figure 42: Effect of HRWRA type on autogenous shrinkage on 0.31 w/cm ratio pastes at dosage 6.5 oz/cwt

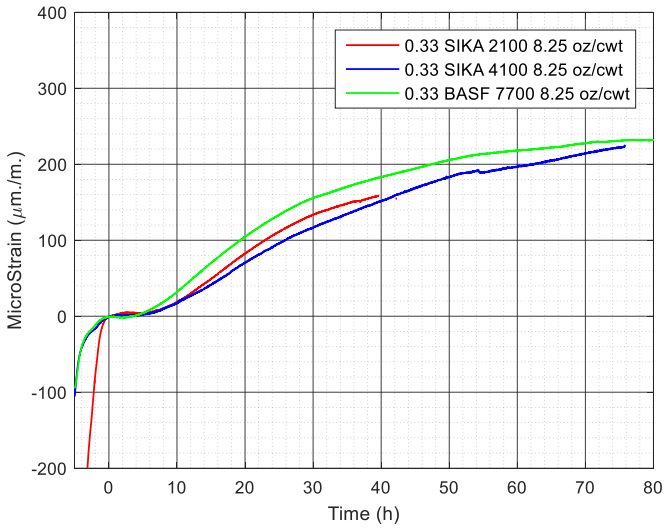

Figure 43: Effect of HRWRA type on autogenous shrinkage on 0.33 w/cm ratio pastes at dosage 8.25 oz/cwt

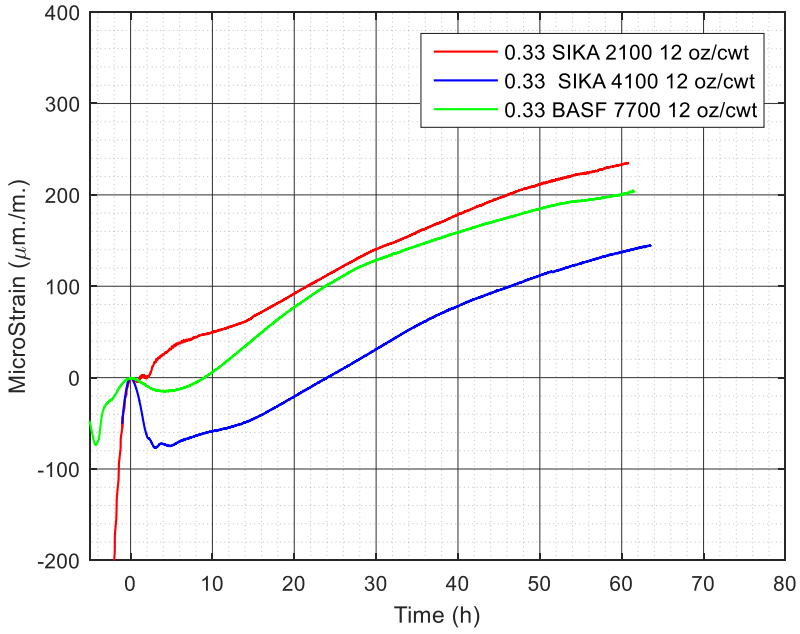

Figure 44: Effect of HRWRA type on autogenous shrinkage on 0.33 w/cm ratio pastes at dosage 12 oz/cwt

Summary of Influence of Admixture Type

Figures 36 – 44 show the influence of admixture type on autogenous shrinkage. In 63% of cases, the BASF 7700 admixture resulted in a lower autogenous shrinkage than the other admixtures. Admixtures with BASF also generally showed a longer period of bleed water absorption indicated by expansion.

4. Influence of Fly Ash Replacement & VMA-Addition (SCC Mix Design)

Figure 45 shows the effect of Rockdale Class F fly ash on autogenous shrinkage of 0.28 and 0.31 w/cm cement pastes. The replacement of cement with fly ash resulted in a decrease of about 50% in autogenous shrinkage, as has previously been observed by other researchers. It has been suggested by Chan et. al. that the reason for this is that as fly ash reacts more slowly than cement, reducing the ability of water to migrate throughout the pore structure [13,14]. A physical

blocker within the hydrating cement paste could lower the capillary pressure developing within the paste, provided its grain size is coarse enough. Figure 46 shows the effect of fly ash on autogenous shrinkage and the effect of a VMA with that fly ash, mimicking an SCC paste. The reduction of autogenous shrinkage due to fly ash is mitigated by the incorporation of VMA. This was not expected; Lin et. al observed a small decrease in surface tension due to incorporation of a VMA [34]. The difference in autogenous shrinkage is within the range of the standard deviation of the mixtures (50 µm/m.) so this result calls for additional testing to verify the correlation.

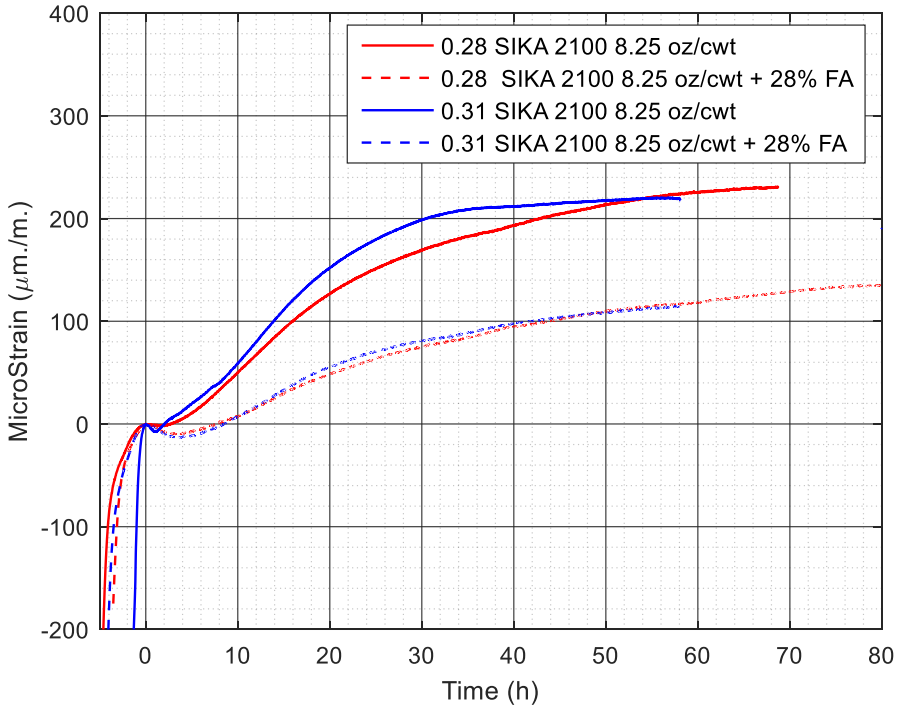

Figure 45: Influence of Fly Ash Addition on Autogenous Shrinkage of paste at constant w/cm ratios

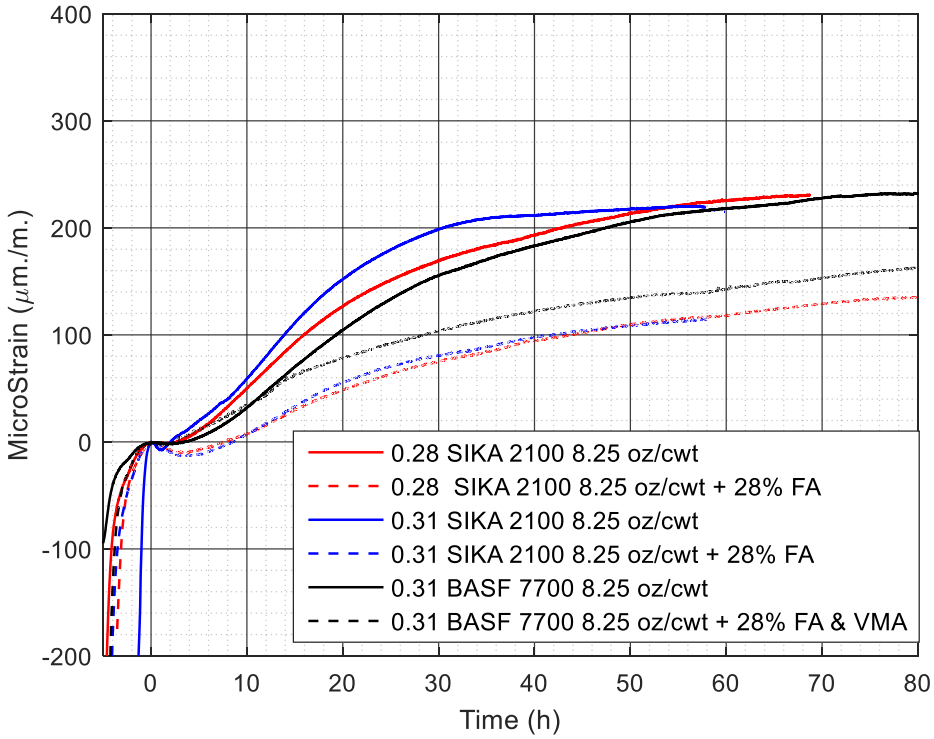

Figure 46: Influence of Fly Ash Addition and VMA addition on Autogenous Shrinkage of paste at constant w/cm ratios

V. CONCLUSION

In this work the effect of HRWRA dosage, HRWRA type, w/cm, addition of fly ash, and incorporation of VMA and fly ash on autogenous shrinkage was evaluated. The motivation of evaluating autogenous shrinkage was to understand their potential to cause cracking in precast mixtures and how to mitigate this shrinkage through mixture design proportioning.

Major findings are as follows:

1. For 75% of mixtures, the largest dosage of polycarboxylate admixture was associated with a reduction in autogenous shrinkage. Beyond 8.25 fl. oz/cwt, increased dosage of polycarboxylate admixture was associated with a reduction in autogenous shrinkage. It is theorized that this is due to a reduction in surface tension of the pore solution caused by the PCE admixture as demonstrated by [32]. Therefore, it is unlikely that the transition from naphthalene to polycarboxylate HRWRA at precast plants in Texas resulted in higher rates of autogenous shrinkage.
2. The 25% of mixtures that did not show the trend noted in 1 were made with HRWRA not agitated before use, suggesting that for this surface tension effect to be applied in practice incorporation of PCE must be carefully monitored
3. Class F Fly ash was demonstrated to be effective in reducing autogenous shrinkage for precast mixtures.
4. A method for normalizing autogenous shrinkage data has been put forward based on the initiation of expansion or peak of shrinkage. The reliability of this method is presented for up to 72 hours in Appendix C. Normalizing autogenous shrinkage data with respect to the maximum of the period of expansion would make autogenous shrinkage results consistent with respect to an arbitrary point so that mixture parameters can be precisely

evaluated with respect to effective autogenous strain without requiring extra associated data to validate an already expensive test method.

Areas for future work to elucidate additional insight from this data include:

- A study on moving time zero based on the end of the bleed bump vs. the peak of the bleed bump and correlation with other independent sources of information about the stiffening of the paste such as internal RH monitoring or ultrasonic pulse velocity measurement monitoring over time
- Characterization of the chemistry of PCE admixtures used to better understand variations in data observed due to admixture type
- Comparing the impact of the admixture types and dosage on surface tension of water using a tensiometer
- Pore structure analysis to examine how PCE impacts pore structure and its role on autogenous shrinkage via mercury intrusion porosimetry (MIP)
- Observe HRWRA impact on crystallization of portlandite

Appendices

Appendix A: Matlab file used to average shrinkage strains at time-zero and determine standard deviations

```
function
[time,strain,tA,strainA,tB,strainB,tC,strainC,stdev]=ldvtgetstrain(filenameA,filenameB,filenameC,str,N,vicatfinalA,vicatfinalB,v
icatfinalC)

% vicatfinalA=8;
% vicatfinalB=8;
% vicatfinalC=8;
finalstrainA=-2;
finalstrainB=-2;
finalstrainC=-2;
finaltA=0;
finaltB=0;
finaltC=0;
% filenameA='31AOU_correctedmixingprocedure.xlsx';
% filenameB='31BOU_correctedmixingprocedure.xlsx';
% filenameC='32COU_correctedmixingprocedure.xlsx';
% str='Mix 32';
N=3;

L0=393.7; %mm (15.5 inches)
%
[TimeA]=xlsread(filenameA,'A:A');
[AmpA]=xlsread(filenameA,'B:B');
tA=zeros(length(TimeA),1);
strainA=zeros(length(AmpA),1);
for i=1:length(TimeA)

   tA(i)=(TimeA(i)-TimeA(1))*24;
   strainA(i)=(AmpA(i)-AmpA(1))/L0;

end

strainA=smooth(tA,strainA,'rlowess');

for i=1:length(tA)

    if tA(i)<vicatfinalA
      if strainA(i)>finalstrainA
         finaltA=tA(i);
         finalstrainA=strainA(i);
         shiftA=i;
      end
    end

end
```

```
tA=tA-finaltA;
strainA=strainA-finalstrainA;

[TimeB]=(xlsread(filenameB,'A:A'));
[AmpB]=xlsread(filenameB,'B:B');
tB=zeros(length(TimeB),1);
strainB=zeros(length(AmpB),1);
for i=1:length(TimeB)

   tB(i)=(TimeB(i)-TimeB(1))*24;
   strainB(i)=(AmpB(i)-AmpB(1))/L0;

end

strainB=smooth(tB,strainB,'rlowess');

for i=1:length(tB)
     if tB(i)<vicatfinalB
       if strainB(i)>finalstrainB
          finaltB=tB(i);
          finalstrainB=strainB(i);
          shiftB=i;
       end
     end
end

tB=tB-finaltB;
strainB=strainB-finalstrainB;


[TimeC]=xlsread(filenameC,'A:A');
[AmpC]=xlsread(filenameC,'B:B');

tC=zeros(length(TimeC),1);
strainC=zeros(length(AmpC),1);

for i=1:length(TimeC)
   tC(i)=(TimeC(i)-TimeC(1))*24;
   strainC(i)=(AmpC(i)-AmpC(1))/L0;

end

strainC=smooth(tC,strainC,'rlowess');

for i=1:length(tC)
   if tC(i)<vicatfinalC
      if strainC(i)>finalstrainC
         finaltC=tC(i);
         finalstrainC=strainC(i);
         shiftC=i;
```

```
        end
    end
end

tC=tC-finaltC;
strainC=strainC-finalstrainC;

strainA=(strainA)*(10^6);
strainB=(strainB)*(10^6);
strainC=(strainC)*(10^6);
shiftAA=0;
shiftBB=0;
shiftCC=0;


if shiftC<shiftA
    if shiftC<shiftB
        shiftAA=-shiftC+shiftA;
        shiftBB=-shiftC+shiftB;
        shiftCC=0;
    end
end
if shiftB<shiftA
    if shiftB<shiftC
     shiftAA=-shiftB+shiftA;
     shiftBB=0;
     shiftCC=-shiftB+shiftC;
    end
end
if shiftA<shiftB
    if shiftC>shiftA
     shiftAA=0;
     shiftBB=-shiftA+shiftB;
     shiftCC=-shiftA+shiftC;
    end
end
if shiftA==shiftB
    if shiftA<shiftC
      shiftAA=0;
      shiftBB=0;
      shiftCC=-shiftA+shiftC;
    end
    if shiftA==shiftC
        shiftAA=0;
        shiftBB=0;
        shiftCC=0;
    end
end
if shiftAA>shiftBB
    if shiftAA==shiftCC
        greatestval=shiftAA;
```

```
    end
    if shiftAA>shiftCC
        greatestval=shiftAA;
    end
    if shiftCC>shiftAA
        greatestval=shiftCC;
    end
elseif shiftBB>shiftCC
    greatestval=shiftBB;
elseif shiftBB<shiftCC
    if shiftAA==shiftBB
        greatestval=shiftCC;
    end
    if shiftAA<shiftBB
        greatestval=shiftCC;
    end
elseif shiftBB>shiftAA
    if shiftBB==shiftCC
        greatestval=shiftBB;
    end
    if shiftBB>shiftCC
        greatestval=shiftBB;
    end
    if shiftCC>shiftBB
        greatestval=shiftCC;
    end
else
    greatestval=0;
end
shortestlength=length(strainA);
shorttime=tA;
timeshift=shiftAA;
if length(strainA)<length(strainB)
    if length(strainA)<length(strainC)
        shortestlength=length(strainA);
        shorttime=tA;
        timeshift=shiftAA;
    end
end
if length(strainB)<length(strainA)
    if length(strainB)<length(strainC)
        shortestlength=length(strainB);
        shorttime=tB;
        timeshift=shiftBB;
    end
end
if length(strainC)<length(strainB)
    if length(strainC)<length(strainA)
        shortestlength=length(strainC);
        shorttime=tC;
        timeshift=shiftCC;
```

```
    end
end

% initialize1=(shortestlength-greatestval)-(greatestval+1)+1;
% StrainAvg=zeros(initialize1,1);
% shorttimeadj=zeros(initialize1,1);
for i=(greatestval+1):shortestlength-greatestval
    StrainAvg(i-(greatestval+1)+1)=(strainA(i+shiftAA)+strainB(i+shiftBB)+strainC(i+shiftCC))/3;
    shorttimeadj(i-(greatestval+1)+1)=shorttime(i+timeshift);
end



% initialize2=(shortestlength-greatestval)-(greatestval+1)+1;
% stdev=zeros(initialize2,1);
% shorttimeadj=zeros(initialize2,1);
for i=(greatestval+1):shortestlength-greatestval

    stdev(i-(greatestval+1)+1)=sqrt((1/(N-1))*(((StrainAvg(i-(greatestval+1)+1)-strainA((i+shiftAA)))^2)+((StrainAvg(i-
(greatestval+1)+1)-strainB(i+shiftBB))^2)+((StrainAvg(i-(greatestval+1)+1)-strainC(i+shiftCC))^2)));

end

time=shorttimeadj;
strain=StrainAvg;


figure
plot(shorttimeadj,stdev)
title(['Standard Deviation of ',str])
xlabel('Time (h)')
ylabel('MicroStrain (\mum./m.)')
axis([-2 80 0 100])
grid


figure
plot(tA,strainA,tB,strainB,tC,strainC,shorttimeadj,StrainAvg)
legend('Sample A','Sample B','Sample C','Average')
title(str)
xlabel('Time (h)')
ylabel('MicroStrain (\mum./m.)')
axis([-5 80 -200 400])
grid

figure
plot(tA,strainA,tB,strainB,tC,strainC)
axis([-5 80 -200 400])
legend('Sample A','Sample B','Sample C')
title(str)
xlabel('Time (h)')
```

```
ylabel('MicroStrain (\mum./m.)')
grid



end
```

Published with MATLAB® R2015b

APPENDIX B: LDVT CORRUGATED TUBE PROCEDURE

Prep Portion

- Measure out appropriate amounts of sieved cement, de-aired water, and admixture
- Place tube over vibrating table within its "holder"
- Use a Q-tip to put mineral oil around the bottom of the funnel and place in tube
- Place mini-slump cone in position with funnel as well
- Have spatula ready

Mix Portion

- Place water and admixture in mixture, scooping the admixture container through the water multiple times
- Place cement in mixer, write down time of w/cm
- Mix on 1 for 30 seconds
- Mix on 2 for 30 seconds
- Rest for 1:30 seconds, using the spatula to scrape sides down into center
- Mix on 2 for 1 minute

Slump Portion

- As quickly as possible, fill the mini-slump cone to the top.
- Use the spatula to give 15 blows to the mini-slump paste
- Lift the mini-slump apparatus up vertically
- Start the timer
- Measure the slump at 10 minutes and 20 minutes

Filling Portion

- Fill in half portions, vibrating each portion about 7.5 minutes (vibrate more if you see lots of entrapped air)
- Clean the top of the tube with oil
- Coat the plastic cap with oil
- Screw on the cap so it is slightly overfilled or closely aligned with the paste on top.
- Place 2 zip ties around the plastic cap. Make sure zip tie tops are aligned with the connection point in the metal cap. Tighten with pliers and cut off excess.
- Place corrugated tubes in half-pipes and use epoxy to place ferro-magnetic plate on tube. Make sure the hole in the metal cap matches up with the top of the plate. Press firmly on plate. Let the epoxy set for 15 minutes.

Placing Portion

- Gently place tube in apparatus using half-tube. The plate must be against the LDVT and the metal cap should be against the bolt. Place Sample A in 1, Sample B in 2, and Sample C in 3.
- Screw bolts into metal cap by hand.
- Use wrench to tighten bolts.
- Right click no computer charts and select ‘Clear Chart’

APPENDIX C: INDIVIDUAL AUTOGENOUS SHRINKAGE MEASUREMENTS

The 3 samples from which averages were taken are shown for every mix, labelled as a number that correlates with the paste mix matrix shown above. The average computed from each of the samples is also shown. In some cases only 1 sample is shown because a plate became dislodged.

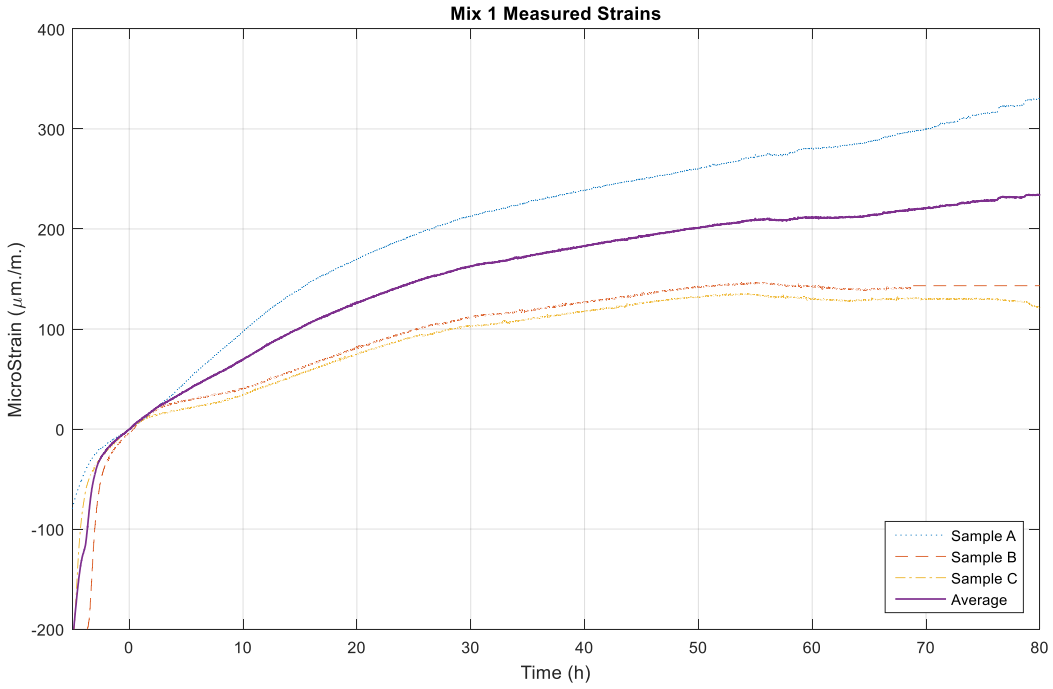

Figure 47: Mix 1 Data

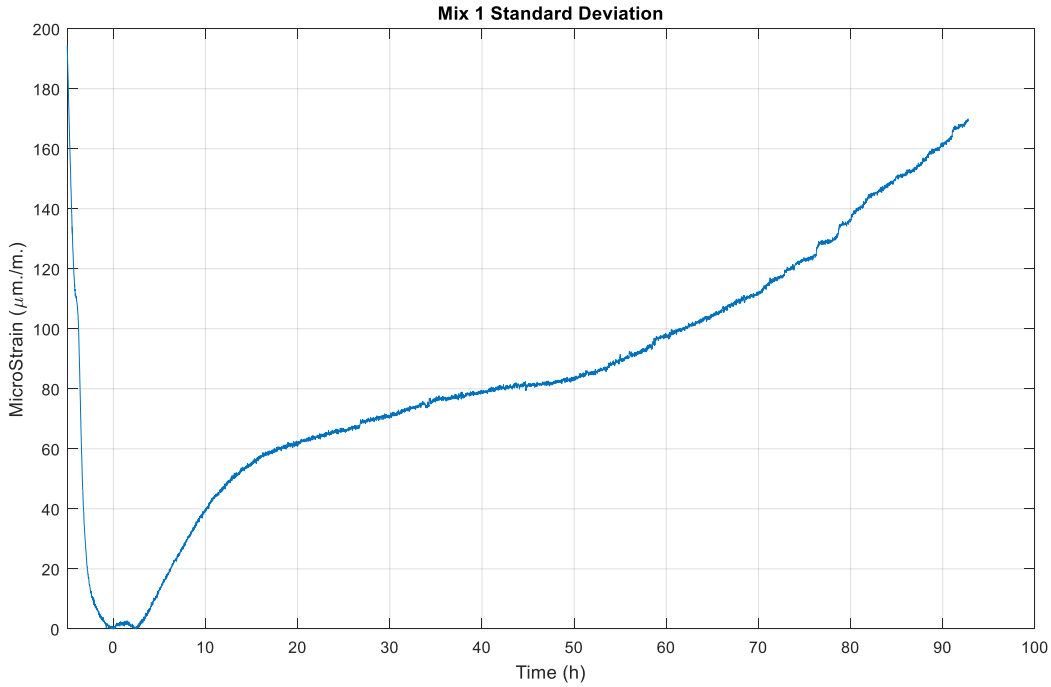

Figure 48: Mix 1 Standard Deviation

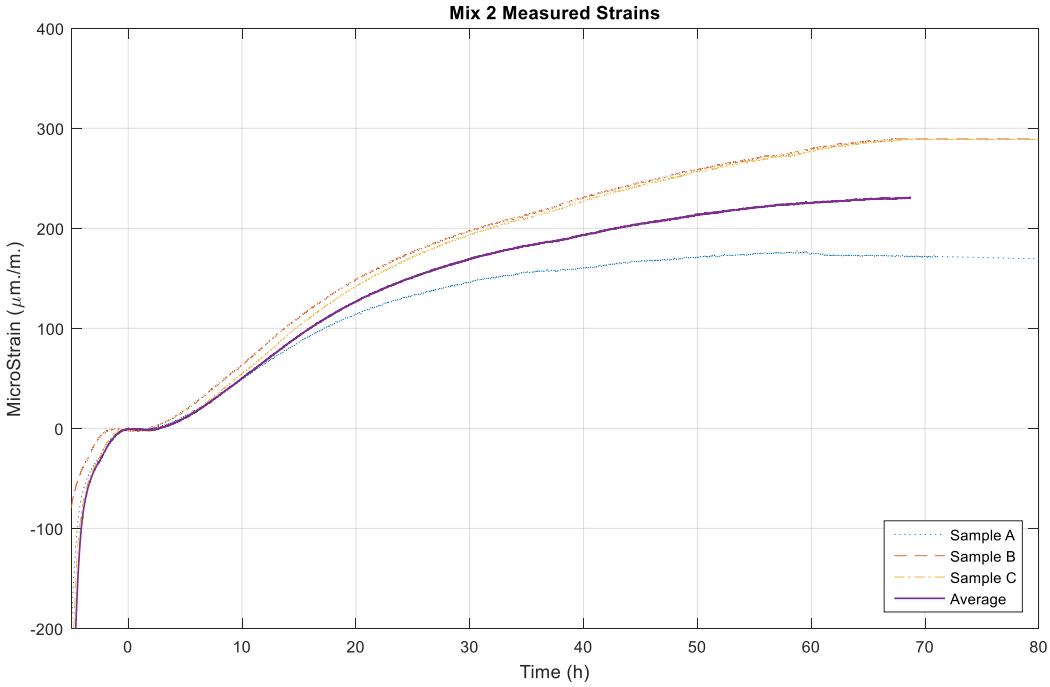

Figure 49: Mix 2 Data

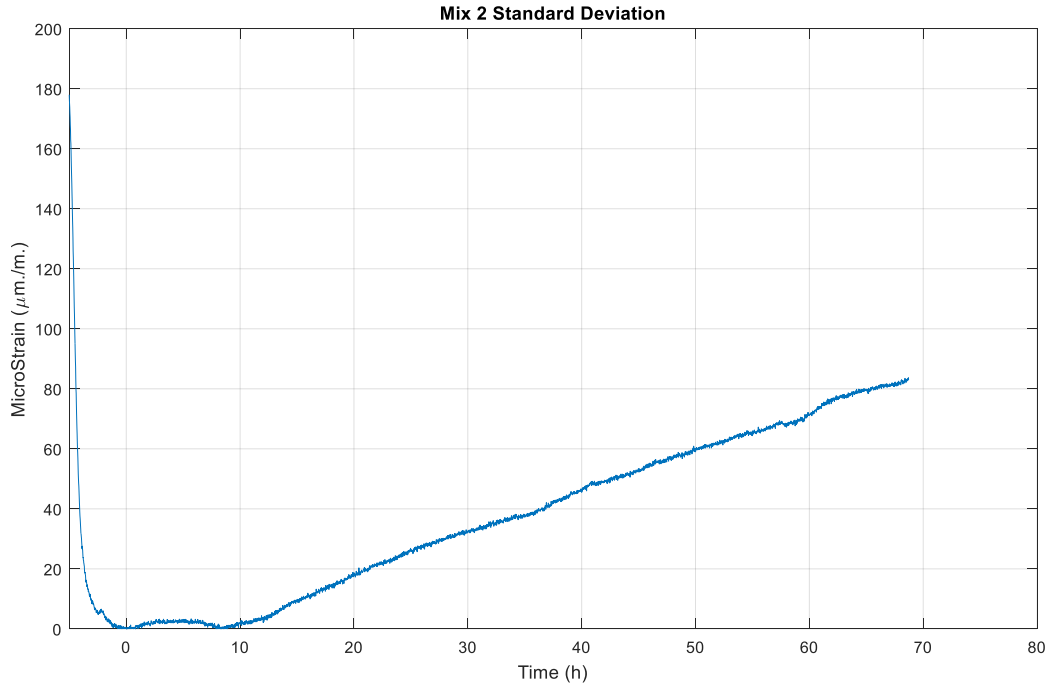

Figure 50: Mix 2 Standard Deviation

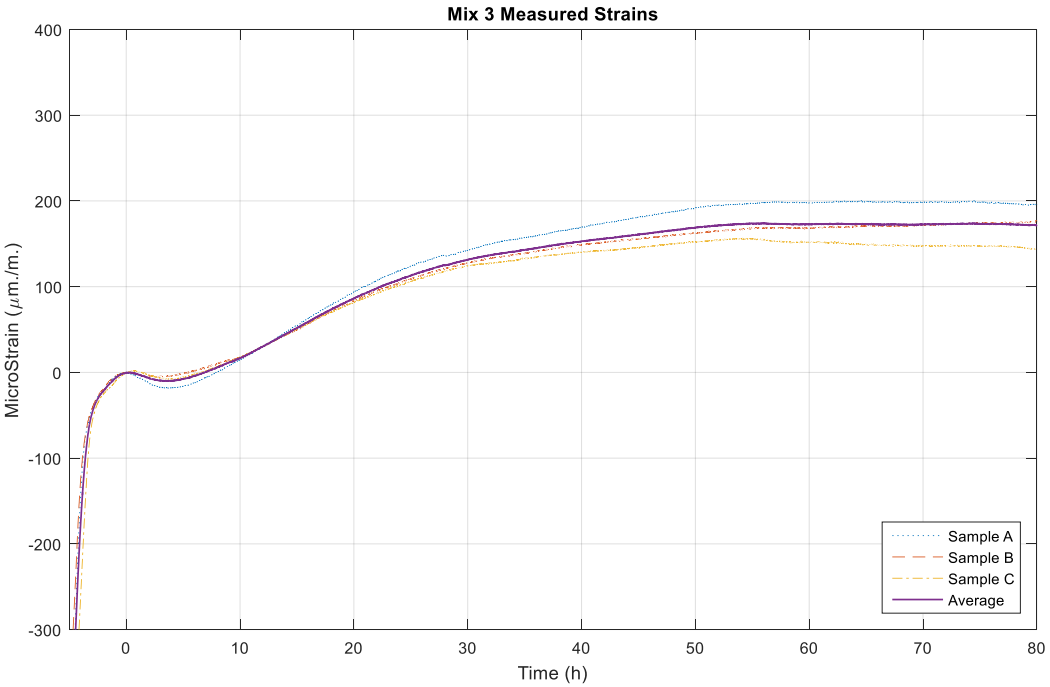

Figure 51: Mix 3 Data

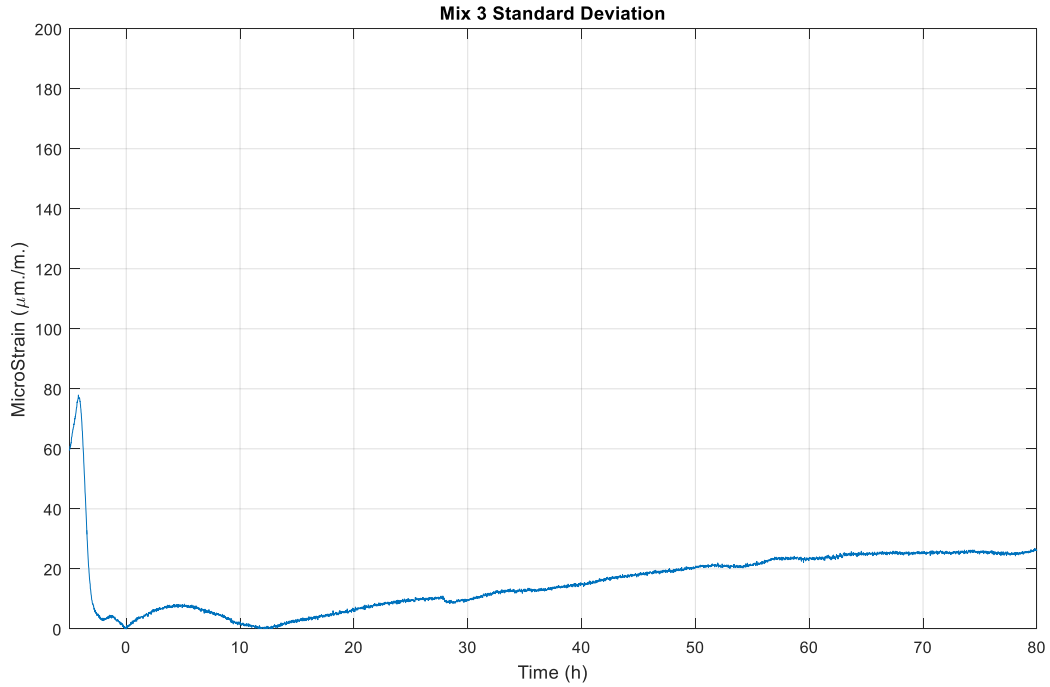

Figure 52: Mix 3 Standard Deviation

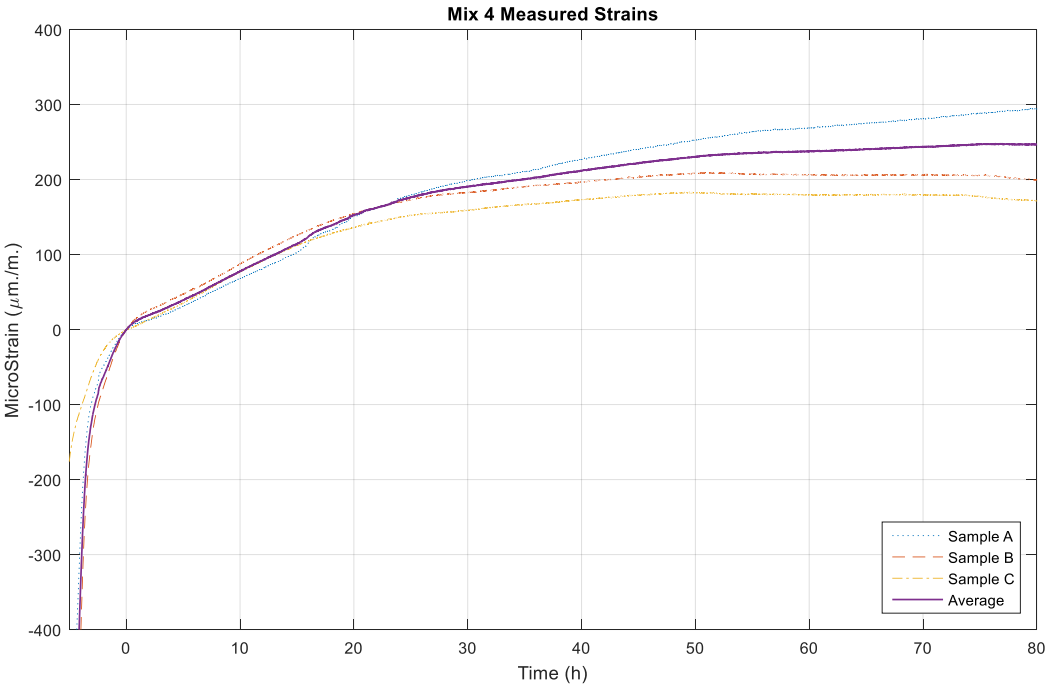

Figure 53: Mix 4 Data

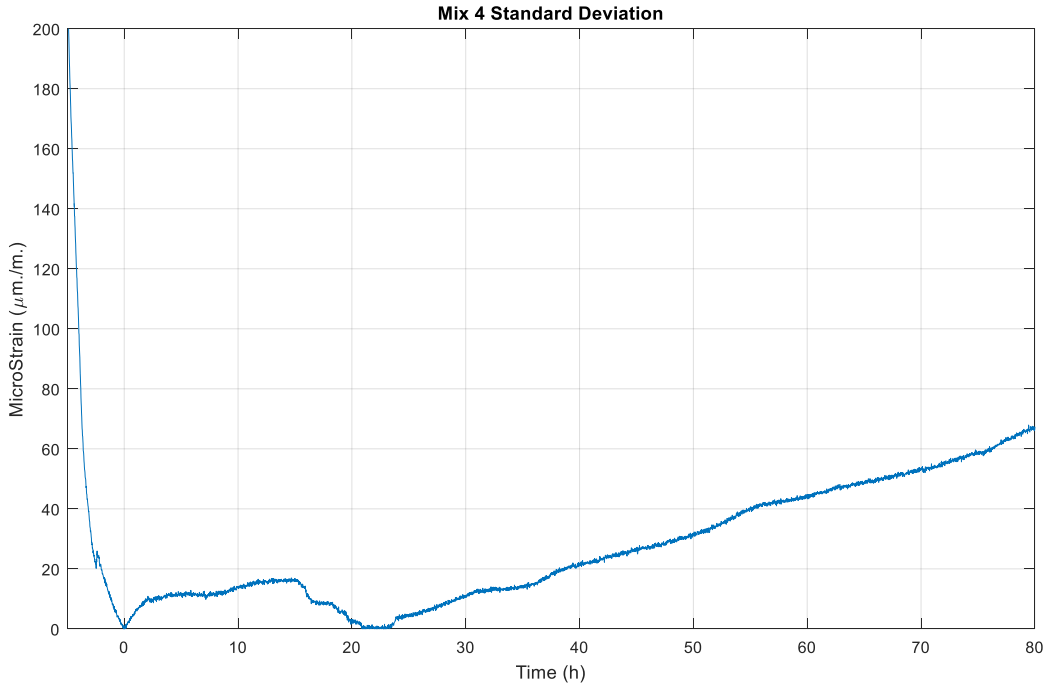

Figure 54: Mix 4 Standard Deviation

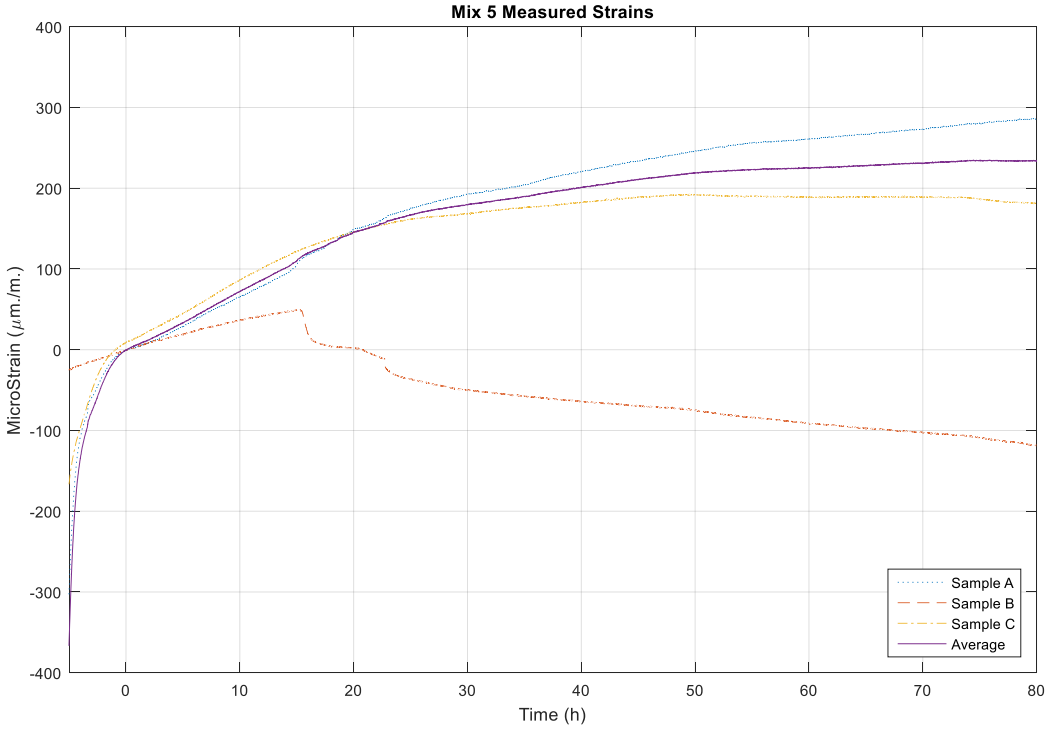

Figure 55: Mix 5 Data

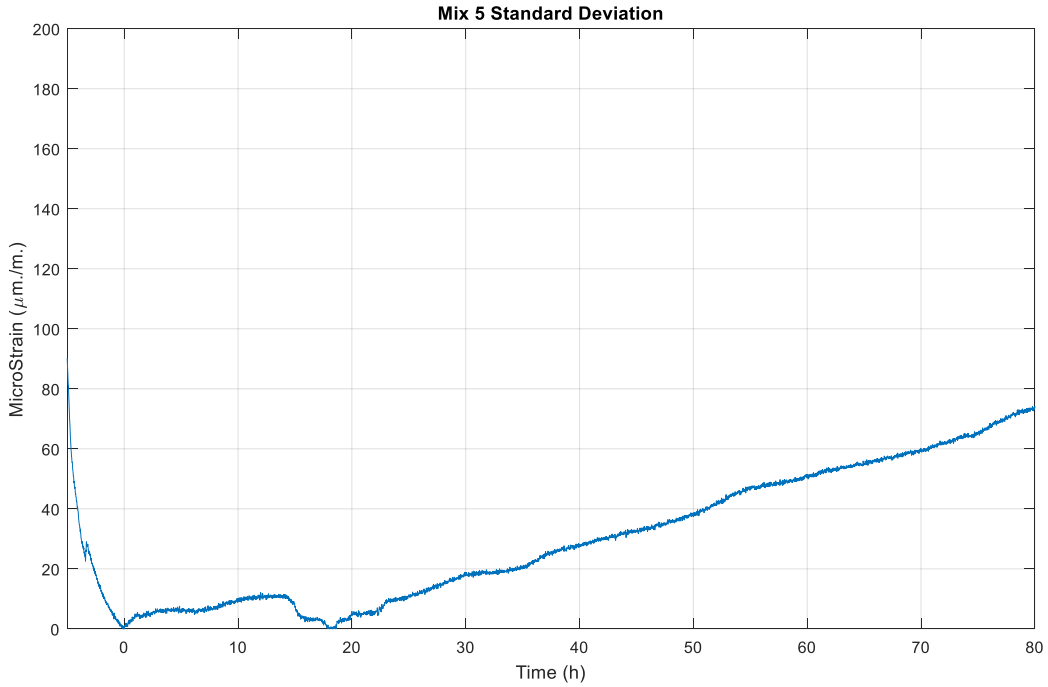

Figure 56: Mix 5 Standard Deviation

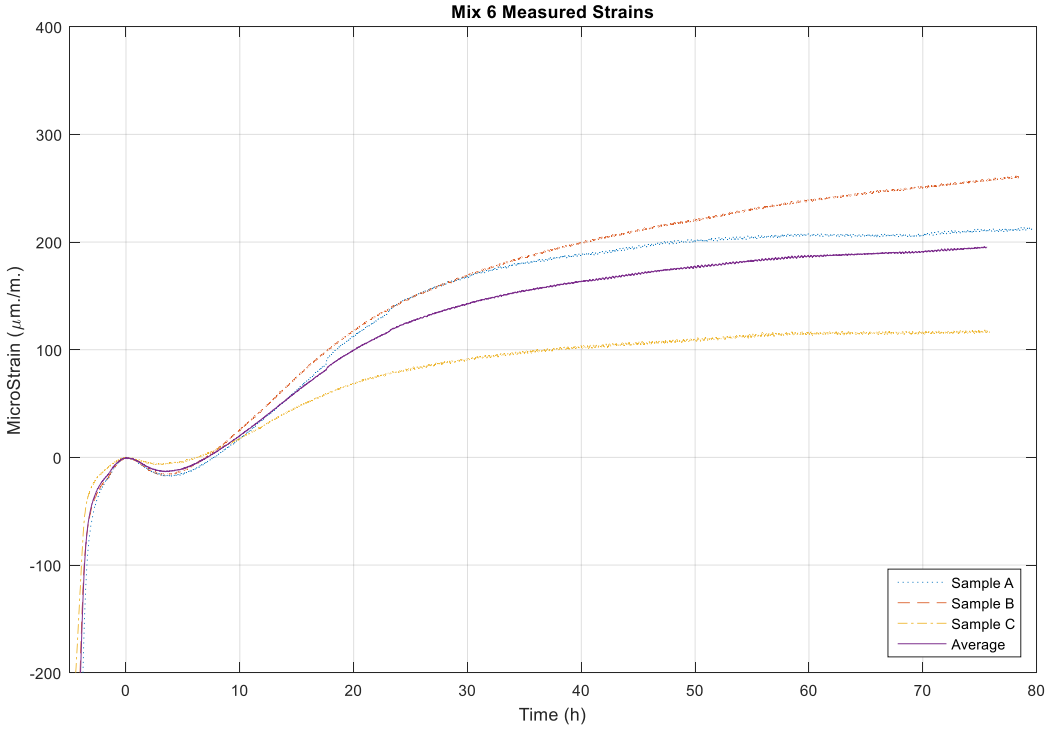

Figure 57: Mix 6 Data

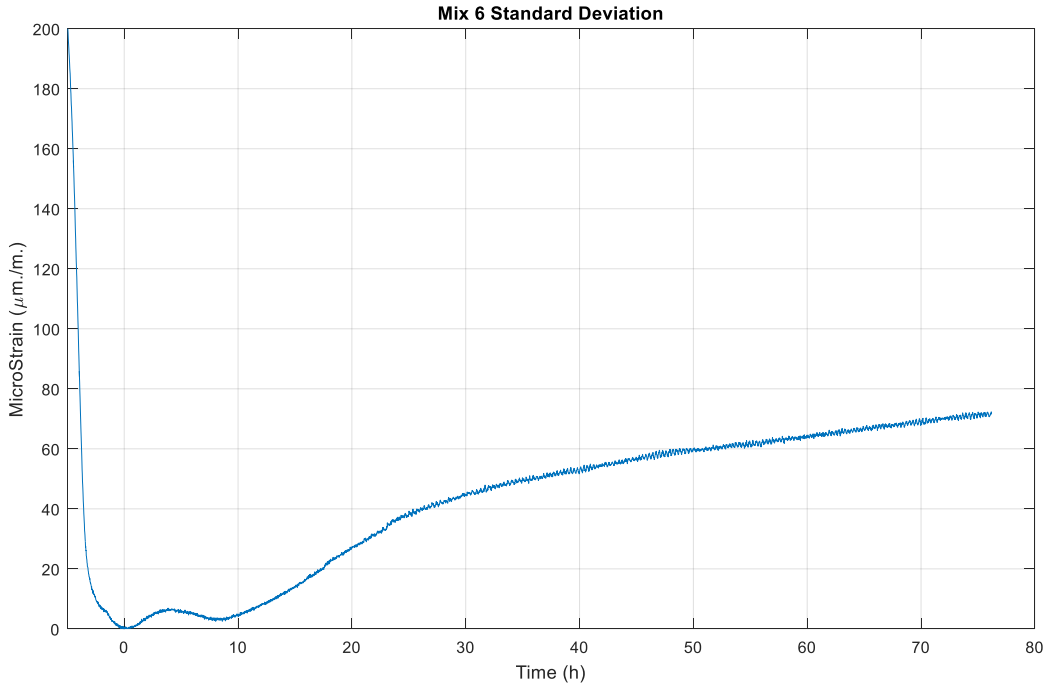

Figure 58: Mix 6 Standard Deviation

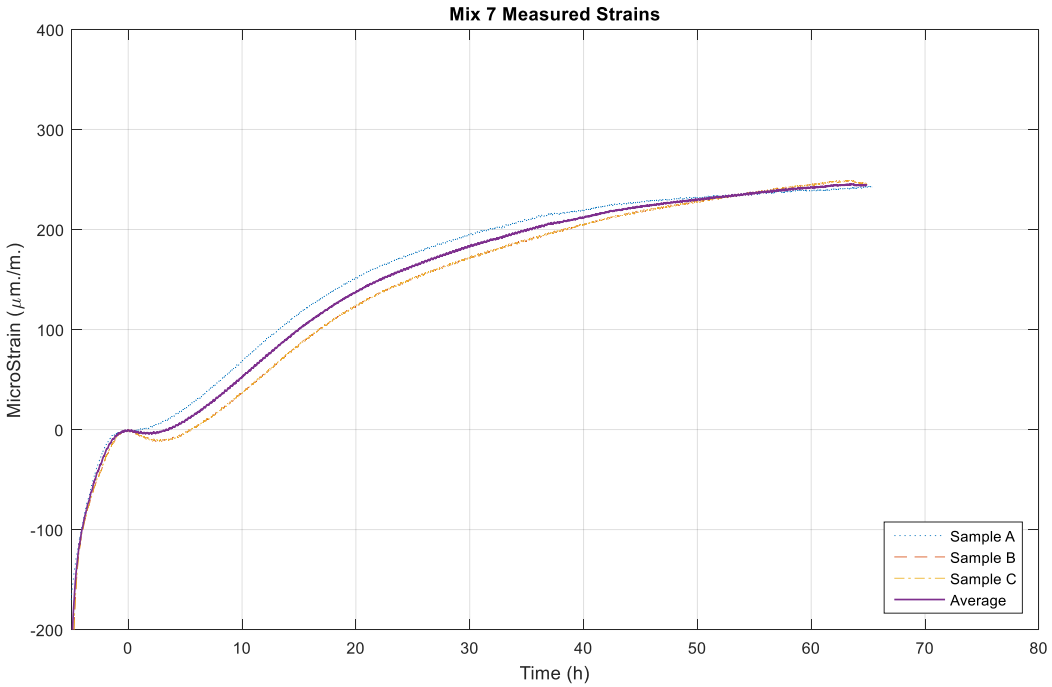

Figure 59: Mix 7 Data

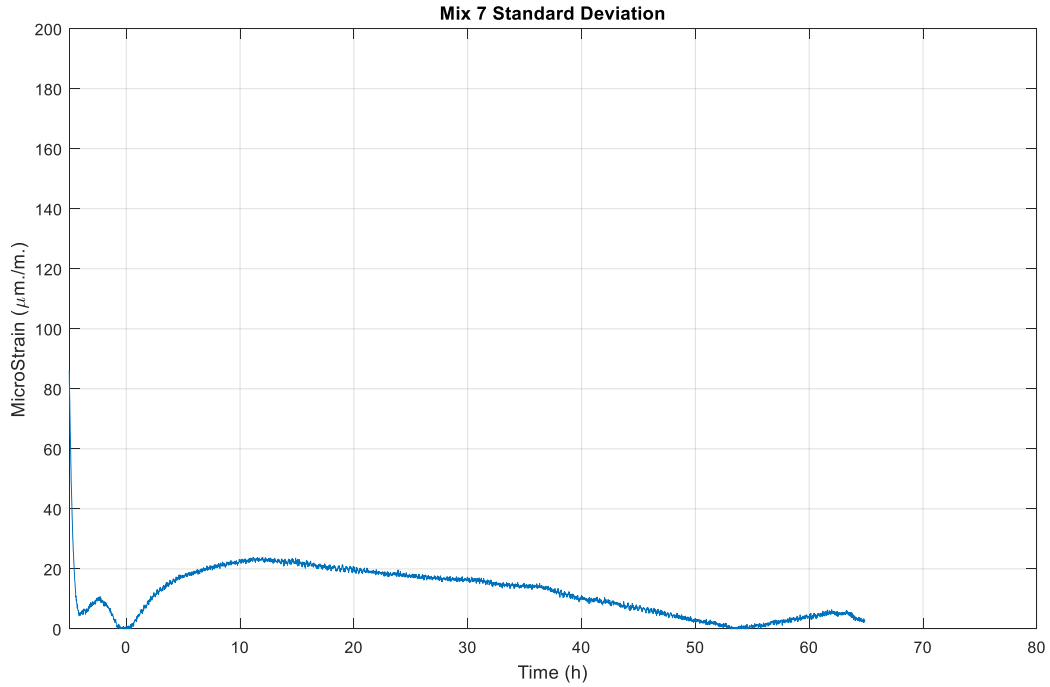

Figure 60: Mix 7 Standard Deviation

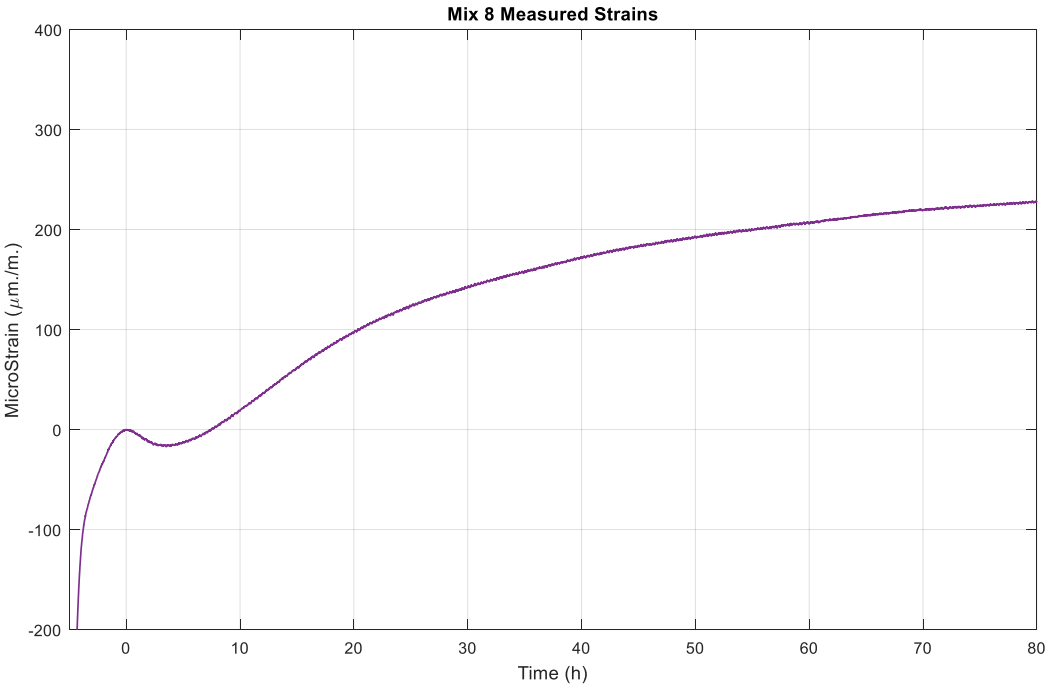

Figure 61: Mix 8 Data

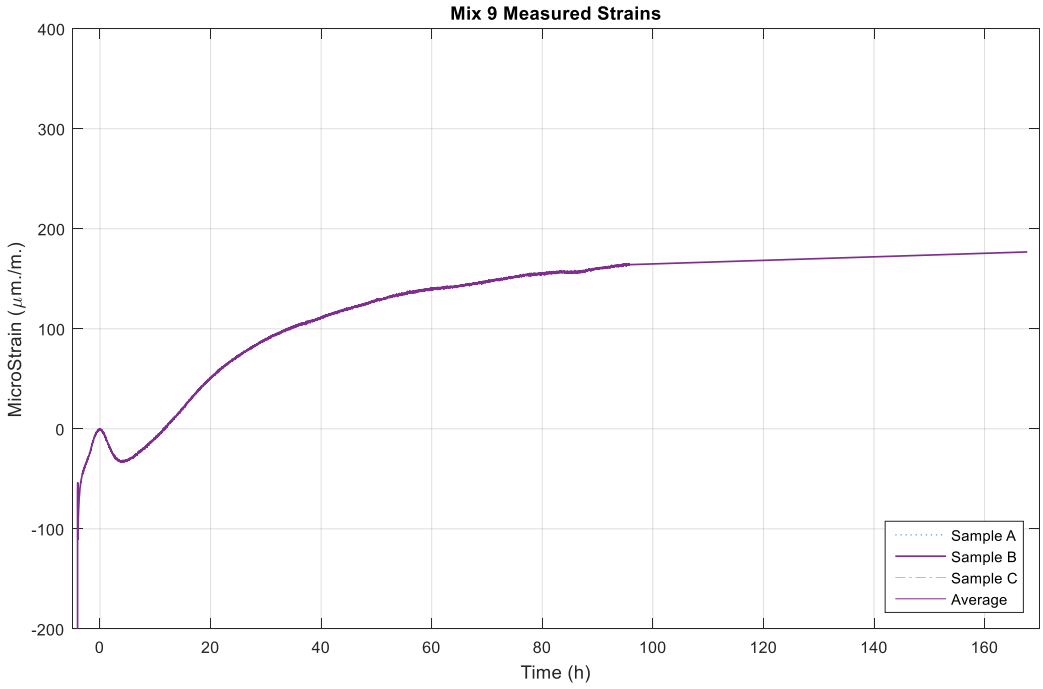

Figure 62: Mix 9 Data

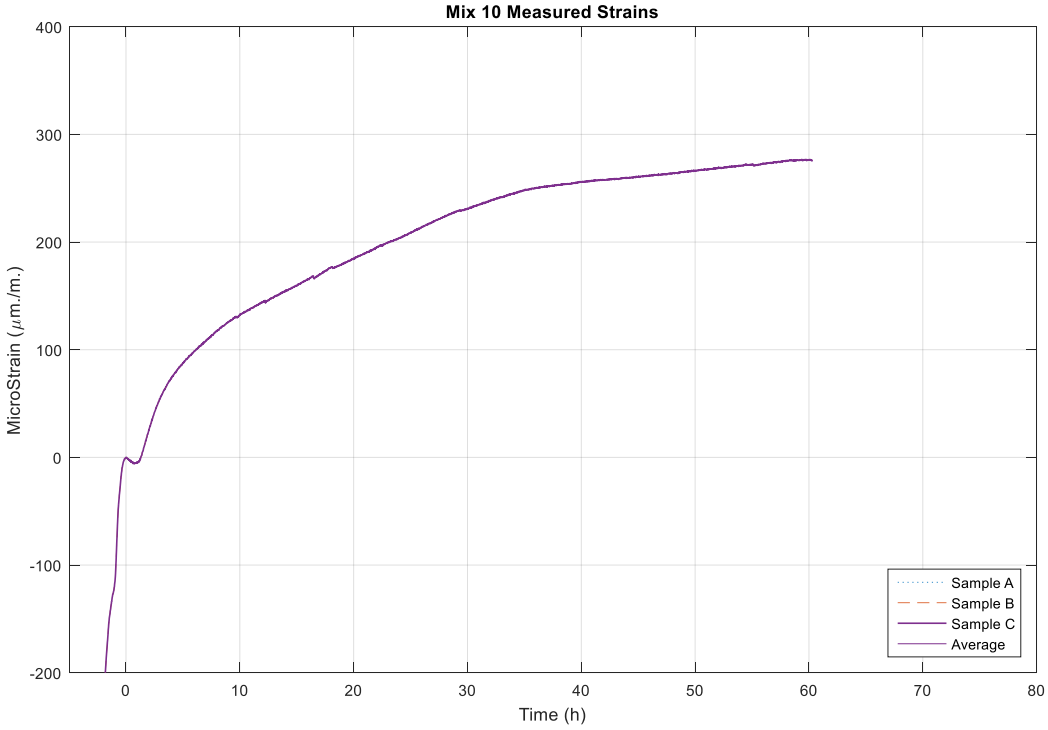

Figure 63: Mix 10 Data

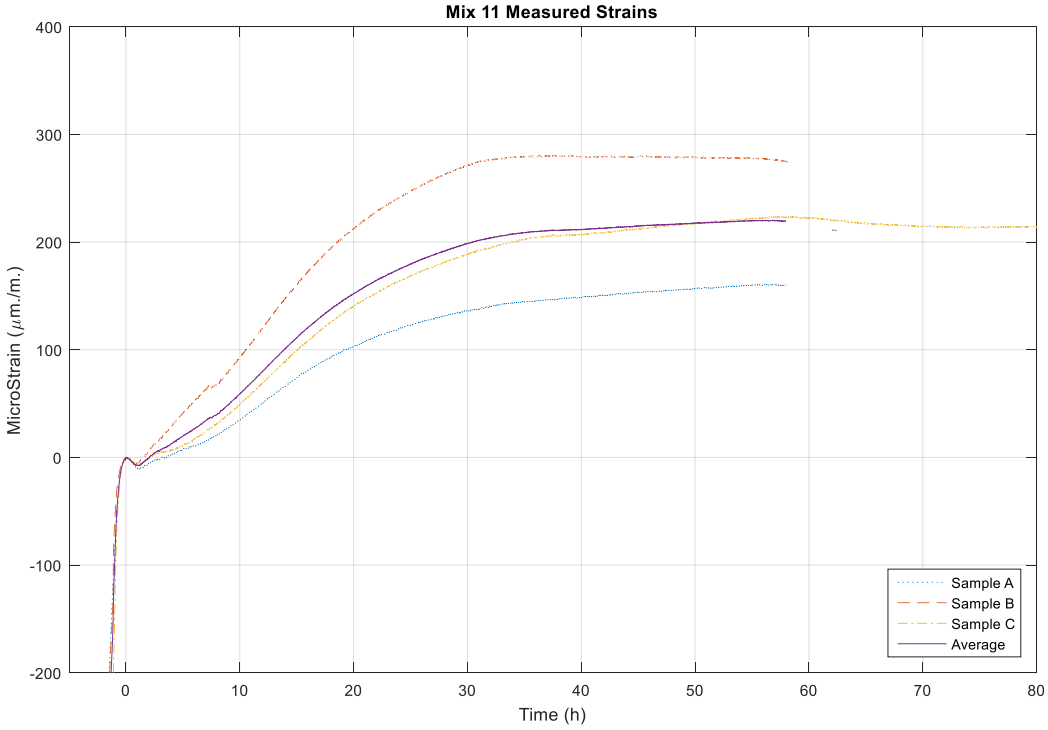

Figure 64: Mix 11 Data

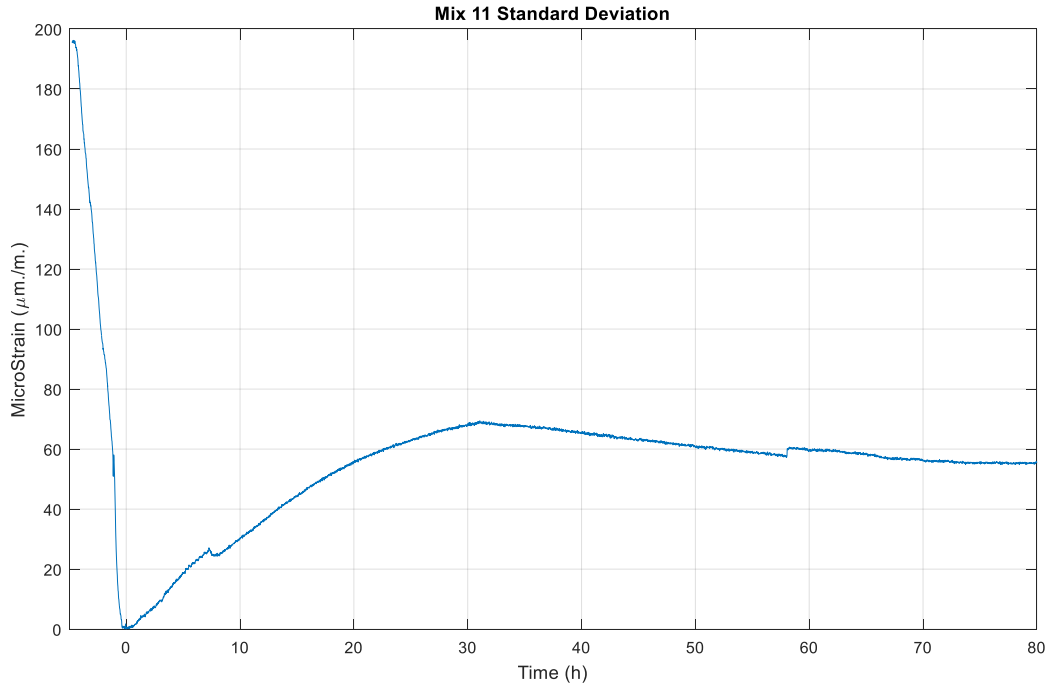

Figure 65: Mix 11 Standard Deviation

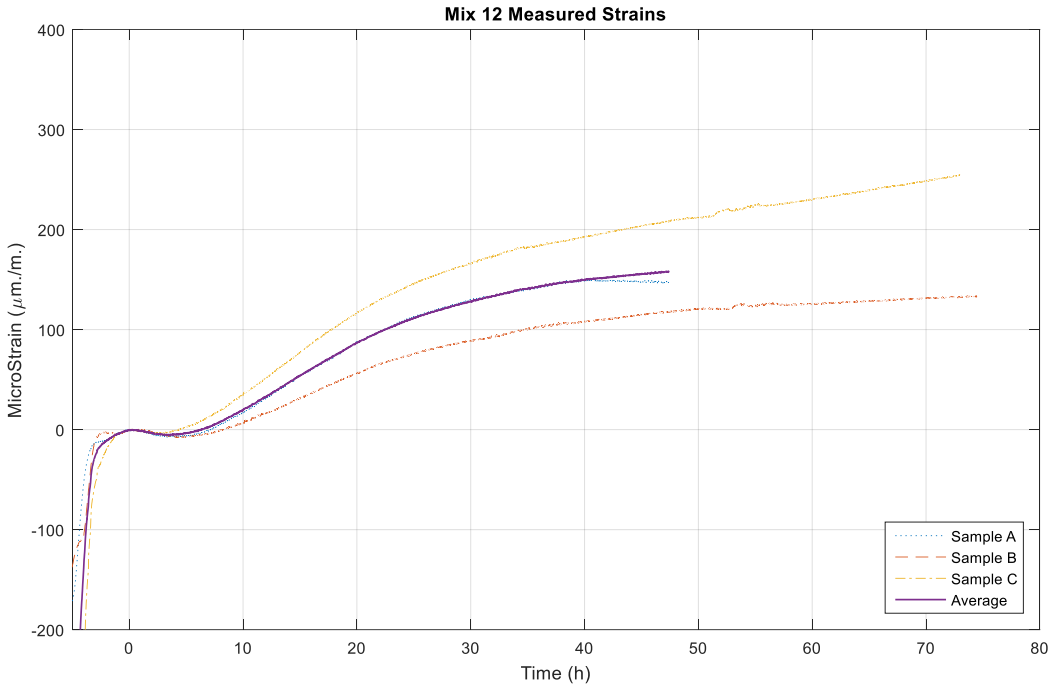

Figure 66: Mix 12 Data

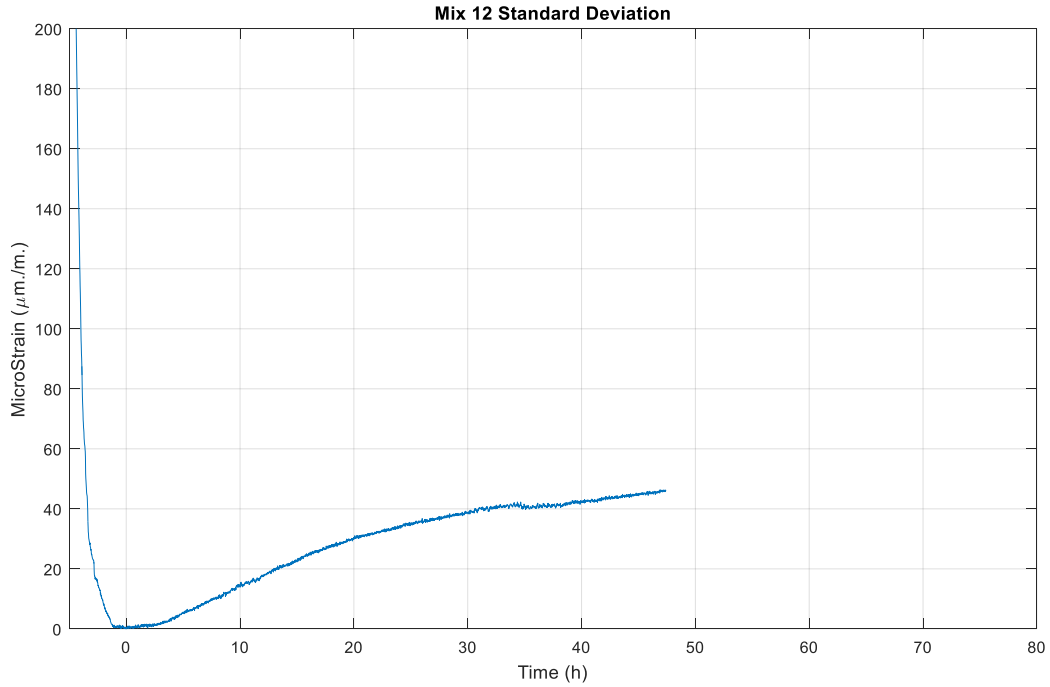

Figure 67: Mix 12 Standard Deviation

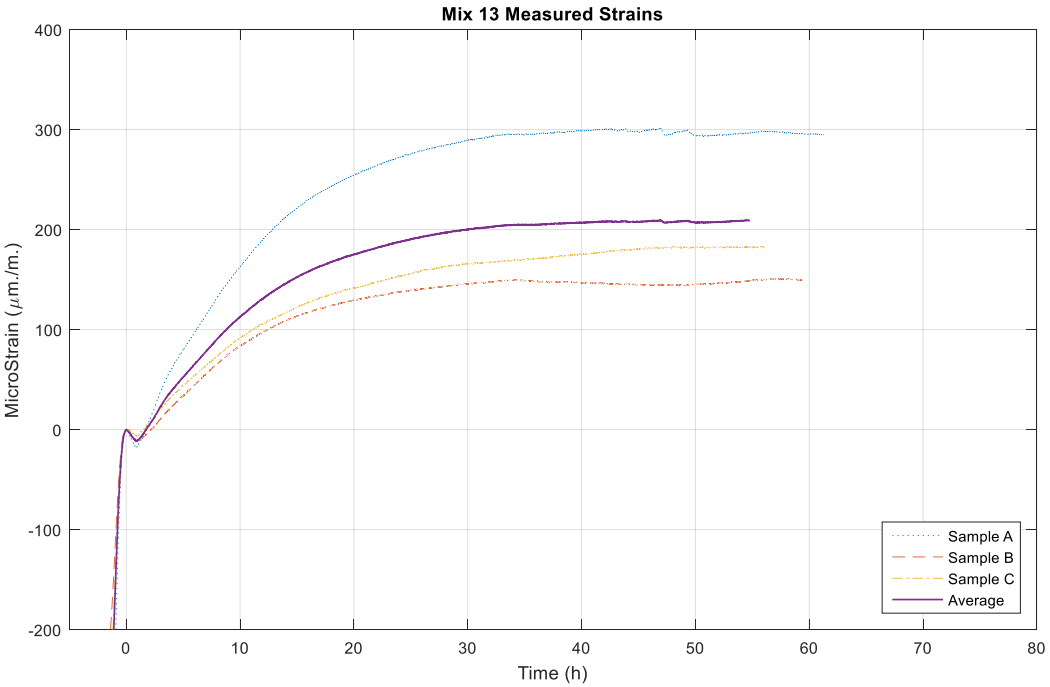

Figure 68: Mix 13 Data

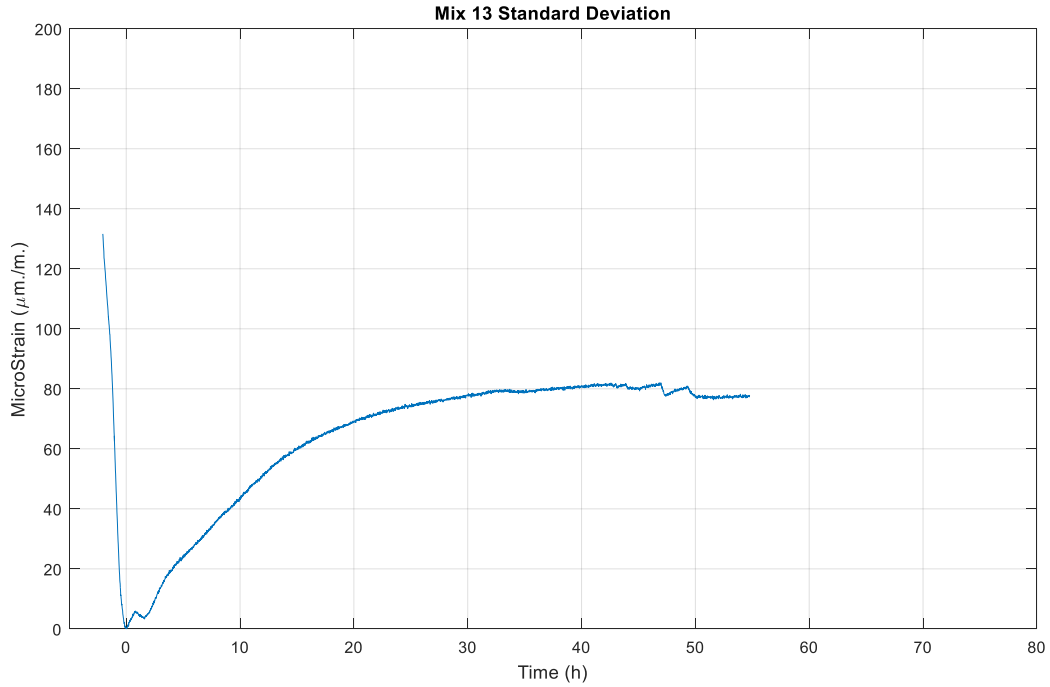

Figure 69: Mix 13 Standard Deviation

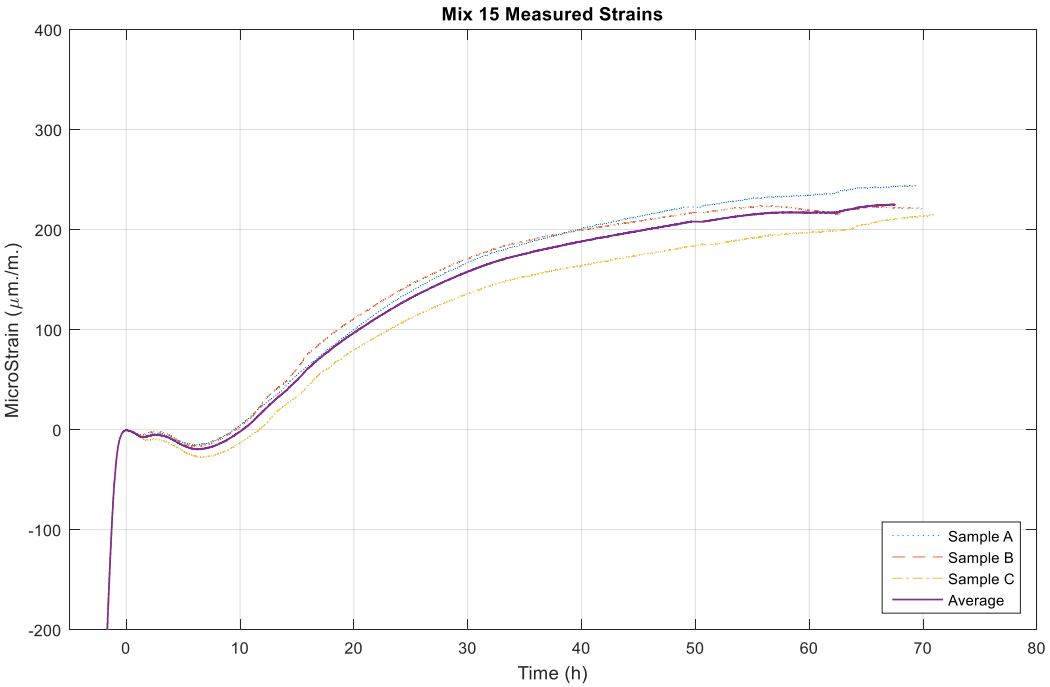

Figure 70: Mix 15 Data

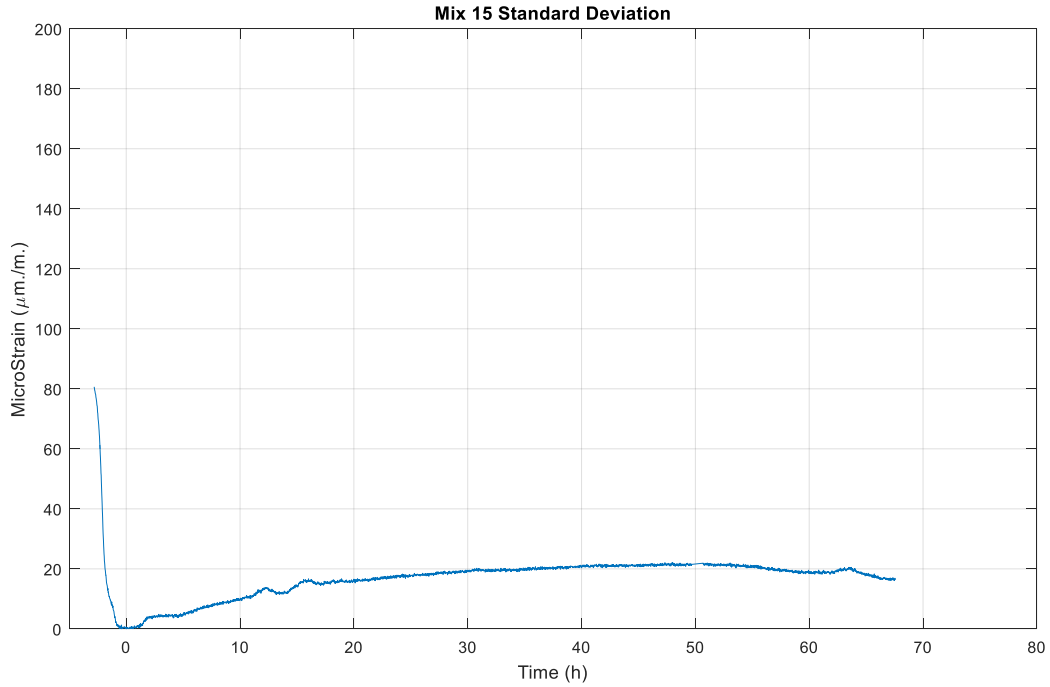

Figure 71: Mix 15 Standard Deviation

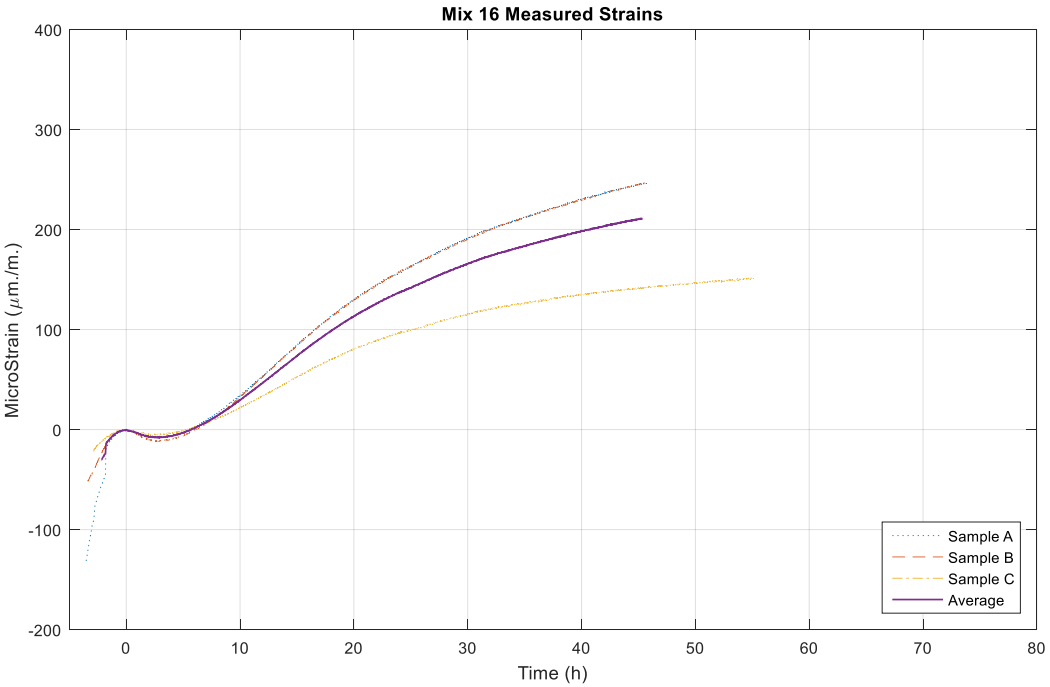

Figure 72: Mix 16 Data

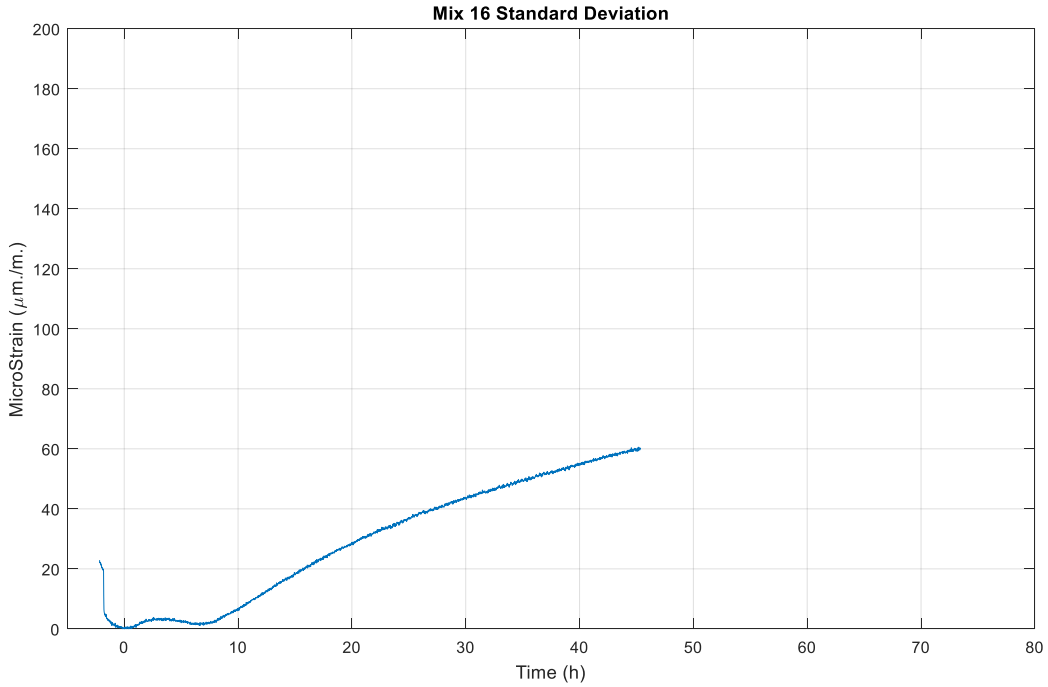

Figure 73: Mix 16 Standard Deviation

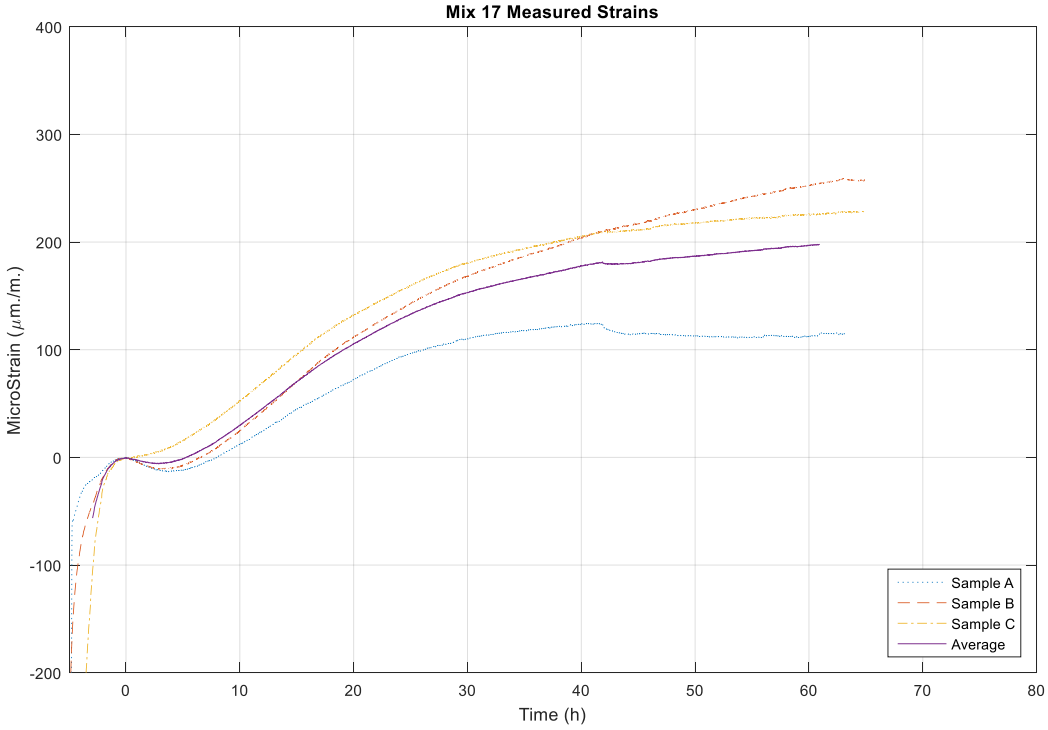

Figure 74: Mix 17 Data

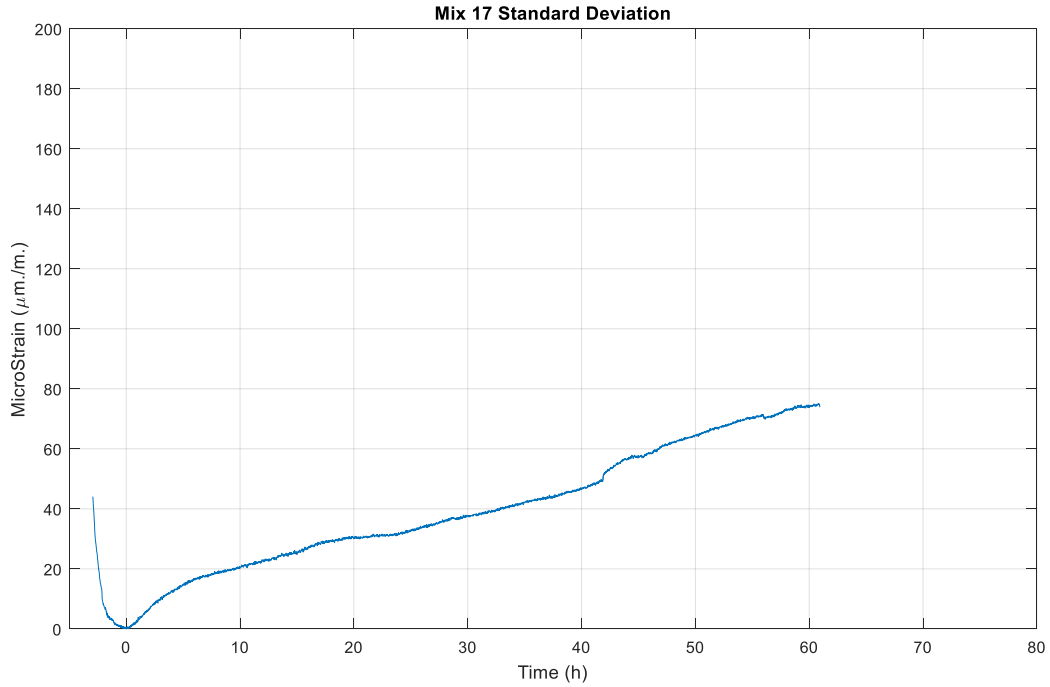

Figure 75: Mix 17 Standard Deviation

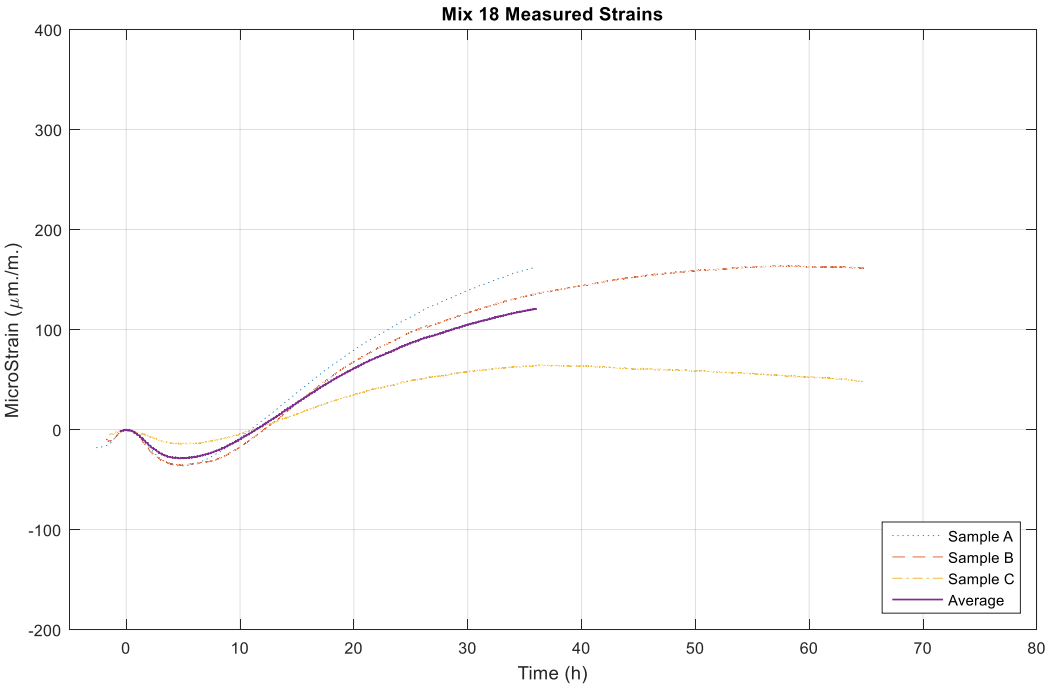

Figure 76: Mix 18 Data

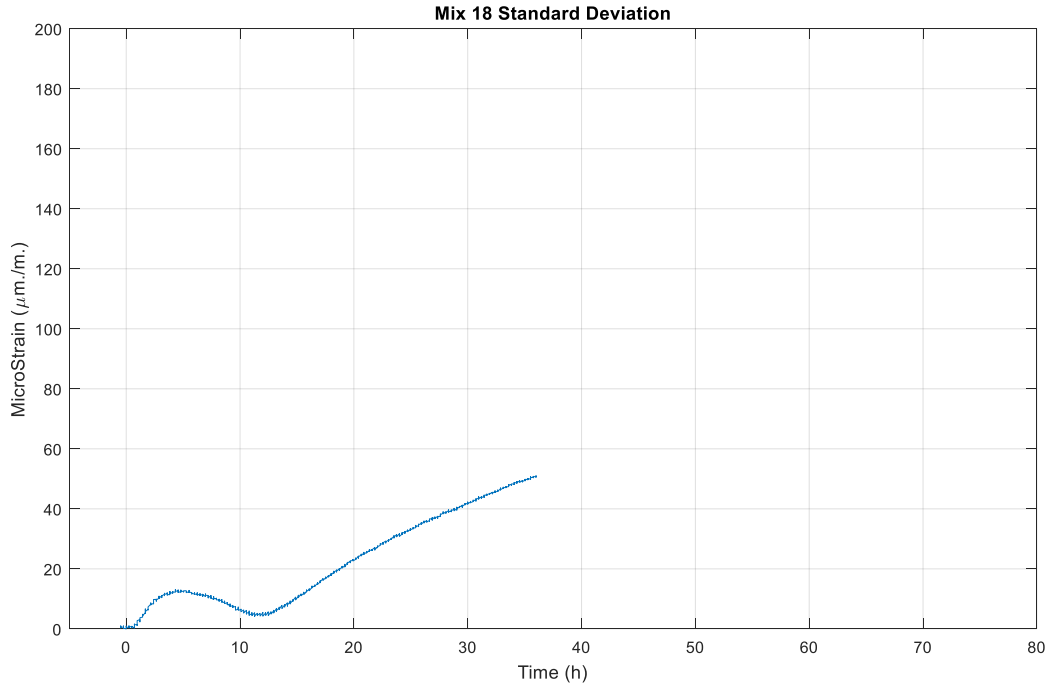

Figure 77: Mix 18 Standard Deviation

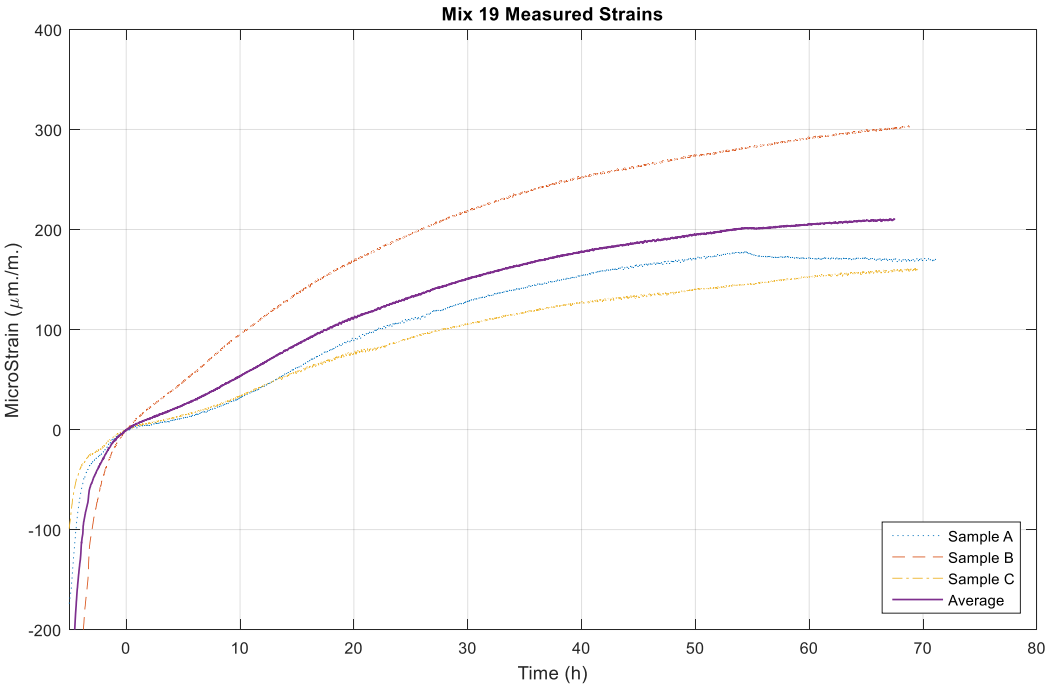

Figure 78: Mix 19 Data

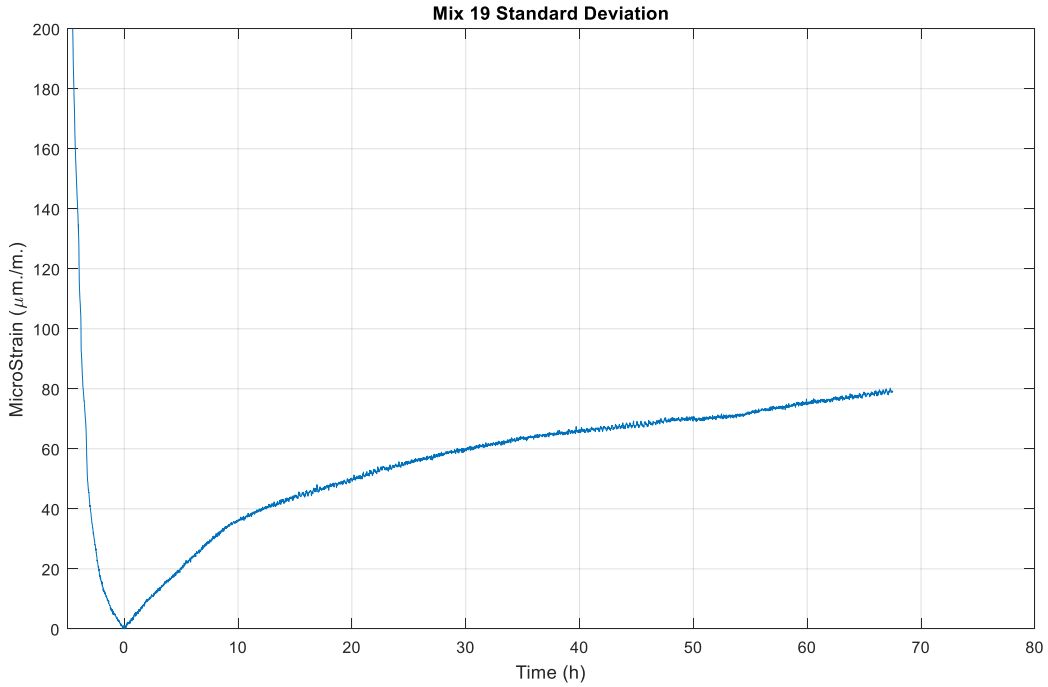

Figure 79: Mix 19 Standard Devation

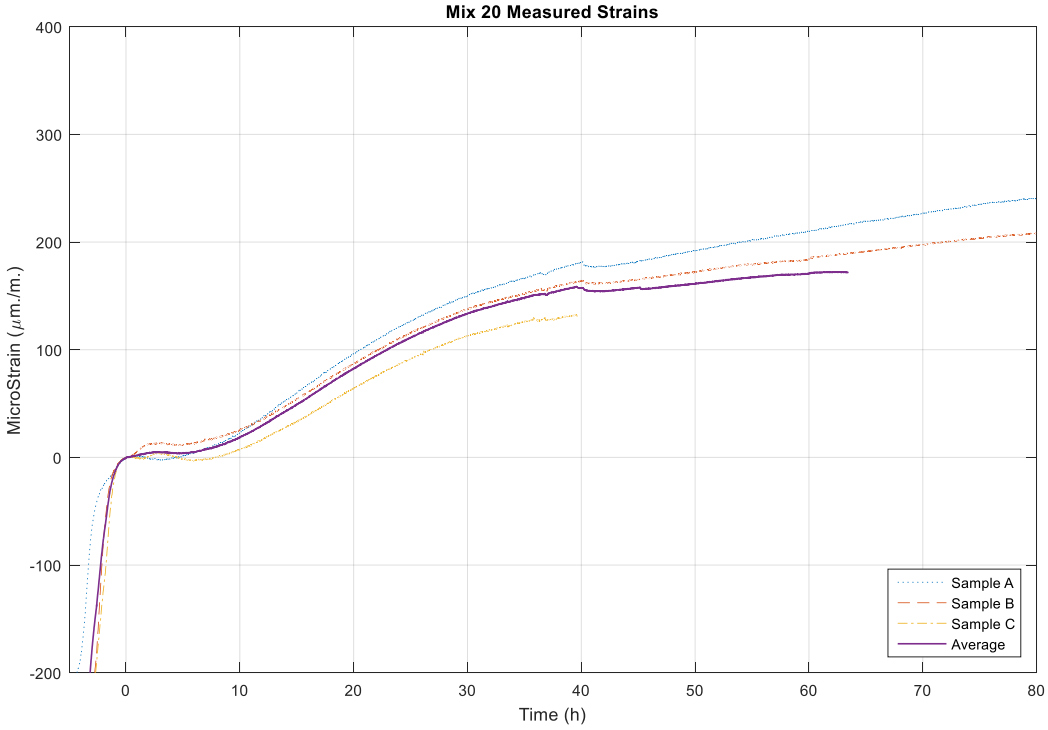

Figure 80: Mix 20 Data

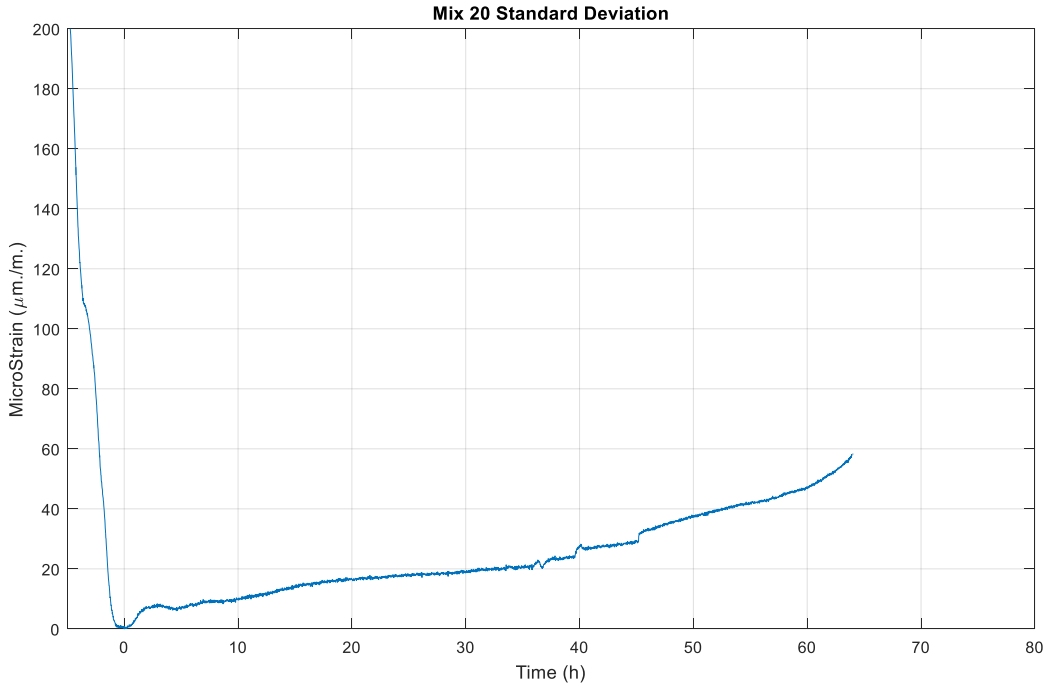

Figure 81: Mix 20 Standard Deviation

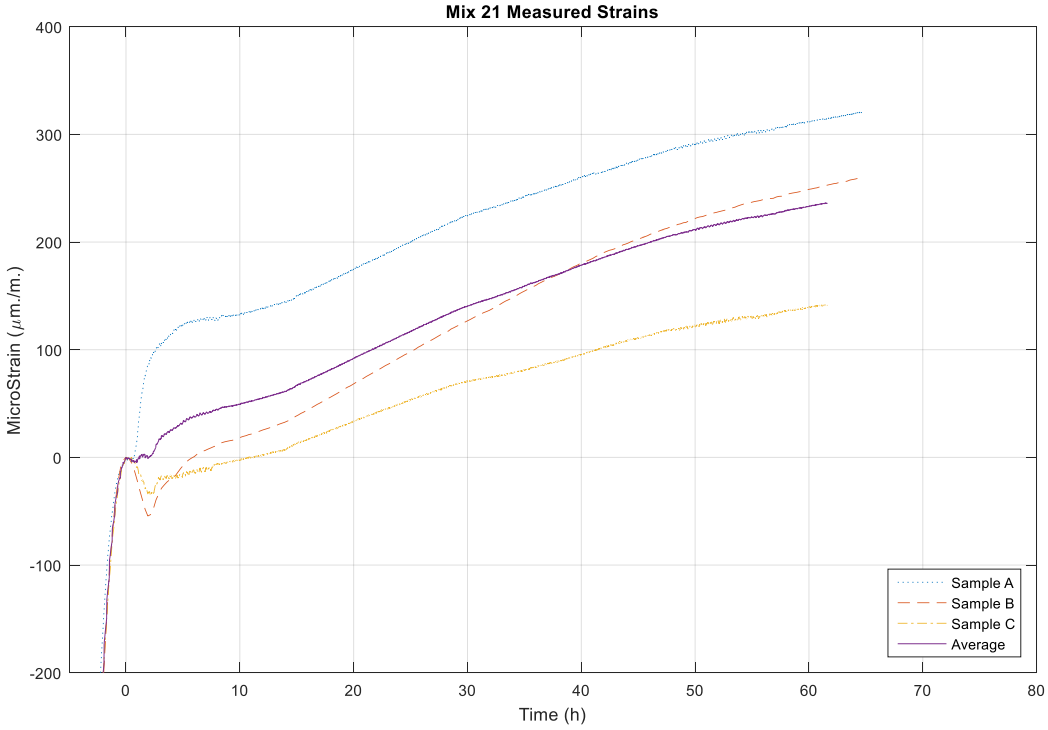

Figure 82: Mix 21 Data

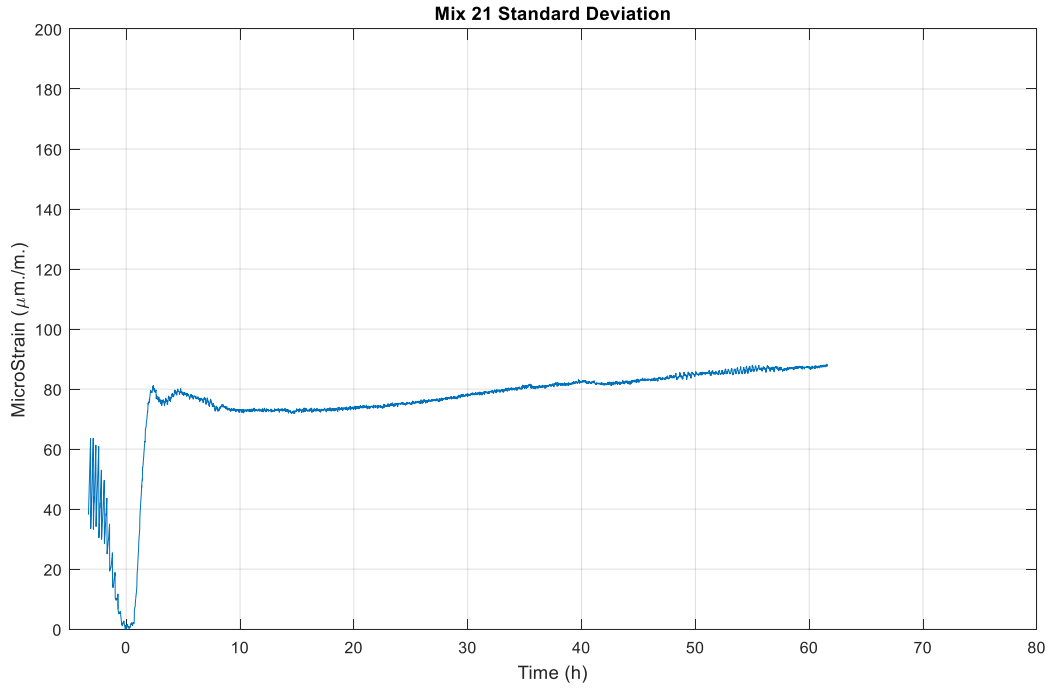

Figure 83: Mix 21 Standard Deviation

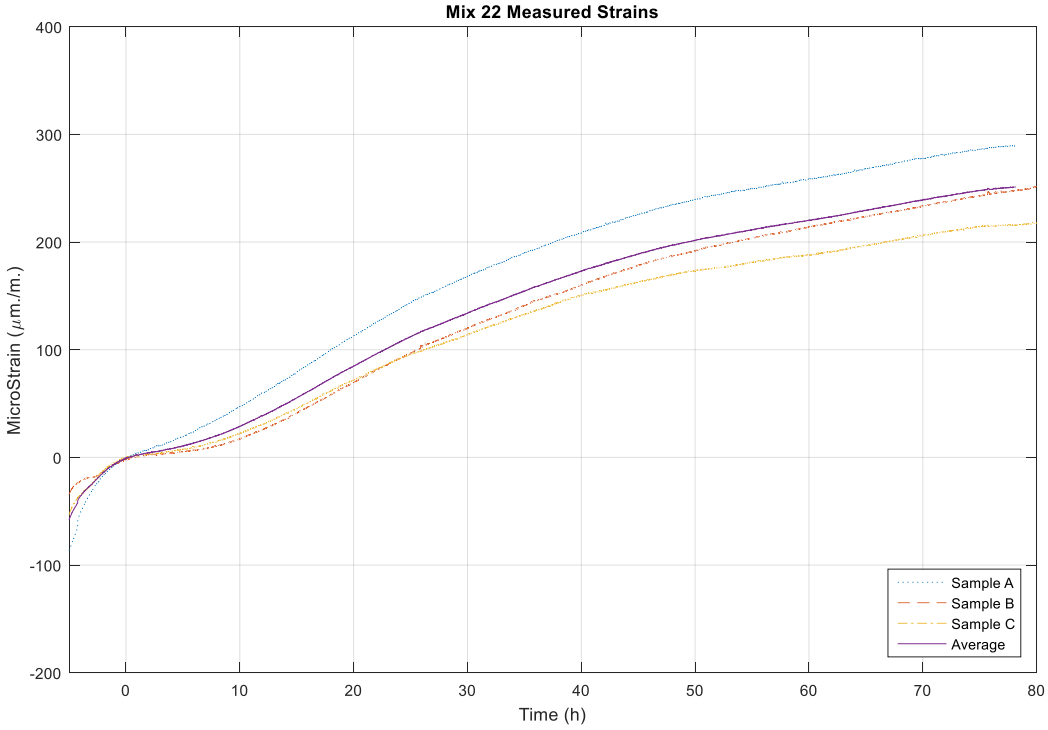

Figure 84: Mix 22 Data Series

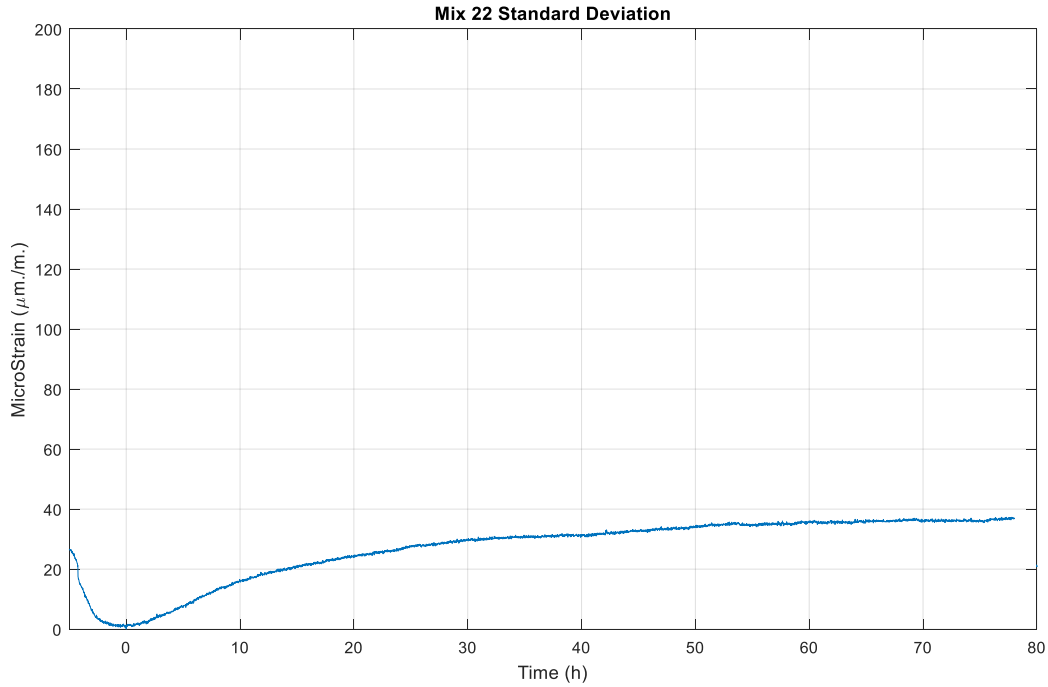

Figure 85: Mix 22 Standard Deviation

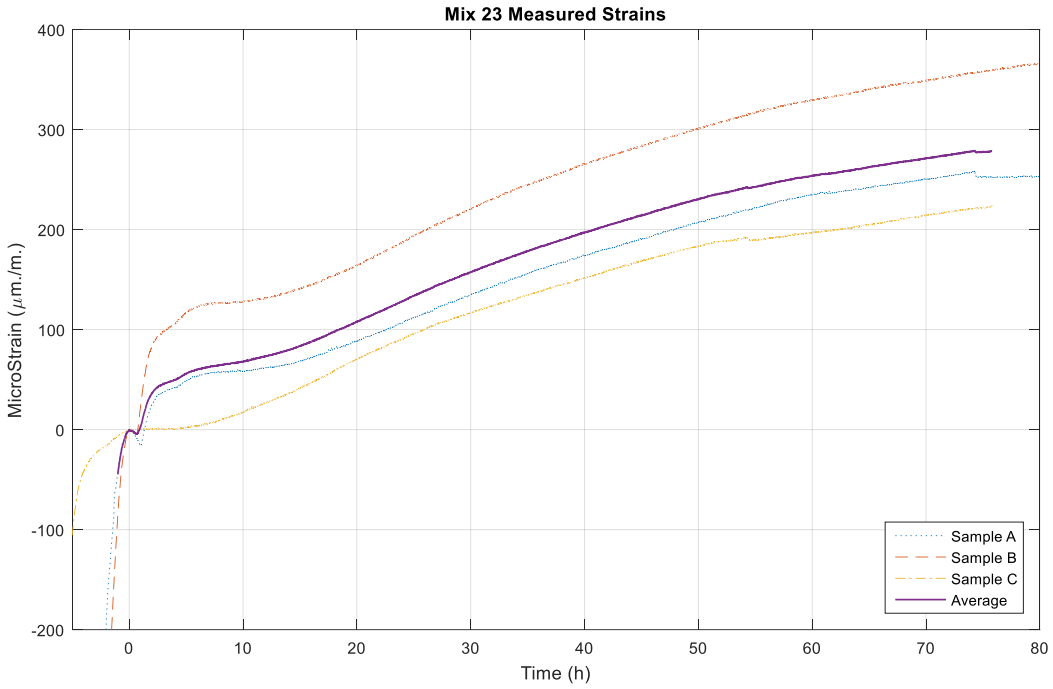

Figure 86: Mix 23 Data

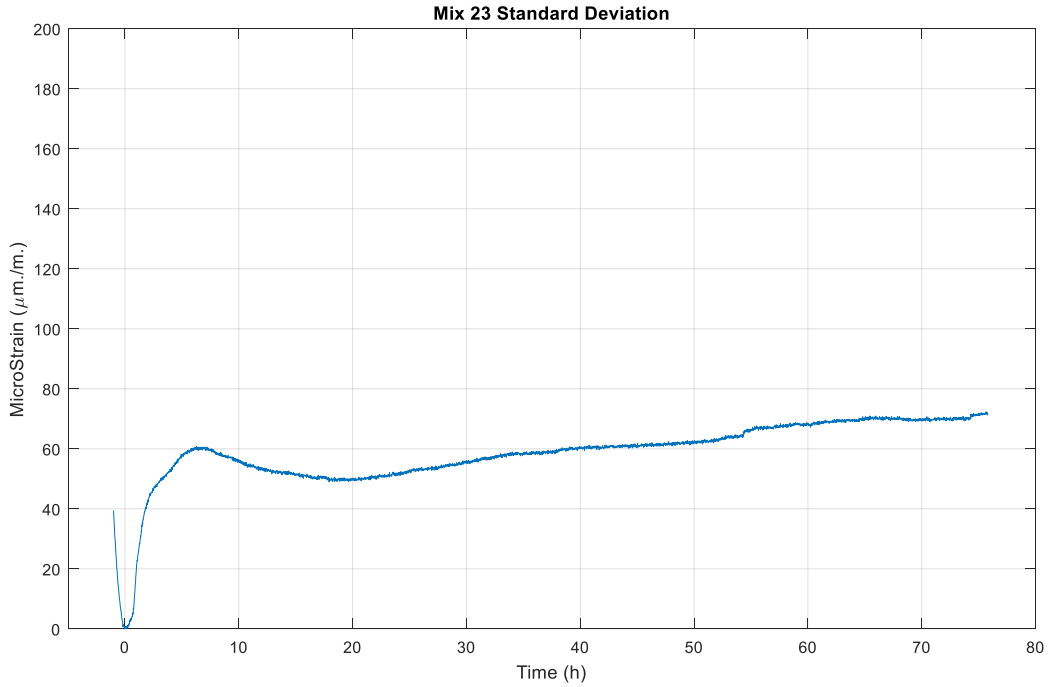

Figure 87: Mix 23 Standard Deviation

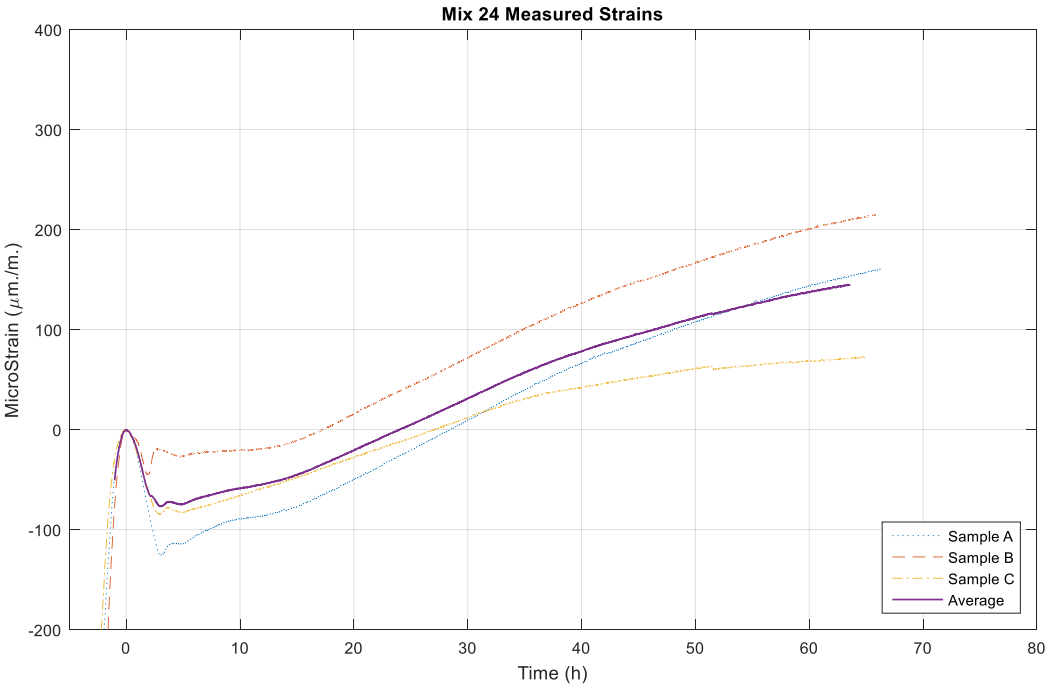

Figure 88: Mix 24 Data

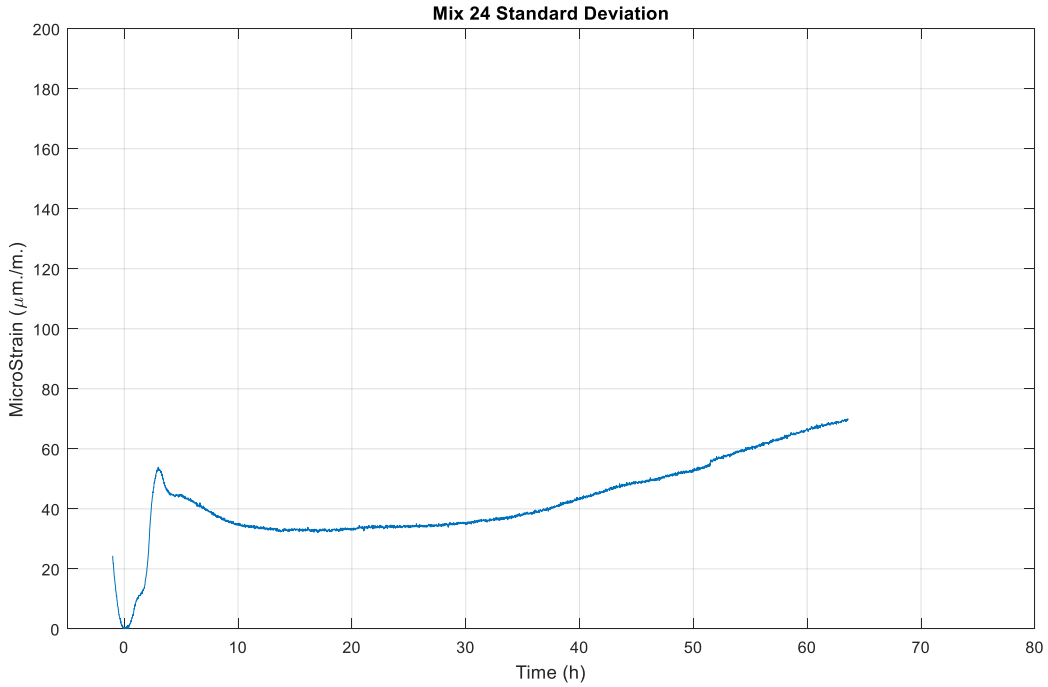

Figure 89: Mix 24 Standard Deviation

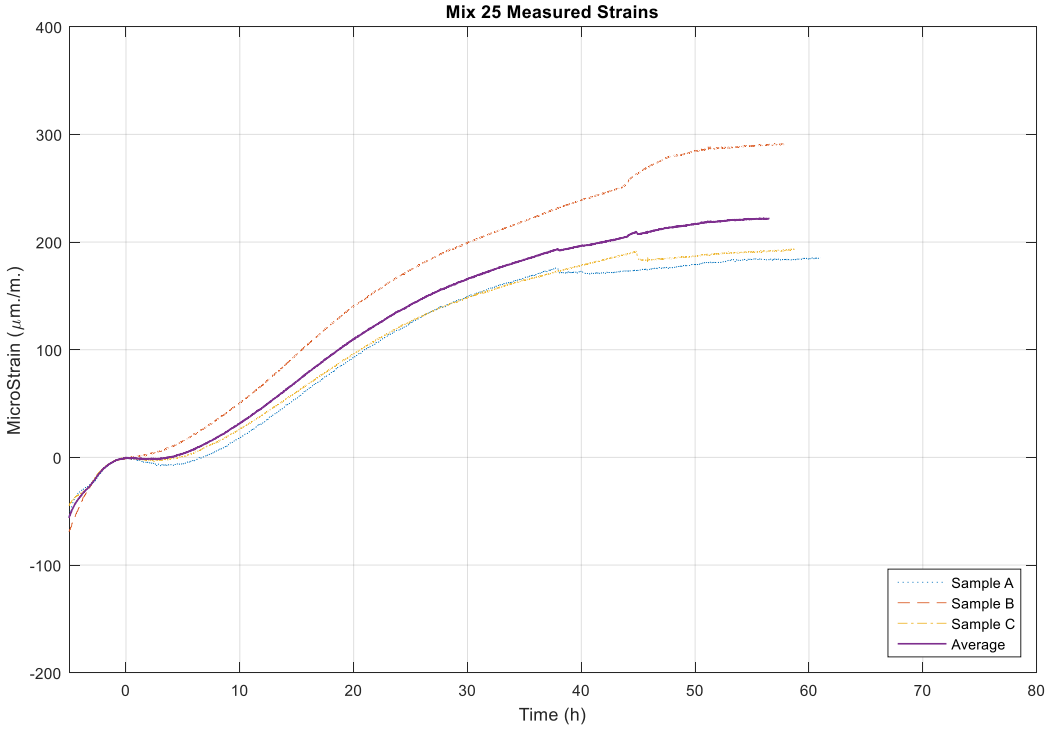

Figure 90: Mix 25 Data

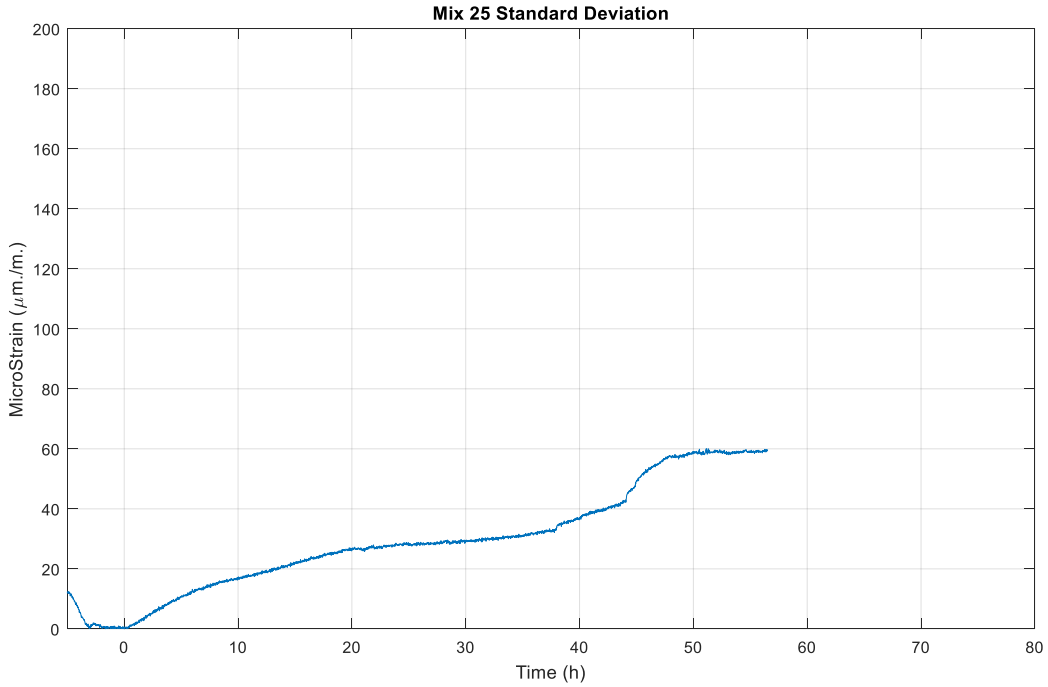

Figure 91: Mix 25 Standard Deviation

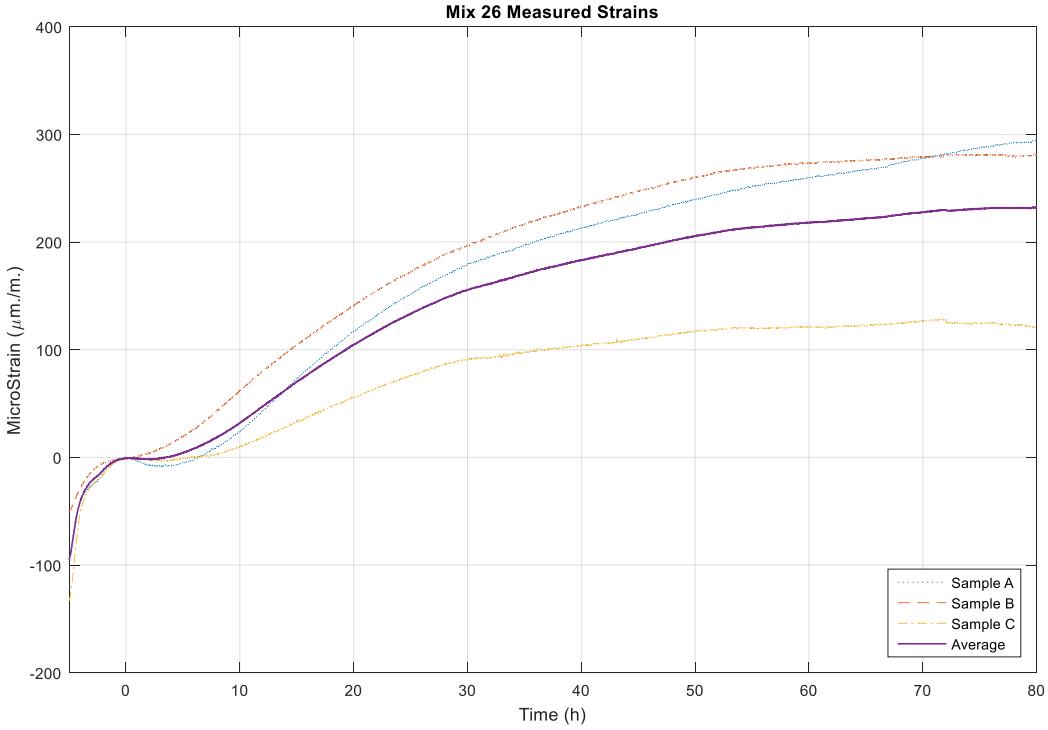

Figure 92: Mix 26 Data

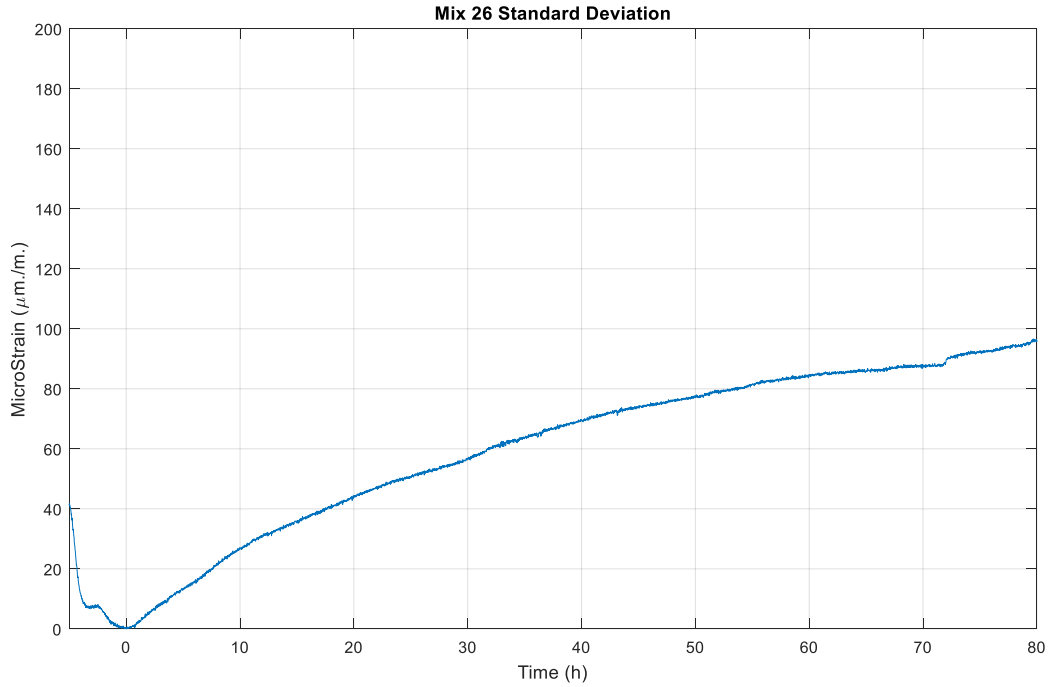

Figure 93: Mix 26 Standard Deviation

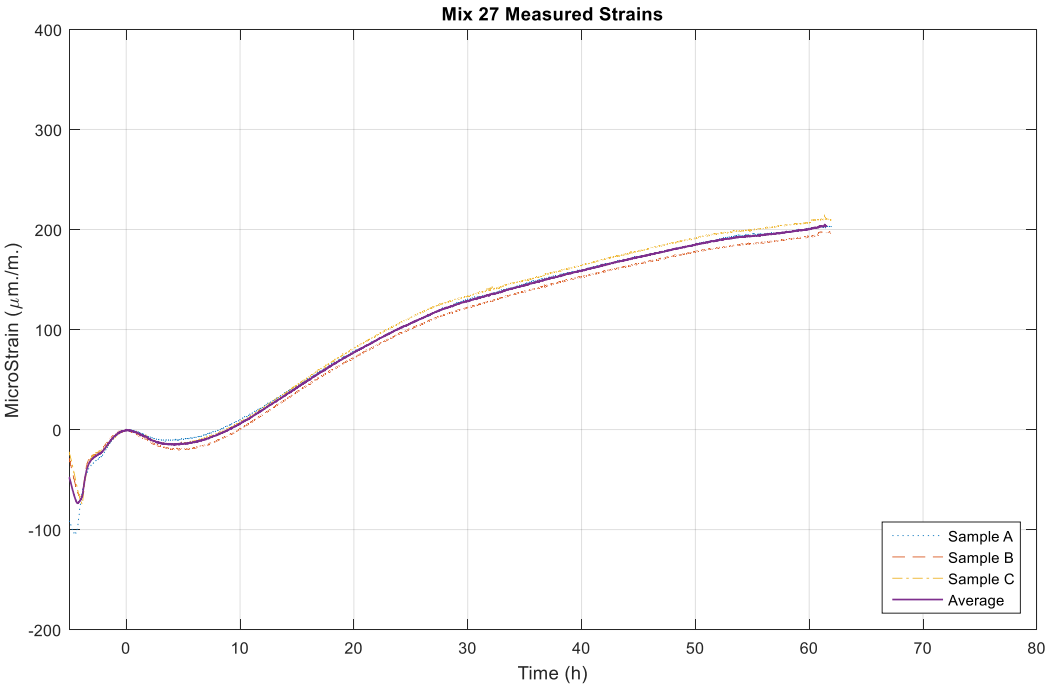

Figure 94: Mix 27 Data

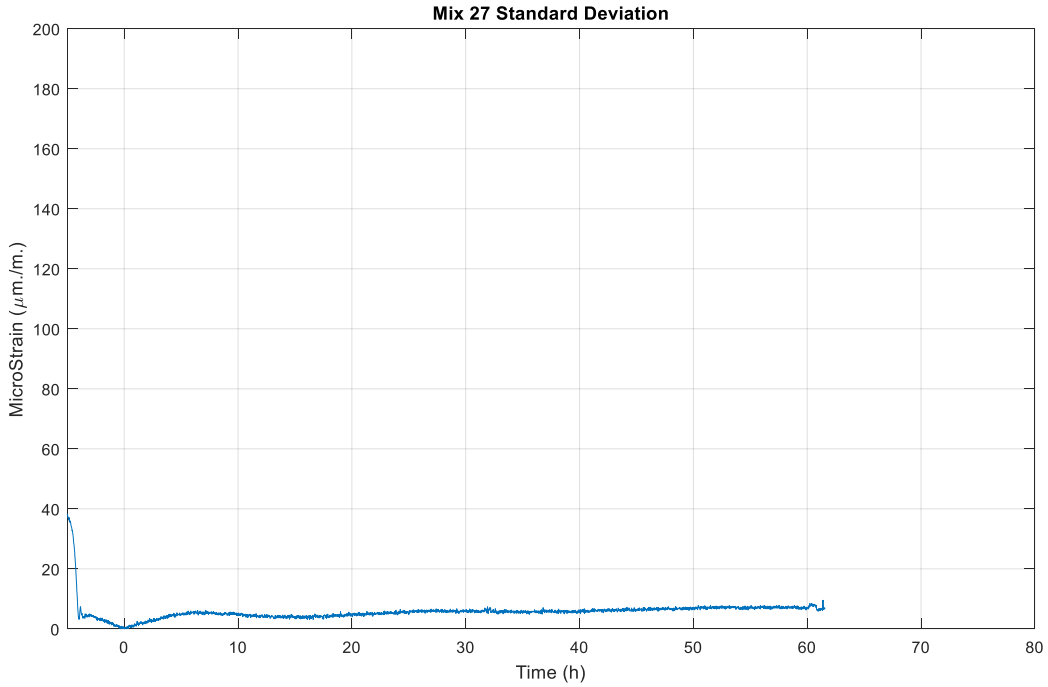

Figure 95: Mix 27 Standard Deviation

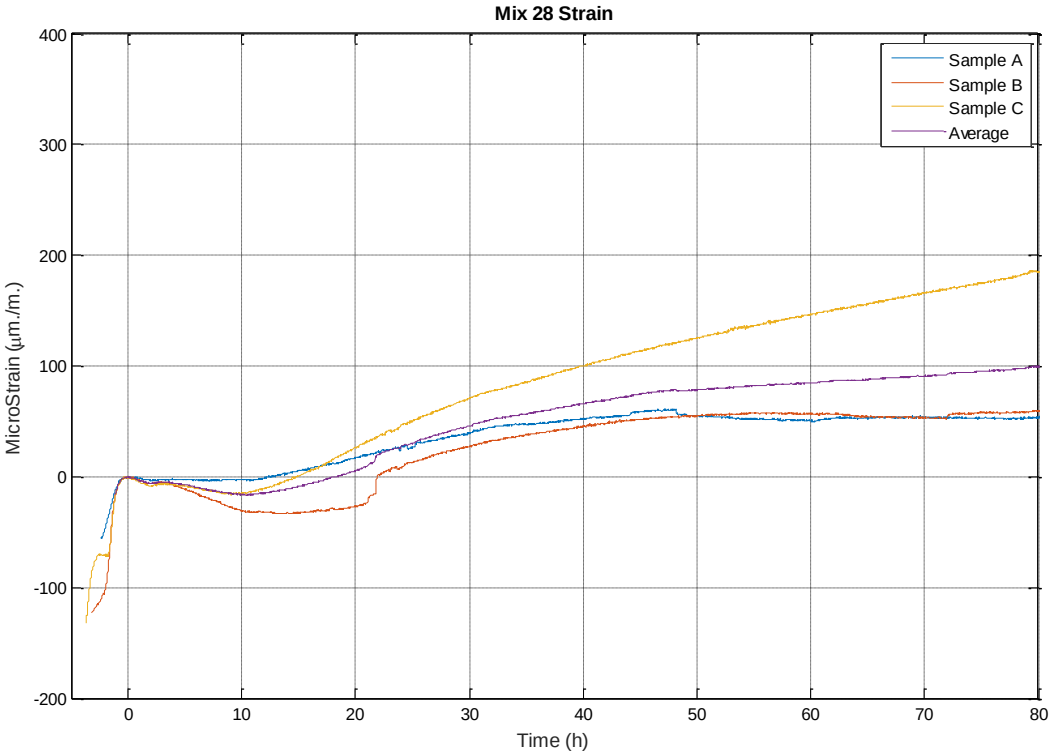

Figure 96: Mix 28 Data

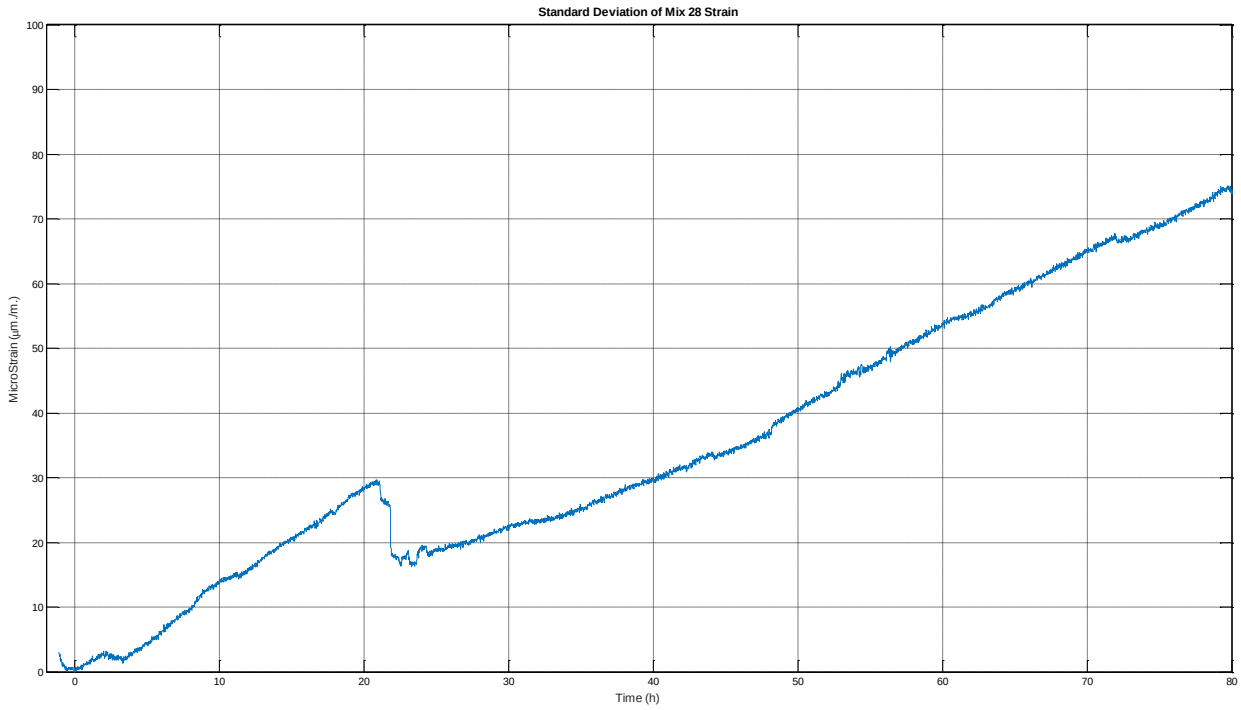

Figure 97: Mix 28 Strain

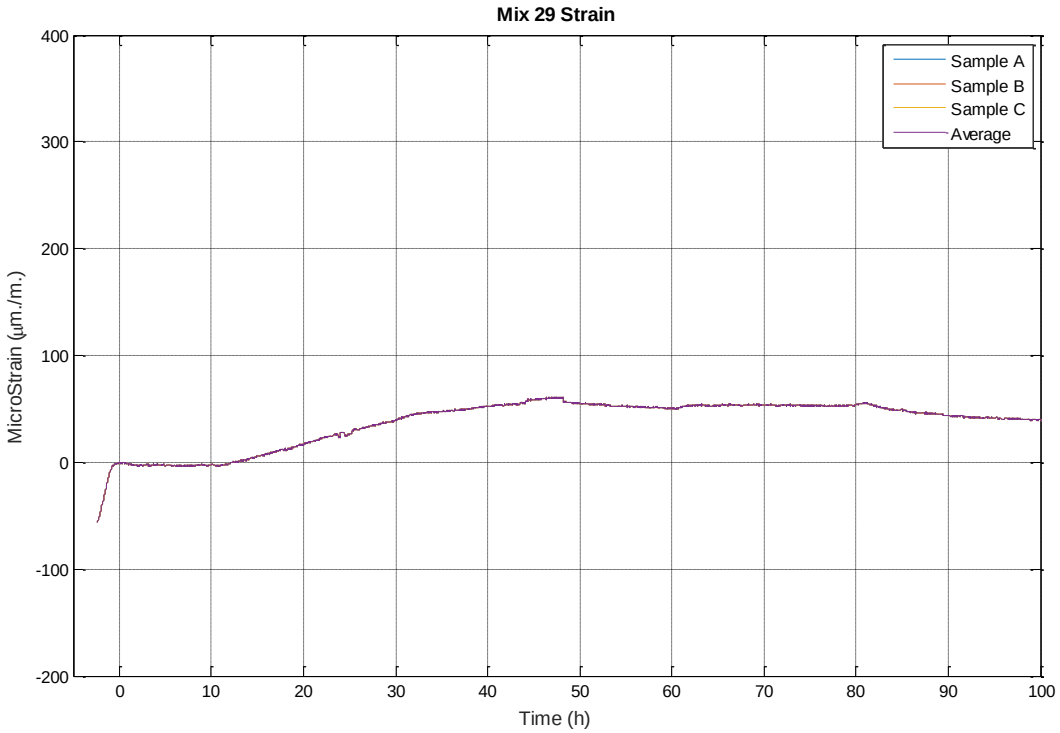

Figure 98: Mix 29 Data

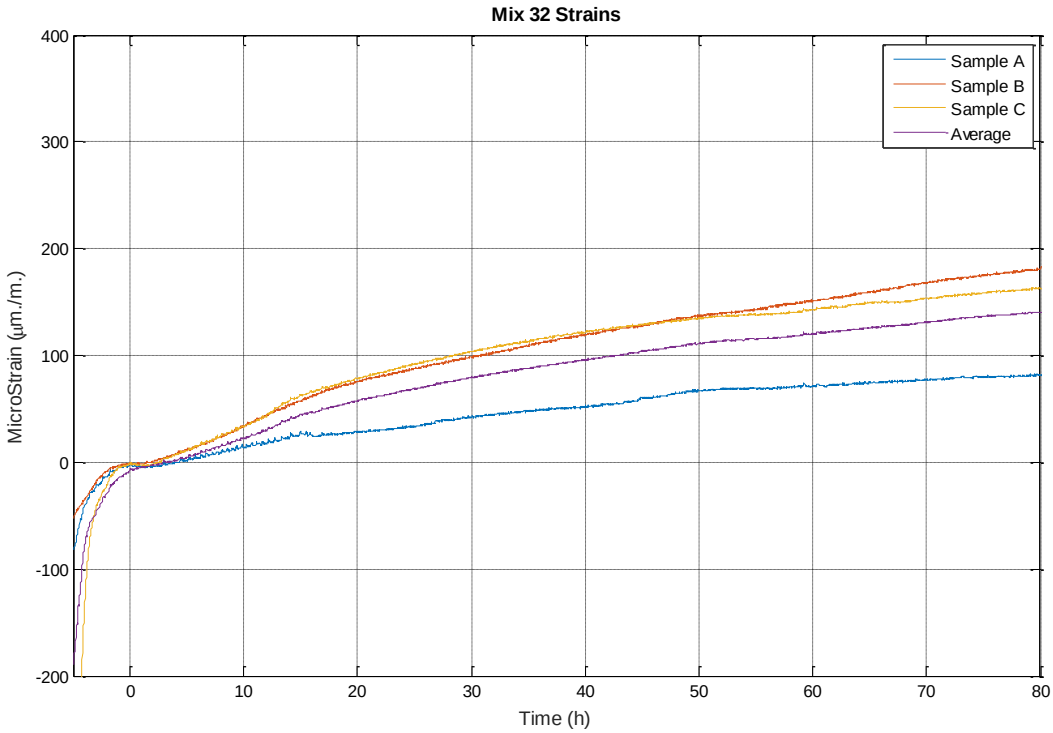

Figure 99: Mix 32 Data

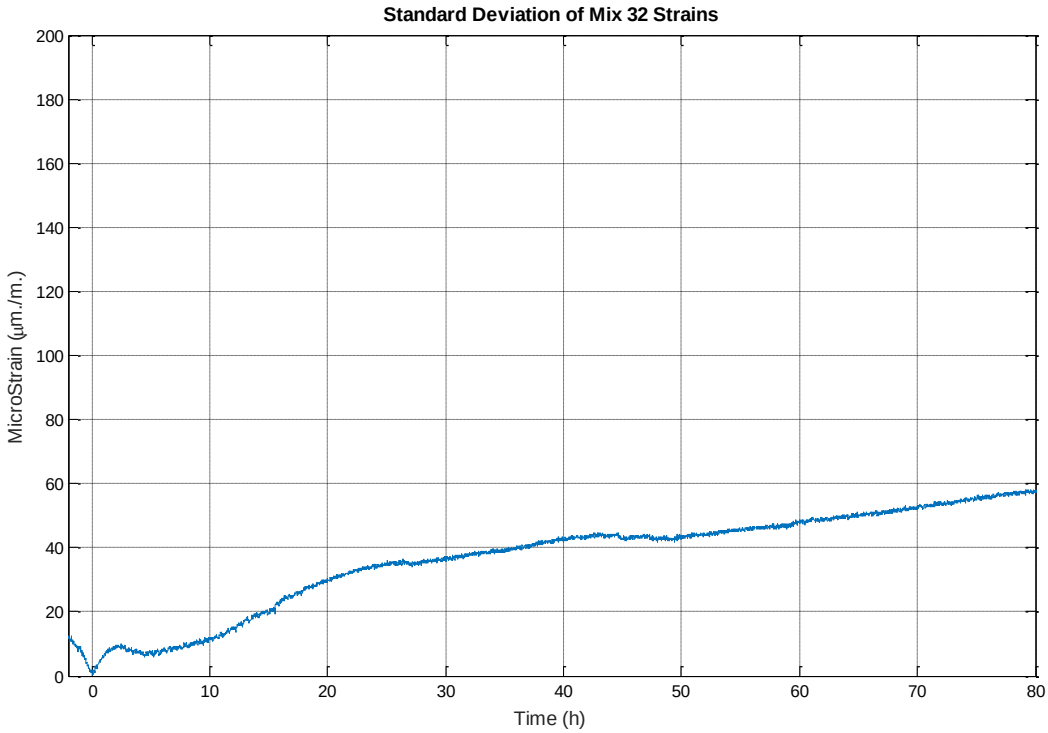

Figure 100: Mix 32 Standard Deviation

References

1. S. Stacey. Evaluation of ASTM C494 Procedure for Polycarboxylate Admixtures used in Precast Concrete Elements. Master's Thesis, Austin, University of Texas, 2016.

2. N. Tiburzi. Evaluation of Volume Changes and Cracking Potential of Low Water-to-Cementitious Material Ratio Concrete Mixtures. Master's Thesis, Austin, University of Texas, 2016.

3. Tiburzi, Nicolas B., Thano Drimalas, and Kevin J. Folliard. "Evaluation of precast bridge girder cracking: The role of volume change." *Cement and Concrete Research* 101 (2017).

4. Powers, T.C. and Brownyard, T.L., "Studies of the Physical Properties of Hardened Portland Cement Paste," Bulletin 22, Portland Cement Association, Chicago, 1948, 992 pp.

5. Jensen, Ole Mejlhede, and Per Freiesleben Hansen. "Water-entrained cement-based materials: I. Principles and theoretical background." *Cement and concrete research* 31, no. 4 (2001): 647-654.

6. Kosmatka, S.H., Kerkhoff, B. and Panarese, W.C., 2011. *Design and control of concrete mixtures*. Portland Cement Assoc.

7. Bentz, Dale P., and Ole Mejlhede Jensen. "Mitigation strategies for autogenous shrinkage cracking." *Cement and Concrete Composites* 26, No. 6 (2004): 677-685.

8. Bisschop Jan (2002) Drying shrinkage microcracking in cement-based material. Ph.D. Thesis, Delft University Press.

9. Maruyama, Ippei, Katsutoshi Beppu, Ryo Kurihara, and Akihiro Furuta. "Action mechanisms of shrinkage reducing admixture in hardened cement paste." *Journal of Advanced Concrete Technology* 14, no. 6 (2016): 311-323.

10. Tazawa, E. And Miyazawa, S. (1994) Autogenous shrinkage of cement paste. Cement and Concrete Research, Vol 25, No. 2, pp. 281-287, 1995.

11. G. Sant. Examining volume changes, stress development and cracking in cement based systems. PhD Thesis, Purdue University, 2007.

12. E. Holt. Early age autogenous shrinkage of concrete. PhD thesis, Seattle, University of Washington, 2001.

13. Chan Y. W., Lui C. Y. and Lu Y. S. Effects of slag and fly ash on the autogenous shrinkage of high performance concrete. Autogenous shrinkage of concrete. In Proc. Int. Workshop. E & FN Spon, London and New York, pp. 221-228.

14. Tangtermsirikul, S. "Effect of chemical composition and particle size of fly ash on autogenous shrinkage of paste." In *Proceedings of an International Workshop on the Autogenous Shrinkage of Concrete. London: E &FN Spon*, pp. 175-185. 1999.

15. Huang, Hao, and Guang Ye. "Examining the “time-zero” of autogenous shrinkage in high/ultra-high performance cement pastes." *Cement and Concrete Research* 97 (2017): 107-114.

16. Sant, Gaurav, Pietro Lura, and Jason Weiss. "Measurement of volume change in cementitious materials at early ages: review of testing protocols and interpretation of results." *Transportation Research Record: Journal of the Transportation Research Board* 1979 (2006): 21-29.

17. Jensen, O. Mejlhede, and P. Freiesleben Hansen. "A dilatometer for measuring autogenous deformation in hardening Portland cement paste." *Materials and Structures* 28, no. 7 (1995): 406-409.

18. ASTM, C. "1698-09,'." *Standard Test Method for Autogenous Strain of Cement Paste and Mortar', American Society for Testing and Materials, ASTM International* (2009).

19. P. Gao, T. Zhang, R. Luo, J. Wei, Q. Yu, Improvement of autogenous shrinkage measurement for cement paste at very early age: Corrugated tube method using non-contact sensors, Constr. Build. Mater. 55 (2014) 57–62, http://dx.doi.org/10.1016/j.conbuildmat.2013.12.086.

20. Mohr, B. J., and K. L. Hood. "Influence of bleed water reabsorption on cement paste autogenous deformation." *Cement and Concrete Research* 40, no. 2 (2010): 220-225.

21. Mailvaganam, Noel P., and M. R. Rixom. *Chemical admixtures for concrete*. CRC Press, 2002.

22. Gelardi, G., and R. J. Flatt. "Working mechanisms of water reducers and superplasticizers." In *Science and Technology of Concrete Admixtures*, pp. 257-278. 2016.

23. Uchikawa, Hiroshi, S. Hanehara, and D. Sawaki. "The role of steric repulsive force in the dispersion of cement particles in fresh paste prepared with organic admixture." *Cement and Concrete Research* 27, no. 1 (1997): 37-50.

24. Nkinamubanzi, P-C., S. Mantellato, and R. J. Flatt. "Superplasticizers in practice." In *Science and technology of concrete admixtures*, pp. 353-377. 2016.

25. Plank, J., E. Sakai, C. W. Miao, C. Yu, and J. X. Hong. "Chemical admixtures—Chemistry, applications and their impact on concrete microstructure and durability." *Cement and Concrete Research* 78 (2015): 81-99.
26. Li, Yinwen, Chaolong Yang, Yunfei Zhang, Jian Zheng, Huilong Guo, and Mangeng Lu. "Study on dispersion, adsorption and flow retaining behaviors of cement mortars with TPEG-type polyether kind polycarboxylate superplasticizers." *Construction and Building Materials* 64 (2014): 324-332.
27. Marchon, D., Mantellato, S., Eberhardt, A.B. and Flatt, R.J., 2016. Adsorption of chemical admixtures. In *Science and Technology of Concrete Admixtures* (pp. 219-256).
28. Holt, Erika. "Very early age autogenous shrinkage: governed by chemical shrinkage or self-desiccation?" In *Proceedings of the Third International Research Seminar in Lund, Lund, Sweden*, pp. 1-25. 2002.
29. Meddah, Mohammed Seddik, and Arezki Tagnit-Hamou. "Pore structure of concrete with mineral admixtures and its effect on self-desiccation shrinkage." *ACI Materials Journal* 106, no. 3 (2009): 241.
30. Li, P. P., Q. L. Yu, and H. J. H. Brouwers. "Effect of PCE-type superplasticizer on early-age behaviour of ultra-high performance concrete (UHPC)." *Construction and Building Materials* 153 (2017): 740-750.
31. Fontana, Patrick, and Birgit Meng. “Influence of mix composition on early-age autogenous deformations of cement pastes.” In *International RILEM Conference on Volume Changes of Hardening Concrete: Testing and Mitigation*, pp. 261-272. RILEM Publications SARL, 2006.

32. Mora-Ruacho, José, Ravindra Gettu, and Antonio Aguado. "Influence of shrinkage-reducing admixtures on the reduction of plastic shrinkage cracking in concrete." *Cement and Concrete Research* 39, no. 3 (2009): 141-146.

33. Tang, Fulvio J., and Sankar Bhattacharja. *Development of an early stiffening test*. No. RP346, RP346. 01T,.1997.

34. Lin, Shih-Tang, and Ran Huang. "Effect of viscosity modifying agent on plastic shrinkage cracking of cementitious composites." *Materials and structures* 43, no. 5 (2010): 651-664.

Vita

Email: cathcarris@gmail.com

Address: 7373 Valley View Lane Apt. 3090, Dallas, TX 75240

This dissertation was typed by Gwen Catherin Carris.